USE OF THE PRINCIPLE OF

CORRESPONDING STATES

IN CHEMICAL PROCESS DESIGN

by

Richard Szczepanski, B.Sc.(Eng), A.C.G.I.

A thesis submitted for the degree of Doctor of Philosophy of the University of London and for the Diploma of Membership of the Imperial College. April, 1979.

Department of Chemical Engineering
and Chemical Technology,
Imperial College,
London, S.W.7.

BIBL.
LONDIN.
UNIV.

Contains

Microfiche

USE OF THE PRINCIPLE OF CORRESPONDING STATES IN CHEMICAL PROCESS DESIGN

by

Richard Szczepanski

ABSTRACT

This thesis explores the possibility of using the principle of corresponding states as a practical method of predicting thermodynamic properties for process design.

New, faster and more reliable ways of solving the basic corresponding states equations for multicomponent mixtures have been developed and include the use of minimization procedures for dealing with flash problems.

Several alternative equations of state for the reference substance (methane) have been developed, covering an extended range of P-ρ-T space, so that reliable corresponding states predictions of the properties of highly volatile substances such as hydrogen are possible. A number of modifications were also included to make the equations more suitable for use in corresponding states procedures.

Using these extended equations of state the corresponding states principle was applied to hydrogen and hydrogen-containing mixtures. The precision is high for volumetric properties but the results for vapour-liquid equilibria show less close agreement with experiment and cast some doubt on the validity of the commonly used molecular shape factor equations {*}.

All of the developments have been incorporated in an easy to use computer package. The algorithms have been made highly reliable and efficient so as to be useable within flowsheeting programmes.

* Leach, J.W., P.S. Chappelear and T.W. Leland, A.I.Ch.E. Journal, 14, 568 (1968).

Acknowledgements

I should like to express my gratitude to Dr. Graham Saville for his unfailing friendship, encouragement, and guidance throughout the course of this work.

Thanks are also due to Selby Angus, Barrie Armstrong, and Marjorie de Reuck of the I.U.P.A.C. Thermodynamic Tables Project Centre at Imperial College for helpful discussions and for permission to make use of their computer programmes.

A grant from the Science Research Council is gratefully acknowledged.

Contents

		page
	TITLE PAGE	1
	ABSTRACT	2
	ACKNOWLEDGEMENTS	3
	CONTENTS	4
	LIST OF TABLES	6
	LIST OF FIGURES	7
	PRINCIPAL SYMBOLS	8
1.	INTRODUCTION	9
2.	THE PRINCIPLE OF CORRESPONDING STATES - THEORY AND APPLICATIONS	16
	2.1 Theoretical background	16
	2.2 A computer package for the prediction of thermodynamic properties	27
	2.3 Performance of the PREPROP thermodynamic package	35
3.	EQUATIONS OF STATE FOR THE REFERENCE SUBSTANCE	49
	3.1 Introduction	49
	3.2 Choice of reference substance	49
	3.3 An extended equation for methane	51
	3.4 Application of Wagner's regression technique to an equation of state for methane	64
	3.5 Conclusions	68
4.	CALCULATION OF VAPOUR-LIQUID EQUILIBRIUM USING MINIMIZATION TECHNIQUES	69
	4.1 Introduction	69
	4.2 Criteria of equilibrium	70
	4.3 The Variable Metric Projection method for minimization	73
	4.4 Formulation of flash problems for minimization	84
	4.5 Computational procedures	95
	4.6 Computational performance	102

		page
5.	HYDROGEN AND HYDROGEN-CONTAINING MIXTURES	106
	5.1 Introduction	106
	5.2 Perfect gas heat capacity for hydrogen	108
	5.3 Effective critical parameters for hydrogen	108
	5.4 Vapour-liquid equilibrium in hydrogen-hydrocarbon mixtures	112
	5.5 Discussion	121
6.	CONCLUSIONS	125
	REFERENCES	127
	APPENDICES	
B.	DERIVATIVES OF CORRESPONDING STATES PARAMETERS FOR THE VAN DER WAALS ONE-FLUID MODEL	132
C.	COEFFICIENTS IN EQUATIONS OF STATE	142

(Note: Appendix A, a listing of computer routines, is included on microfiche inside the back cover).

List of Tables

page

Chapter 2

2.1 Comparison of calculation times for the CHESS and PREPROP thermodynamic packages. 37

2.2 Binary interaction parameters for the argon-oxygen system. 46

Chapter 3

3.1 A comparison of some high-accuracy equations of state. 50

3.2 Triple point temperatures for some common substances. 52

3.3 Comparison of equations of state for methane. 60

Chapter 4

4.1 Number of function evaluations required for vapour-liquid equilibrium calculations. 102

Chapter 5

5.1 Classical critical constants for hydrogen. 105

5.2 Numerical values for coefficients in equation (5.1). 107

5.3 Critical parameters and acentric factor for hydrogen. 109

5.4 Comparison of predicted and experimental compressiblity factors in hydrogen-hydrocarbon mixtures. 110

5.5 Pressure and composition deviations in bubble point calculations for methane-heptane mixtures. 113

5.6 Experimental data for hydrogen-hydrocarbon systems. 116

5.7 Comparison of calculated and experimental bubble point data for binary systems. 117

5.8 Binary interaction parameters used in ternary systems. 118

5.9 Comparison of predicted and experimental bubble point data for ternary systems. 121

5.10 Comparison of calculated and experimental bubble point data for some binary systems - using modified shape factors. 123

List of Figures

page

Chapter 2

2.1 Intermolecular potentials for two substances. 15
2.2 Structure of the PREPROP thermodynamic package. 26
2.3 Flow diagram for dew point temperature calculation. 28
2.4 Comparison of calculated and experimental results for HCl. 36
2.5 Computation times for dew/bubble point calculations. 38
2.6 Proportion of time spent on parts of dew/bubble point calculations. 38
2.7 Vapour-liquid equilibrium in the nitrogen-methane system at 171 K. 40
2.8 Dew point locus for a methane-heptane mixture. 40
2.9 Isotherms of an equation of state. 42
2.10 Difference in calculated temperature due to change in reference equation. 44
2.11 Number of theoretical plates required in distillation of an oxygen-argon mixture. 47

Chapter 3

3.1 Lines of constant Z and F for methane. 56
3.2 Isotherms for methane equation C. 62
3.3 Isotherms for equation D 62
3.4 Isotherms for equation E. 67

Chapter 4

4.1 Infeasible steps. 81
4.2 Flash process. 85
4.3 Allocation function and derivative. 94

Chapter 5

5.1 Dew point compositions for methane-heptane mixtures. 111
5.2 Experimental and predicted vapour-liquid equilibria for a methane-hydrogen mixture. 114
5.3 Vapour-liquid equilibrium in the hydrogen-methane system. 119
5.4 Dew points for hydrogen-propane mixtures. 120

Principal Symbols

A	Helmholtz free energy
C	heat capacity
c	number of components
F	fugacity/pressure ratio
f	corresponding states parameter for energy
fug	fugacity
G	Gibbs free energy
H	enthalpy
h	corresponding states parameter for volume
k	Boltzmann constant
N	number of molecules
n	number of moles
P	pressure
Q	canonical ensemble partition function
R	molar gas constant
r	molecular position
S	entropy
T	temperature
U	intermolecular potential, internal energy
V	volume
x	mole fraction in liquid phase
y	mole fraction in vapour phase
Z	compressibility factor
ε	vapour fraction
η	binary interaction parameter for volume
θ	temperature shape factor
μ	chemical potential
ξ	binary interaction parameter for energy
ρ	density
ϕ	volume shape factor
ω	acentric factor

Superscripts

c	critical
mol	molecular
L	liquid
pg	perfect gas
R	reduced
res	residual
V	vapour
σ	saturation state
'	configurational

Subscripts

i,j,k,ℓ	Component identifiers
x	equivalent substance
o	reference substance

CHAPTER 1

Introduction

A knowledge of thermodynamic properties is a fundamental requirement of all design activities in the chemical industry. Ideally, the designer would prefer to use correlations based on accurate experimental measurements of the property concerned but even for pure substances these are not always available. When one considers the number of possible binary and multicomponent systems of interest to the chemical industry one immediately realizes that it is not practicable to carry out measurements on all of them. Methods of predicting and correlating thermodynamic properties are both, therefore, of great importance and their use has become routine, particularly in computer aided design procedures.

In preliminary design calculations or feasibility studies, done by hand, a relatively small quantity of data of limited accuracy may be sufficient. But a flow-sheeting or simulation programme will require a large quantity of data and the data source must be automatic. The cost of data in terms of computing resources (and hence money) now becomes important - simulation of a chemical plant will typically require many thousands of property evaluations. The user will wish to choose the data source and level of approximation used as appropriate to the problem.

The requirements of both types of usage may be satisfied by a computerised thermodynamic package and this thesis is directed towards such an approach. For convenience, the collection of routines which perform the thermodynamic calculations can be divided from the routines which provide the interface with the user. An interactive system (based on a telex terminal or visual display unit) can be a simple and quick way of obtaining a few data points. A sophisticated, and necessarily complex, interactive interface is needed to make such a system easy to use and reliable. The interface with a design programme is relatively simple but, in addition to being reliable, the main thermodynamics routines must be fast.

Data from computers present the intrinsic danger that they may be accepted without proper scrutiny. In the case of a design package even obviously incorrect values may not be detected unless the programme fails. Some means of assessing the quality of data should be provided, and a distinction must be made between a complete failure giving no sensible values and a case where a result is obtained, but to fewer decimal places than originally specified.

The thermodynamic properties of most interest to engineers are the enthalpy and phase equilibrium of mixtures. The latter is entirely determined by departures from perfect gas behaviour and is by far the more difficult to predict. Methods for predicting vapour-liquid equilibrium may be grouped into three categories and each one is discussed below.

Methods based on equations of state use a single equation to calculate component fugacities in both phases. The first equation to gain wide use among chemical engineers was the Redlich-Kwong {1.1}

$$P = \frac{RT}{v - b} - \frac{a}{T^{\frac{1}{2}} v(v + b)} \qquad (1.1)$$

This simple equation with two adjustable parameters is of limited accuracy, particularly in representing the volumetric properties of the liquid phase. To use this equation for mixtures one requires some combining rules for the coefficients a and b. The problem of finding mixing rules is common to all equations of state as applied to mixtures. It is customary to use the following rules for the Redlich-Kwong parameters

$$\left.\begin{aligned} a &= \sum_i \sum_j x_i x_j a_{ij} \\ b &= \sum_i x_i b_i \end{aligned}\right\} \qquad (1.2)$$

Better accuracy, but at the expense of increased complexity, is provided by the well known equation of Benedict, Webb, and Rubin {1.2}. The B.W.R. equation predicts volumetric properties of both phases

reasonably well but there is now the problem of how to determine the eight constants for each substance. A large quantity of experimental data is required to fix eight constants uniquely. Finding mixing rules for all the constants is now a real problem and the only solution is a trial and error strategy trying all likely combinations. This has, of course, been done for the B.W.R. equation and even for the twenty constant Bender equation {1.3} which is an extended form of the B.W.R. Very accurate results are possible for mixtures provided the constants for the pure components are all evaluated from the same type of data covering similar ranges of temperature and pressure. However, the number of substances for which there are enough data to fix the constants in these equations is small.

The second class of methods take as their starting point the fundamental equation for phase equilibrium

$$fug_i^V = fug_i^L \qquad (1.2)$$

and write this as

$$fug_i^V = \gamma_i^{(P^+)} x_i fug_i^{o(P^+)} \exp\left(\int_{P^+}^{P} \frac{\bar{v}_i dP}{RT}\right) \qquad (1.3)$$

where $\gamma_i^{(P^+)}$ is the activity coefficient at system temperature T and reference pressure P^+ and $fug_i^{o(P^+)}$ is the fugacity of component i in some standard state at the reference pressure P^+ and temperature T. The exponential term is usually called the Poynting correction and involves the partial molar volume $\bar{v}_i$. Separate correlations can be used for each term in equation (1.3).

It is usual to calculate the vapour phase fugacity from an equation of state. The equation need only be applicable in the gas phase and at low to moderate pressures reasonable fugacities can be obtained from the virial equation or the Redlich-Kwong equation.

A great number of empirical equations have been used to represent liquid phase activities. One of the more successful equations is that due to Wilson {1.4}. According to this equation the activity coefficient

for a component in a binary mixture is given by

$$\ln \gamma_1 = -\ln(x_1 + \Lambda_{12}\, x_2) + x_2\left[\frac{\Lambda_{12}}{x_1 + \Lambda_{12}\, x_2} - \frac{\Lambda_{21}}{\Lambda_{21}x_1 + x_2}\right] \qquad (1.4)$$

In Wilson's derivation the two adjustable parameters Λ_{12} and Λ_{21} are related to pure component molar volumes and characteristic energy differences by

$$\left.\begin{aligned} \Lambda_{12} &= \frac{v_2}{v_1}\ \exp\left[\frac{-(\lambda_{12} - \lambda_{11})}{RT}\right] \\ \Lambda_{21} &= \frac{v_1}{v_2}\ \exp\left[\frac{-(\lambda_{12} - \lambda_{22})}{RT}\right] \end{aligned}\right\} \qquad (1.5)$$

Practice differs over which set of parameters, Λ_{12} and Λ_{21} or $(\lambda_{12} - \lambda_{11})$ and $(\lambda_{12} - \lambda_{22})$, is fitted to experimental data. It is found that the energy differences in equations (1.5) can be treated as constants only over small temperature intervals, making extrapolation difficult. The main disadvantage of the Wilson equation is that it cannot predict immiscibility. Renon's NRTL equation {1.5} is of a similar form to the Wilson equation but has an extra adjustable parameter which also makes it applicable to partially miscible systems. Both equations may be generalised to multicomponent mixtures with no extra parameters.

The Poynting correction may be treated in a variety of ways. Very often it is completely neglected and at low pressures the error introduced is small. At higher pressures the correction must be included. The molar volume of the pure component is frequently substituted for the partial molar volume and is assumed constant over the pressure interval.

The remaining term is the fugacity of the standard state. It is convenient to take this as the fugacity of the pure liquid at the system temperature and reference pressure. In principle this fugacity can be calculated from an equation of state for the pure component in the vapour phase. If a component in the liquid is above its critical

temperature then standard state fugacities, as defined above, cannot be obtained. In such cases different standard states must be used for different components and the whole procedure becomes very complex.

The equation of state approach and the hybrid method for calculating vapour-liquid equilibrium are both highly empirical. They are widely used but contain many parameters which must be evaluated by fitting experimental data for pure components and mixtures. The methods work well provided they are not extrapolated beyond the temperature and pressure range of the data originally used in determining the parameters. They are particularly useful in correlating existing data and may be predictive when applied to multicomponent systems.

Theoretical methods based on statistical thermodynamics form the third class. Only the corresponding states principle has gained wide use by chemical engineers. Although the principle dates back to the time of van der Waals its theoretical foundation was first established by Pitzer {1.6} in 1931. He showed that any two parameter intermolecular potential of the form

$$U = \varepsilon f\left(\frac{r}{\sigma}\right) \qquad (1.6)$$

(where r is the distance between two molecules, ε is an energy parameter, and σ a distance parameter) the compressibility factor is a universal function of reduced temperature and volume

$$Z = Z\,(T^R, V^R) \qquad (1.7)$$

Equation (1.7) only holds rigorously for spherical, or near spherical, molecules such as argon and methane. Rowlinson {1.7} showed that equation (1.6) also applies to molecules with angle-dependent potentials but the parameters must now be considered functions of temperature. The deviation from "simple fluid" behaviour is monotonic and can be shown to have the effect of lowering the vapour-pressure of substances with non-spherical molecules. Pitzer used this fact to define his acentric factor ω, which characterises departures from the simple corresponding states principle embodied in equation (1.7). The extended

principle is often used in the form

$$Z = Z^{o}(P^{R},T^{R}) + \omega Z^{1}(P^{R},T^{R}) \qquad (1.8)$$

where Z^{o} is a simple fluid term and Z^{1} a deviation term - both are available in the form of charts.

Theoretically based methods are not yet sufficiently developed to deal with all the systems of industrial interest. It is true, however, that progress in *prediction* can only be made with methods soundly based on theory. This work is concerned with the corresponding states principle and its use as a practical method in process design.

The criteria by which any method must be judged, from a practical point of view, are accuracy, reliability, computational efficiency, ease of use, and range of applicability. The work in this thesis is addressed to all of these aspects. In the following chapter the statistical mechanical basis of the corresponding states principle is described together with its practical implementation in a thermodynamic package. The time required for a corresponding states calculation has been reduced to a point where it is comparable with the times for simple empirical procedures. This is achieved through the use of efficient numerical methods and by replacing some iterative calculations with analytic solutions. A new method is introduced for solving flash problems by applying a minimization algorithm to appropriate energy functions.

An equation of state for a reference substance is a basic feature of the modern corresponding states principle. A highly accurate equation is required but these tend to be complex and behave wildly outside their range of validity. Some new equations of state for methane have been devloped to overcome this problem and to extend the range of applicability to high temperatures. Using these equations it is possible to include hydrogen in a corresponding states treatment by fitting pseudo-critical parameters to the experimental data. Predictions for hydrogen-containing mixtures are compared with a wide range of experimental data.

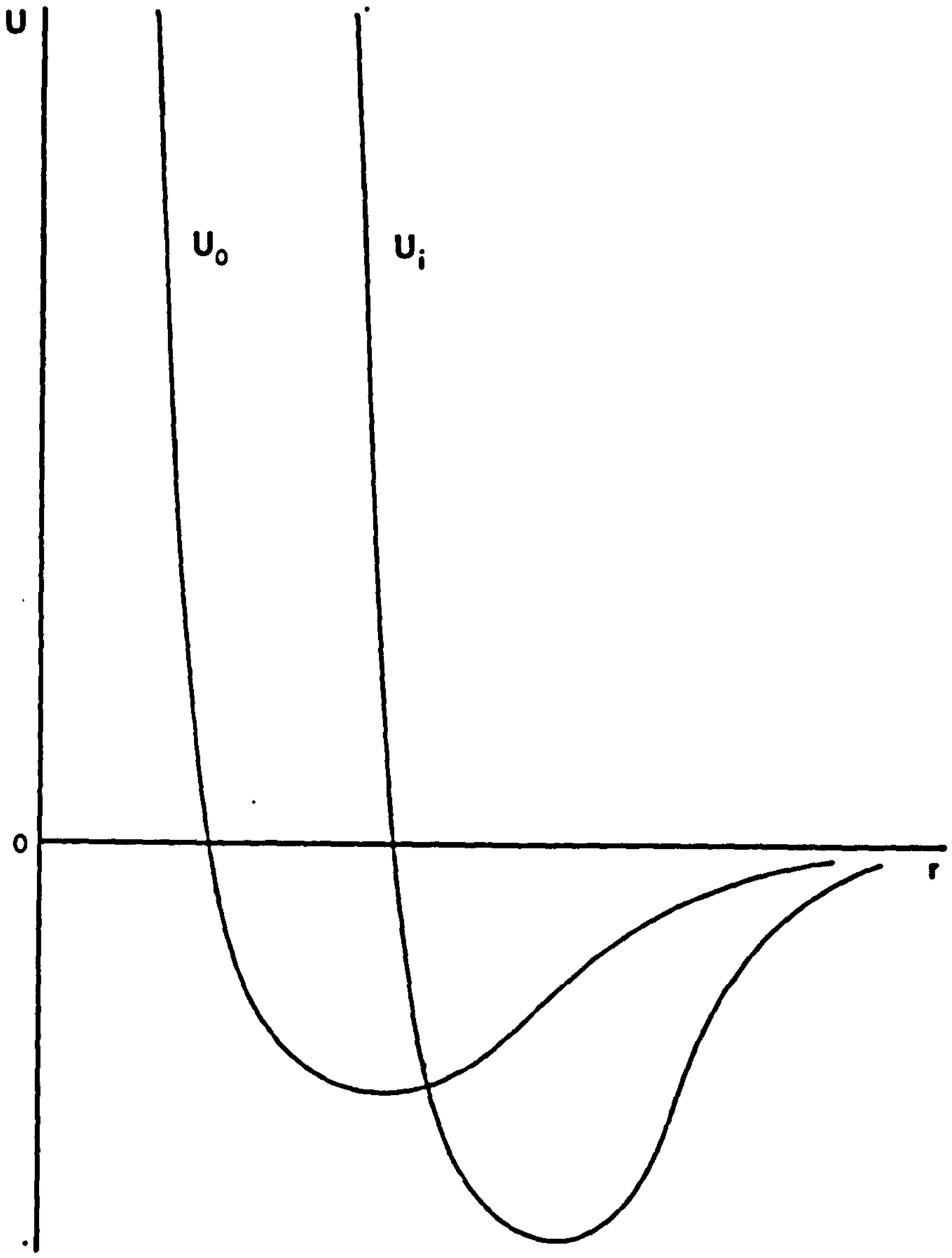


Figure 2.1 Intermolecular potentials for two substances

CHAPTER 2

The Principle of Corresponding States - Theory and Application

2.1 Theoretical Background

The thermodynamic properties of a system containing fixed amounts of substances at given volume and temperature can be calculated from the canonical ensemble partition function. The Helmholtz free energy is related to the partition function by

$$A = -kT \ln Q \qquad (2.1)$$

and the other thermodynamic properties may be calculated from the free energy. The partition function may be factorised into a molecular part, which depends only on the nature of individual molecules, and a configurational part, which depends on interactions between molecules:

$$Q = Q^{mol}\, Q' \qquad (2.2)$$

2.1.1 Simple Molecules

For a pure substance made up of spherical molecules the configurational integral may be written as

$$Q' = \frac{1}{N!} \int_V \cdots \int e^{-U/kT}\, d\underline{r}_1 \,\ldots.\, d\underline{r}_N \qquad (2.3)$$

where U is the potential energy of the configuration due to intermolecular forces, and $\underline{r}_i$ is the position vector of molecule i. This integral is difficult to evaluate in practice but for simple molecules the intermolecular potentials are similar and the variation between substances may be characterised by a few parameters.

Two hypothetical pair potentials are shown in Figure 2.1. We assume these may be scaled by an energy factor f_{ii}, and a distance factor $h_{ii}^{1/3}$, in order to superimpose the two curves. Substances for which this scaling is possible are said to be conformal. Extending this argument to the more general potential, $U(\underline{r}_1, \underline{r}_2, \ldots., \underline{r}_N)$, which depends on all

interactions we have

$$\frac{U_i[(\underline{r}_i)_1, \ldots, (\underline{r}_i)_N]}{f_{ii}} = U_o[(\underline{r}_o)_1, \ldots, (\underline{r}_o)_N] \qquad (2.4)$$

and

$$(\underline{r}_o) = (\underline{r}_i)/h_{ii}^{1/3} \qquad (2.5)$$

Substituting into equation (2.3) for the configurational integral gives

$$Q_i'(V,T) = \frac{1}{N!}\int_V \cdots \int \exp\left[\frac{-U_i[(\underline{r}_i)_1, \ldots, (\underline{r}_i)_N]}{k(T/f_{ii})}\right] d(\underline{r}_i)_1 \ldots, d(\underline{r}_i)_N$$

$$Q_o'\left(\frac{V}{h_{ii}}, \frac{T}{f_{ii}}\right) = \frac{1}{N!}\int_{\left(\frac{V}{h_{ii}}\right)} \cdots \int \exp\left[\frac{-U_o[(\underline{r}_o)_1, \ldots, (\underline{r}_o)_N]}{k(T/f_{ii})}\right] d(\underline{r}_o)_1 \ldots d(\underline{r}_o)_N$$

Differentiating equation (2.5)

$$d(\underline{r}_i) = h_{ii}\, d(\underline{r})_o$$

and hence

$$Q_i'(V,T) = h_{ii}^N\, Q_o'\,(V/h_{ii}, T/f_{ii}) \qquad (2.6)$$

From equations (2.1), (2.2) and (2.6) the configurational Helmholtz free energy of the substance i is

$$A_i'(V,T) = f_{ii} A_o'(V/h_{ii}, T/f_{ii}) - NkT \ln h_{ii} \qquad (2.7)$$

Equation (2.7) allows the configurational properties of substance i to be calculated from a knowledge of the properties of substance o, the "reference" substance.

In practice this is not the most convenient way of expressing the relationship. It is more useful to work in terms of the residual properties rather than the configurational properties. The residual part of any property, X^{res}, is here defined as the difference between the total property and value in the perfect gas state at the same volume and temperature,

$$X^{res} = X - X^{pg} \tag{2.8}$$

The intermolecular potential for the perfect gas is zero and hence the configurational integral in equation (2.3) becomes

$$Q' = V^N/N!$$

It follows that

$$A^{pg} = A^{mol} + NkT\ (\ln\ (N/V) - 1),$$

$$A^{res} = A' - NkT\ (\ln\ (N/V) - 1),$$

and $$A_i^{res} = f_{ii}\ A_o^{res}\ (V/h_{ii}, T/f_{ii}) \tag{2.9}$$

The residual Helmholtz free energy may be related to the equation of state by

$$P = -\left(\frac{\partial A}{\partial V}\right)_T = \rho^2 \left(\frac{\partial A}{\partial \rho}\right)_T$$

therefore

$$A = \int_0^\rho P\ \frac{d\rho}{\rho^2} \qquad \text{at constant temperature.}$$

For a perfect gas,

$$A^{pg} = \int_0^\rho \rho RT\ \frac{d\rho}{\rho^2}$$

hence

$$A^{res}(\rho, T) = \int_0^\rho (P - \rho RT)\ \frac{d\rho}{\rho^2} \tag{2.10}$$

The other residual properties may be related to those of the reference substance by ordinary thermodynamic manipulations:

$$\left.\begin{aligned}
&\text{internal energy,} && U_i^{res}(V,T) = f_{ii}U_o^{res}(V/h_{ii},T/f_{ii}) \\
&\text{entropy,} && S_i^{res}(V,T) = S_o^{res}(V/h_{ii},T/f_{ii}) \\
&\text{enthalpy,} && H_i^{res}(V,T) = f_{ii}H_o^{res}(V/h_{ii},T/f_{ii}) \\
&\text{pressure} && P_i(V,T) = (f_{ii}/h_{ii})P_o(V/h_{ii},T/f_{ii}) \\
&\text{fugacity,} && fug_i(V,T) = (f_{ii}/h_{ii})fug_o(V/h_{ii},T/f_{ii})
\end{aligned}\right\} \quad (2.11)$$

and in terms of the equation of state the residual properties are:

$$\left.\begin{aligned}
U^{res}(\rho,T) &= \int_0^\rho \left[P - T\left(\frac{\partial P}{\partial T}\right)_\rho\right] \frac{d\rho}{\rho^2} \\
S^{res}(\rho,T) &= \int_0^\rho \left[R\rho - \left(\frac{\partial P}{\partial T}\right)_\rho\right] \frac{d\rho}{\rho^2} \\
H^{res}(\rho,T) &= U^{res}(\rho,T) + P/\rho - RT \\
\ln\left[\frac{fug(\rho,T)}{P}\right] &= \ln\left(\frac{RT\rho}{P}\right) + \frac{P}{\rho RT} - 1 + \frac{A^{res}(\rho,T)}{RT}
\end{aligned}\right\} \quad (2.12)$$

2.1.2 Non-spherical Molecules and Mixtures

For non-spherical molecules the potential energy of the system will depend on the orientations of the molecules as well as their positions. If it is assumed that the potential is a sum of pair interactions between molecules, i.e.

$$U = \sum_{j>i} \sum U_{ij} \quad (2.13)$$

then it is possible to derive an approximate expression for the configurational integral {2.1},

$$Q' = \frac{1}{N!} \int \cdots \int \exp\left(\frac{-U^*}{kT}\right) d\underline{r}_1 \cdots d\underline{r}_N \quad (2.14)$$

The angle-averaged potential, U* in equation (2.14), is a function of temperature. If it is assumed to be conformal with the reference substance then equation (2.9) still applies but the parameters h_{ii} and f_{ii} are now functions of temperature.

For mixtures the problems are greater since the potential will depend not only on positions of molecules but also on the assignment of molecules by species to these positions. In *one fluid* models of mixtures it is assumed that the potential energy of the mixture may be replaced by a position averaged potential, which is the same for all components i.e. the potential of a hypothetical equivalent substance.

Equation (2.3) may be generalised to give the configurational integral of a mixture of spherical molecules interacting with a common potential U_x

$$Q' = \frac{1}{\prod_{i=1}^{c} N_i!} \int \cdots \int \exp\left(\frac{-U_x}{kT}\right) d\underline{r}_1 \cdots d\underline{r}_N \qquad (2.15)$$

where $N = \sum_{i=1}^{c} N_i$

Writing this in terms of the configurational integral for N molecules of the equivalent substance x gives

$$Q' = \frac{N!}{\prod_{i=1}^{c} N_i!} Q'_x \qquad (2.16)$$

The configurational Helmholtz free energy follows from equation (2.1)

$$A' = A'_x + NkT \sum_{i=1}^{c} x_i \ln x_i \qquad (2.17)$$

where $x_i = N_i/N$.

Using the one fluid model all the configurational properties of the mixture may be calculated from equations (2.17) and (2.7). There remains

the problem of finding corresponding states parameters f_x and h_x, replacing f_{ii} and h_{ii} in equation (2.7), which relate the properties of the equivalent substance to those of the reference substance.

2.1.3 Corresponding States Parameters

For conformal pure substances with spherical molecules the parameters are constants by definition. In particular the substances must correspond at the critical point, hence from the pressure relation in equation (2.11)

$$\left.\begin{aligned} V_i^c &= h_{ii}\, V_o^c \\ T_i^c &= f_{ii}\, T_o^c \end{aligned}\right\} \qquad (2.18)$$

In the case of non-spherical molecules the parameters are functions of temperature. The corresponding states to which the parameters refer may be defined by any two of equations (2.11). Following Rowlinson and Watson {2.2} we use

$$\left.\begin{aligned} Z_i(V,T) &= Z_o(V/h_{ii}, T/f_{ii}) \\ \text{and} \quad A_i'(V,T) &= f_{ii} A_o'(V/h_{ii}, T/f_{ii}) - NkT \ln h_{ii} \end{aligned}\right\} \qquad (2.19)$$

Leach et al. {2.3} introduced *molecular shape factors*, θ and ϕ, defined by

$$\left.\begin{aligned} f_{ii} &= \left(\frac{T_i^c}{T_o^c}\right) \theta_i\, (V_i^R, T_i^R) \\ \text{and} \quad h_{ii} &= \left(\frac{V_i^c}{V_o^c}\right) \phi_i\, (V_i^R, T_i^R) \end{aligned}\right\}, \qquad (2.20)$$

They produced a correlation for the shape factors by solving equations equivalent to (2.19) using experimental data for hydrocarbons:

$$\left.\begin{aligned}
\theta_i &= 1 + (\omega_i - \omega_o)\,[0.0892 - 0.8493\ \ln T_i^R \\
&\qquad + (0.3063 - 0.4506/T_i^R)(V_i^R - 0.5)] \\
\phi_i &= \left(\frac{Z_o^c}{Z_i^c}\right)\{1 + (\omega_i - \omega_o)\,[0.3903\ (V_i^R - 1.0177) \\
&\qquad - 0.9462\ (V_i^R - 0.7663)\ \ln T_i^R]\}
\end{aligned}\right\} \qquad (2.21)$$

where $T_i^R = T/T_i^c$ and $V_i^R = V/V_i^c$ for pure components. The reduced temperatures and volumes are restricted to $T_i^R < 2.0$ and $0.5 < V_i^R < 2.0$, values outside these ranges are set to the limits. The acentric factor characterises departures from sphericity and is defined by

$$\omega = -1.0 - \log_{10}(P^\sigma/P^c) \qquad (2.22)$$

(at $T^R = 0.7$)

In mixtures there is the further complication that the parameters for the hypothetical equivalent substance, f_x and h_x, are also functions of composition. The theoretical justification for the van der Waals one-fluid model of mixtures is discussed by Leland et al. {2.4}. In terms of this model the corresponding states parameters for the equivalent substance are

$$\left.\begin{aligned}
h_x &= \sum_i \sum_j x_i\, x_j\, h_{ij} \\
f_x &= \frac{\sum_i \sum_j x_i\, x_j\, f_{ij}\, h_{ij}}{h_x}
\end{aligned}\right\} \qquad (2.23)$$

In equations (2.23) terms like h_{ii} and f_{ii} are obviously pure component parameters but for unlike interactions, where $i \neq j$, combining rules are necessary. It is common to write

$$f_{ij} = \xi_{ij} \, (f_{ii} \, f_{jj})^{1/2}$$

$$\text{and} \quad h_{ij} = \eta_{ij} \left(\frac{h_{ii}^{1/3}}{2} + \frac{h_{jj}^{1/3}}{2} \right)^3 \qquad \Bigg\} \quad (2.24)$$

The binary interaction parameters ξ_{ij} and η_{ij} are constants, usually close to unity, which must be determined from experimental data on binary systems.

For mixtures Leach et al. {2.3} show that the equations

$$T_i^R = \frac{\theta_i \, T}{T_o^c \, f_x}$$

$$\text{and} \quad V_i^R = \frac{\phi_i \, V}{V_o^c \, h_x} \qquad \Bigg\} \quad (2.25)$$

are consistent with the requirement that calculated mixture properties are invariant when the reference substance is changed. Equations (2.25) must be used together with equations (2.20) and (2.21) to calculate the corresponding states parameters in equations (2.23) and (2.24).

2.1.4 Thermodynamic Properties of Mixtures of non-spherical molecules

From the definition of corresponding states in equations (2.19) we have

$$Z(V,T,x) = Z_o(V_o,T_o)$$

$$A^{res}(V,T,x) = f_x A_o^{res}(V_o,T_o) \qquad (2.26)$$

$$V_o = V/h_x \quad , \quad T_o = T/f_x$$

Equations for the fugacity of a component in a mixture and for the internal energy are derived by Gunning {2.5}, the enthalpy and entropy

follow immediately since H = U + PV and A = U - TS. The results used in this work are summarised below:

$$RT \ln\left[\frac{fug_i(V,T,x)}{x_i fug_x(V,T,x)}\right] = U_o^{res}(V_o,T_o)\ \Delta_i f_x$$

$$+ \frac{RT}{h_x}\left[Z_o(V_o,T_o) - 1\right]\ \Delta_i h_x \qquad (2.27)$$

$$fug_x(V,T,x) = \left(\frac{f_x}{h_x}\right) fug_o(V_o,T_o) \qquad (2.28)$$

$$H_x^{res} = f_x H_o^{res}(V_o,T_o) - TU_o^{res}(V_o,T_o)\left(\frac{\partial f_x}{\partial T}\right)_V$$

$$- \frac{RT^2}{h_x}(Z_o - 1)\left(\frac{\partial h_x}{\partial T}\right)_V \qquad (2.29)$$

$$S_x^{res} = S_o^{res}(V_o,T_o) - U_o^{res}(V_o,T_o)\left(\frac{\partial f_x}{\partial T}\right)_V$$

$$- RT(Z_o - 1)\left(\frac{\partial h_x}{\partial T}\right)_V \qquad (2.30)$$

where Δ_i is the differential operator

$$\left(\frac{D}{Dx_i} - \sum_{j=1}^{c} x_j \frac{D}{Dx_j}\right)_{V,T}$$

and (D/Dx_i) denotes differentiation with respect to x_i in which all other mole fractions are treated as independent variables.

The total mixture properties follow from equations (2.8) and (2.17)

$$\left.\begin{aligned} A &= \sum_{i=1}^{c} x_i A_i^{pg} + RT \sum_{i=1}^{c} x_i \ln x_i + A_x^{res} \\ H &= \sum_{i=1}^{c} x_i H_i^{pg} + H_x^{res} \\ S &= \sum_{i=1}^{c} x_i S_i^{pg} - R \sum_{i=1}^{c} x_i \ln x_i + S_x^{res} \end{aligned}\right\} \quad (2.31)$$

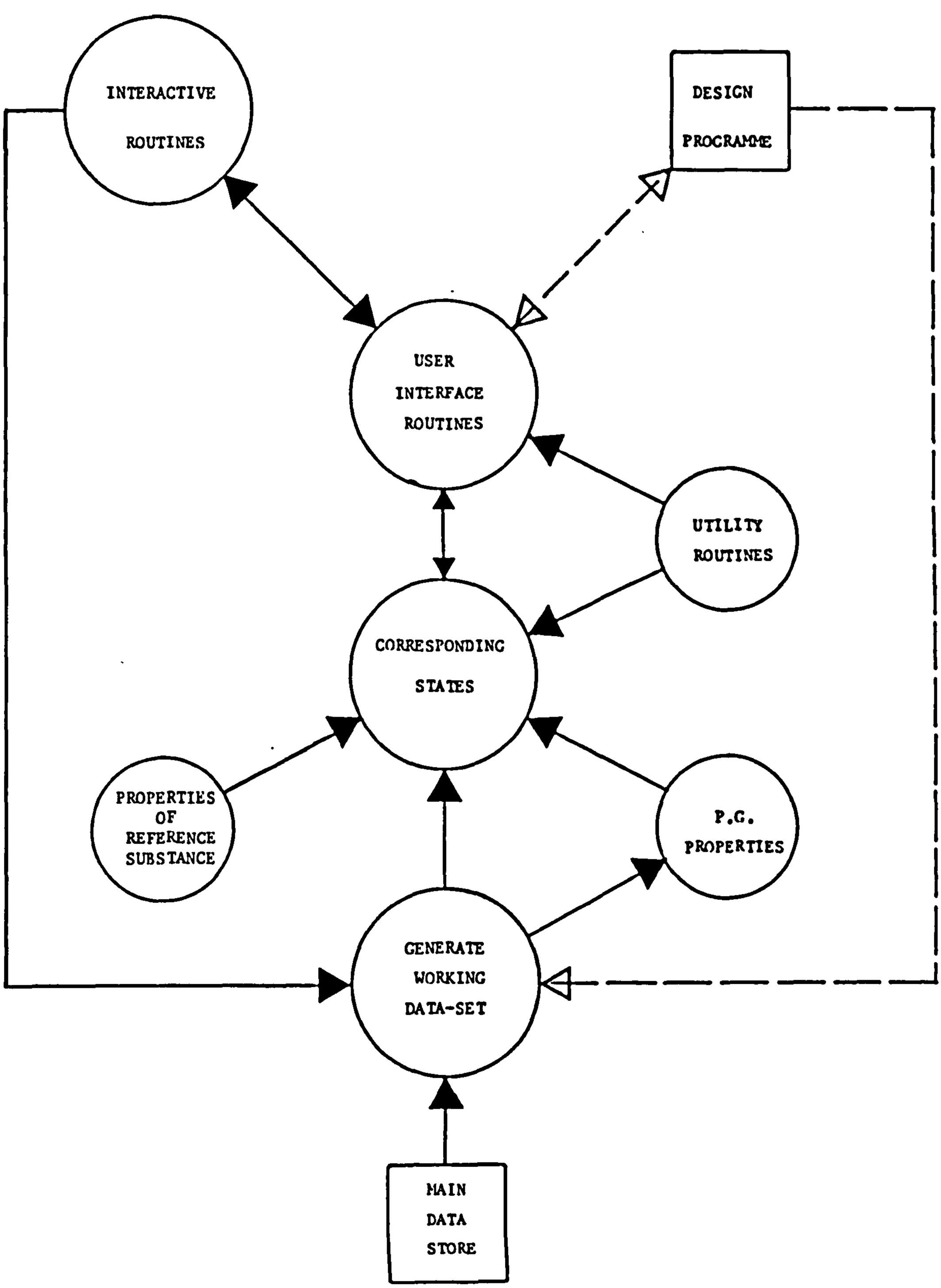
Thermodynamic properties in the perfect gas state can be calculated accurately by the methods of statistical mechanics. Equations for the perfect gas heat capacity as a function of temperature are often available and hence we can easily calculate the entropy and enthalpy using the equations

$$\left.\begin{aligned} S^{pg}_{(\rho,T)} &= \int_{T^+}^{T} \frac{C_p^o}{T} dT + R \ln\left(\frac{P^+}{\rho RT}\right) + S^+ \\ H^{pg}(T) &= \int_{T^+}^{T} C_p^o \, dT + H^+ \end{aligned}\right\} \quad (2.32)$$

where P^+ and T^+ are standard conditions, S^+ and H^+ are arbitrary constants.

Equation (2.20) to (2.32) together with (2.12) form a complete statement of how the properties of a mixture may be calculated using the corresponding states principle. The method requires an equation of state for a reference substance and shape factor equations. For each component we need an equation for the perfect gas heat capacity and must know the critical properties, acentric factor, and binary interaction parameters.

Figure 2.2 Structure of the PREPROP thermodynamic package



2.2 A Computer Package for the Prediction of Thermodynamic Properties

2.2.1 Introduction

The package described here is based on the corresponding states principle. It has been developed both as a research tool and a practical implementation of theory - with full consideration of reliability, robustness, range of applicability, and computational efficiency. The package as a whole has acquired the name PREPROP but in fact the structure is highly modular. The basic components and their interconnections are illustrated in Figure 2.2.

Listings of the FORTRAN code are included (on microfiche) in Appendix A. A comprehensive introduction forms the first part of the package and the routines themselves are fully documented and self-explanatory. The remainder of this section will discuss the strategy and features of the main components of the package.

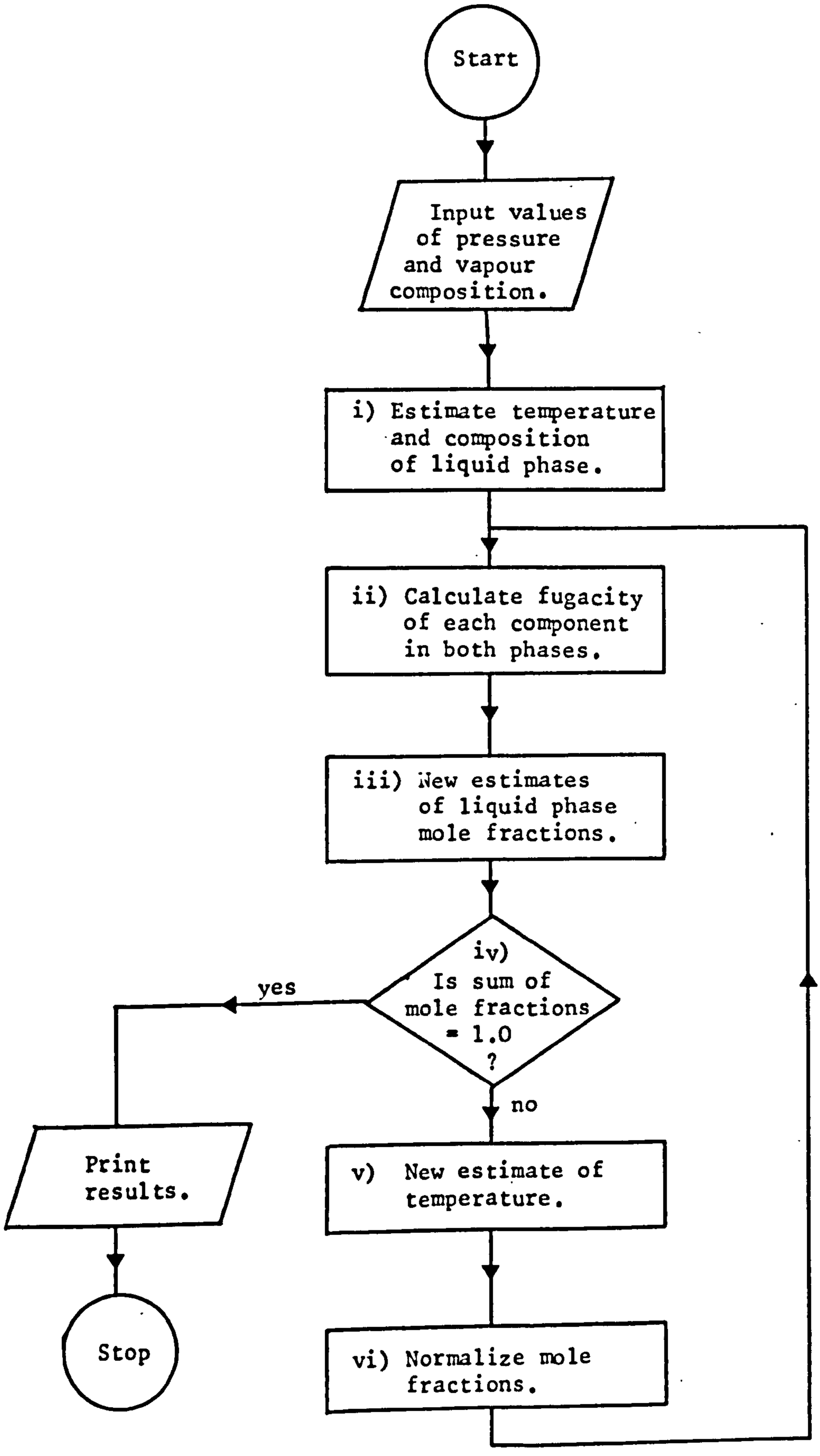
2.2.2 Interactive Operation

Interactive computing, from the point of view of the user of thermodynamic data, has already been mentioned in Chapter 1. For development purposes it provides rapid and simple means for testing and error detection, particularly in complex programmes such as PREPROP.

The interactive routines may be divided into two groups. The first contains the main executive routine and also one for writing out an appropriate message to the user when input data are required. The executive assembles the information needed to solve a problem, calls the thermodynamics routines, and writes out the results. The second group deals with input operations. The user may enter any number of numeric and/or character data on each line of input. Lines are decoded and the information passed to the executive.

Operation of the interactive system is very flexible. Parts of the problem specification, eg. number of components, may be changed at any time. Help is provided for users unfamiliar with the system, lists of commands, codes for substances, etc., may be displayed. The most important aid to research, and also to programme development, is the ability to selectively activate WRITE statements in many of the thermodynamics routines. If a calculation fails, extra information is

Figure 2.3 Flow diagram for dew point temperature calculation



immediately available and usually allows the problem to be identified - whether it be fundamental or merely a programming error.

The interactive interface not only makes PREPROP simple to use in a general way but also, because of its great flexibility, allows research work to be carried out with maximum effect.

2.2.3 User Level Routines

The routines in this category will solve a complete problem, eg. dew point temperature, provided it is specified in a correct way. The method of solution and the details of the corresponding states procedure do not need to be considered by the user.

A single input/output COMMON block is used for communication with these routines. The number of components, substance identifiers, mole fractions, etc., must be specified and after a successful calculation the results are placed in the block. At no point in the package are user-specified variables changed. If the calculation fails an error flag is set to inform the user and an error code indicates where the failure occurred. Routines are provided for the calculation of total properties (ONEPHS), or excess properties (EXCESS), in a one phase mixture. Routines LIQVAP and DBPRES calculate vapour-liquid equilibrium when pressure or temperature and amount of one phase are specified - including the limiting cases of dew and bubble points. Flash calculations at constant pressure and temperature, enthalpy, or entropy are discussed in detail in Chapter 4.

Dew/Bubble Point Calculations

The algorithm used here differs substantially from that published by Watson and Rowlinson {2.6}. A flow diagram for a dew point temperature calculation is shown in Figure 2.3.

i) First estimates - Raoult's law is used to estimate T and x_i in the same way as for flash calculations (see section 4.5.1).

ii) Calculation of fugacities - this is done at two temperatures, T_o and T_1, to give finite difference derivatives. A temperature increment of 1 K is satisfactory.

iii) New mole fractions are estimated by $x_i(T) = x_i(T) fug_i^V(T)/fug_i^L(T)$, where the superscripts V and L refer to gas and liquid phases respectively. Mole fractions are estimated at T_o and T_1.

iv) If S_o (the sum of mole fractions at T_o) is equal to 1.0, a solution has been found.

v) Otherwise, update the temperature. We assume $\ln S \propto 1/T$, this can be justified by use of Raoult's law

$$P\, y_i = P_i^\sigma\, x_i$$

$$\therefore \quad \Sigma x_i = P\, \Sigma y_i / P_i^\sigma$$

A reasonable representation of the vapour pressure curve is $\ln P_i^\sigma = A_i/T + B_i$, hence

$$\left(\frac{\partial \Sigma x_i}{\partial T}\right) = \frac{P}{T^2} \frac{\Sigma y_i A_i}{P_i^\sigma} = \frac{1}{T^2} \Sigma A_i x_i$$

If $\ln \Sigma x_i = A/T + B$ then $\left(\frac{\partial \Sigma x_i}{\partial T}\right) = \frac{-A}{T^2} \Sigma x_i$. It is reasonable to assume that for real mixtures $\ln \Sigma x_i$ will be closer to linearity in 1/T than Σx_i in T - this is confirmed by experience. If this assumption holds, and taking a temperature increment $T_o - T_1 = 1.0$, then the updating formula is

$$T_{new} = \frac{T_o T_1}{T_o - \frac{\ln(S_1)}{\ln (S_1/S_o)}}$$

vi) The mole fractions must be normalized before returning to step ii).

In the algorithm, as programmed, convergence acceleration is applied at step iii), and in step ii) fugacities are only evaluated at a single temperature once the change in temperature calculated in step v) is small. Watson and Rowlinson repeat steps ii) and iii) until the compositions do not change and then introduce an outer iterative loop to adjust the temperature. Convergence on composition is only important near the final temperature and the single update in step iii) is all that is required. The algorithm used here combines temperature and composition adjustments in one loop. In practice, convergence on the temperature is rapid followed by a few iterations which make small changes to the mole fractions.

Dynamic Accuracy Criteria

In the algorithm given above there are three levels of iterative calculation and each one requires an accuracy criterion to determine convergence. The outermost loop iterates on the sum of mole fractions. Calculation of shape factors in step ii) involves an iteration, and within this is an iterative solution of the equation of state to get the density. There is little point in calculating the density or shape factors very accurately when the sum of mole fractions is far from unity, but better values are required as the outermost iteration converges. The accuracy criteria are varied dynamically throughout the calculation to reflect these considerations. The two inner criteria are tightened as the sum of mole fractions approaches unity.

2.2.4 Corresponding States Routines

The routines described here calculate shape factors, corresponding states parameters, and their derivatives. These are used together with the properties of the reference substance and perfect gas properties to evaluate total mixture properties.

Shape Factors and Corresponding States Parameters - Routine VDW1

The calculation involves equations (2.20), (2.21), and (2.23) - (2.25). An iterative solution is necessary since the reduced temperatures and volumes depend on the shape factors through equations (2.25) and the shape factors are themselves functions of reduced volume and temperature. By initially setting shape factors to unity, $V_i^R = V/V_i^c$, and $T_i^R = T/T_i^c$ the iteration converges rapidly using successive

substitution. Both V_i^R and T_i^R can be iterated upon simultaneously, there is no need for the much longer nested iteration used by Gunning {2.5}. It is much more common for the pressure to be specified rather than the density and hence the equation of state must be solved at each iteration for the shape factors.

The square root and cube root terms in equations (2.24) impose a significant computational penalty when the number of components in a mixture is large. For c components $(c - 1)c/2$ square roots and cube roots must be evaluated for every shape factor iteration. Fortunately, values of h_{ii} and f_{ii} lie in a limited range and fast approximating functions are available {2.7}. Approximations are also used for the logarithmic terms in equations (2.21).

Derivatives of the Corresponding States Parameters

To calculate fugacities from equation (2.27) requires composition derivatives of the corresponding states parameters represented by $\Delta_i f_x$ and $\Delta_i h_x$. The enthalpy and entropy, in equations (2.29) and (2.30), involve temperature derivatives $(\partial h_x/\partial T)_V$ and $(\partial f_x/\partial T)_V$. Differentiation of equations (2.20) - (2.25) gives expressions which are not simple since h_x and f_x depend on the shape factors which are themselves functions of temperature and composition. Watson and Rowlinson {2.6} suggest an iterative scheme but in fact a complete analytic solution is possible. A full derivation of the following equations will be found in Appendix B.

For the composition derivatives we have

$$\left.\begin{aligned} \Delta_i h_x &= A_1 \Delta_i h_x + A_2 \Delta_i f_x - E_i \\ \Delta_i f_x &= B_1 \Delta_i f_x + B_2 \Delta_i h_x - F_i \end{aligned}\right\} \qquad (2.33)$$

where A_1, A_2, B_1, and B_2 are constants for the mixture, independent of the component i. The temperature derivatives give very similar expressions

$$\left.\begin{aligned}\left(\frac{\partial h_x}{\partial T}\right) &= A_1 \left(\frac{\partial h_x}{\partial T}\right) + A_2 \left(\frac{\partial f_x}{\partial T}\right) - C_1 \\ \left(\frac{\partial f_x}{\partial T}\right) &= B_1 \left(\frac{\partial f_x}{\partial T}\right) + B_2 \left(\frac{\partial h_x}{\partial T}\right) - C_2\end{aligned}\right\} \qquad (2.34)$$

where C_1 and C_2 are constants and A_1, A_2, B_1, and B_2 are the same as in equations (2.33). The identical structure of equations (2.33) and (2.34) allows the two sets of derivatives to be conveniently evaluated in parallel with no extra penalty in computation time. The structure is best shown by writing the equations in matrix form

$$\begin{bmatrix} A_1-1 & A_2 \\ B_2 & B_1-1 \end{bmatrix} \begin{bmatrix} \left(\frac{\partial h_x}{\partial T}\right) & \Delta_1 h_x & \Delta_2 h_x & \cdots \\ \left(\frac{\partial f_x}{\partial T}\right) & \Delta_1 f_x & \Delta_2 f_x & \cdots \end{bmatrix} = \begin{bmatrix} C_1 & E_1 & E_2 & \cdots \\ C_2 & F_1 & F_2 & \cdots \end{bmatrix} \qquad (2.35)$$

Although no explicit matrix inversion is necessary the elements of the 2 x 2 inverse are used to solve all the equations. The analytic method is, computationally, very much faster than the iterative procedure; according to one report the gain in speed is a factor of seven {2.8}.

2.2.5 Perfect Gas Properties

Perfect gas enthalpies and entropies are evaluated from equations (2.32) and an equation for the perfect gas heat capacity is required for each substance. Equations found in the literature are of various forms and to directly abstract as many as possible a comprehensive formulation is used for the perfect gas heat capacity,

$$C_p^o = C_1 + C_2 T + C_3 T^2 + C_4 T^3 + C_5 T^4 + C_7 T^6 + C_8/T + C_9/T^2$$

$$+ C_{10}/T^3 + C_{12} T^{1/3} + C_{13} T^{2/3} + \frac{C_{11} u^2 e^u}{(e^u - 1)^2} \qquad (2.36)$$

where $u = c_{14}/T$.

Generally, only a few of these constants are non-zero for any given substance. Equation (2.36) requires fourteen storage locations for each substance - this represents more than twice the storage needed for the rest of the corresponding states procedure (see section 2.2.7). It is suggested, therefore, that later versions of PREPROP should use a simpler equation with the correct limiting behaviour. Thompson {2.9} has published a two constant equation that satisfies this requirement but the accuracy is not high. An ideal equation, with coefficients, clearly still has to be developed.

2.2.6 Properties of the Reference Substance

The choice of reference substance and equation of state is discussed fully in Chapter 3. For the purposes of this section it is assumed that we have a single equation of state, applicable to both gas and liquid phases, and that the equation gives equal fugacities for co-existing phases.

Residual properties of the reference substance are calculated from equations (2.12). The integrals for the residual entropy, residual internal energy, and fugacity are closely related and are most conveniently evaluated in a single routine, SUFREF. The pressure is calculated as a function of density and temperature in routine PREF. The derivative $(\partial P/\partial \rho)_T$ is used in solving the equation of state and is evaluated in routine DPREF.

Data required for the reference substance consist of coefficients for the equation of state, values of the critical parameters, the acentric factor, and a first estimate used in solving for the density of a liquid phase.

2.2.7 Data for Pure Components

The following data are required for each substance included in the package:

critical density, temperature, and compressibility factor,

acentric factor,

coefficients for perfect gas heat capacity equation,

standard state enthalpy and entropy.

This totals 20 storage locations per substance. If the binary interaction

parameters (defined in equation (2.24)) differ from unity and values are available they are stored in sequential form together with an identification code - three storage locations are needed for each binary.

Data from the main storage blocks must be transferred to working arrays for use by the package. Routine GNRATE extracts data for the components of a mixture. It must be the first routine called and must be called again whenever the components are changed.

2.2.8 Utility Routines

The equation of state for the reference substance gives pressure as a function of density and temperature. A non-linear equation solver is required since the pressure, and not the density, is usually specified. The routine provided uses a combination of bisection, the secant method, and Newton's method (as appropriate) to overcome numerical difficulties and ensure very fast convergence.

The flash equilibrium algorithms described in Chapter 4 require a minimisation routine capable of dealing with nonlinear constraints. The Variable Metric Projection method is used for this purpose and details will be found in Chapter 4.

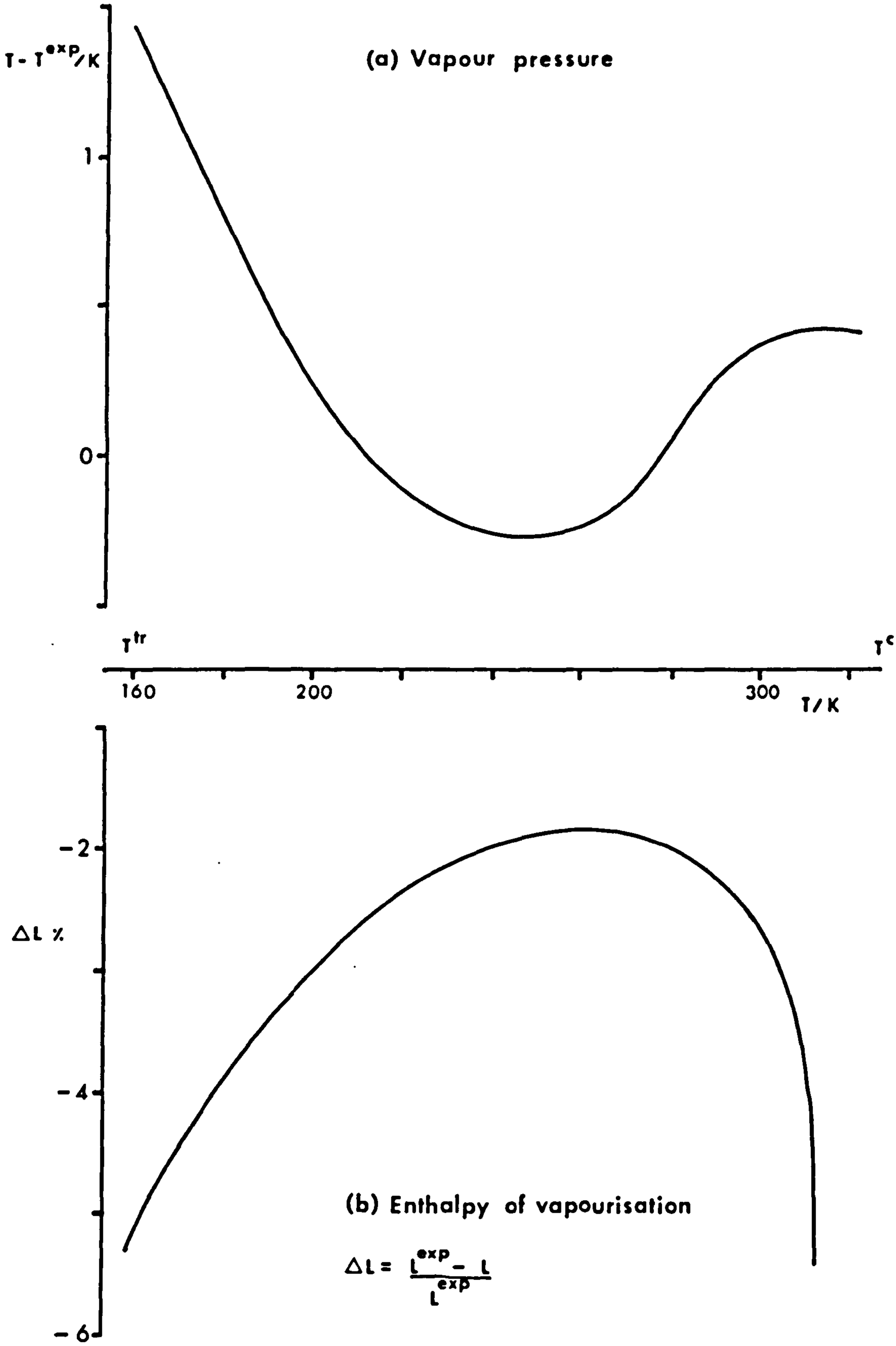
The numerical methods mentioned above are by no means the only ones possible. Suitable library routines should be available at any large computer centre.

2.3 Performance of the PREPROP Thermodynamic Package

2.3.1 Accuracy

The ingredients of the predictive procedure are the reference equation of state, the corresponding states principle, the shape factor equations, and the van der Waals one-fluid theory of mixtures. It is hardly surprising that predictions are worst for mixtures of dissimilar molecules, particularly if some are highly non-spherical. Gunning {2.5} carried out extensive comparisons between experimental data (mainly on hydrocarbon systems) and predictions. The agreement found was generally good except for systems containing carbon dioxide, toluene, and decane. Mollerup {2.10} has examined many liquefied natural gas and related

Figure 2.4 Comparison of calculated and experimental results for HCl {2.24}



(a) Vapour pressure

(b) Enthalpy of vapourisation

$$\Delta L = \frac{L^{exp} - L}{L^{exp}}$$

mixtures and has found excellent agreement between the data and predictions. Although polar substances are usually excluded from the corresponding states principle, Figure 2.4 shows surprisingly good predictions of the vapour pressure and enthalpy of vapourisation for hydrogen chloride. Saville {2.11} has found similar results for acetone and ammonia.

The question of accuracy is intimately connected with the problem of sensitivity, which is considered in more detail in section 2.3.4. It is important to realise that a predictive method which relies on the minimum of input data must be sensitive to that data if it is to be applicable to a wide range of systems. Calculation of vapour-liquid equilibrium in mixtures containing species of widely differing volatility and molecular size is particularly ill conditioned. It is important to have good values of all parameters, including the binary interaction parameters, if meaningful predictions are to be made.

2.3.2 Computation Times

It is widely believed that use of the corresponding states principle is prohibitively expensive in computing time compared with other methods. In industry the use of the principle, in its modern form, is probably confined to areas such as natural gas processing or air separation where the great accuracy is considered worth the extra computer time.

The corresponding states procedure is very complex compared with methods such as the Chao-Seader correlation {2.12} which is embodied in seven simple equations. Considerable progress has been made in reducing the time required for a corresponding states calculation by the techniques described in section 2.2. Table 2.1 compares the times for dew and bubble point calculations using PREPROP and the CHESS implementation of the Chao-Seader correlation {2.13}.

Table 2.1 Comparison of calculation times for the CHESS and PREPROP thermodynamic packages

Pressure/MPa	Calculation Time		PREPROP/CHESS
	Bubble Point		Dew Point
0.1	1.3		1.7
1.0	1.6		2.2
5.0	3.9		3.8

Figure 2.5 Computation times for dew/bubble point calculations

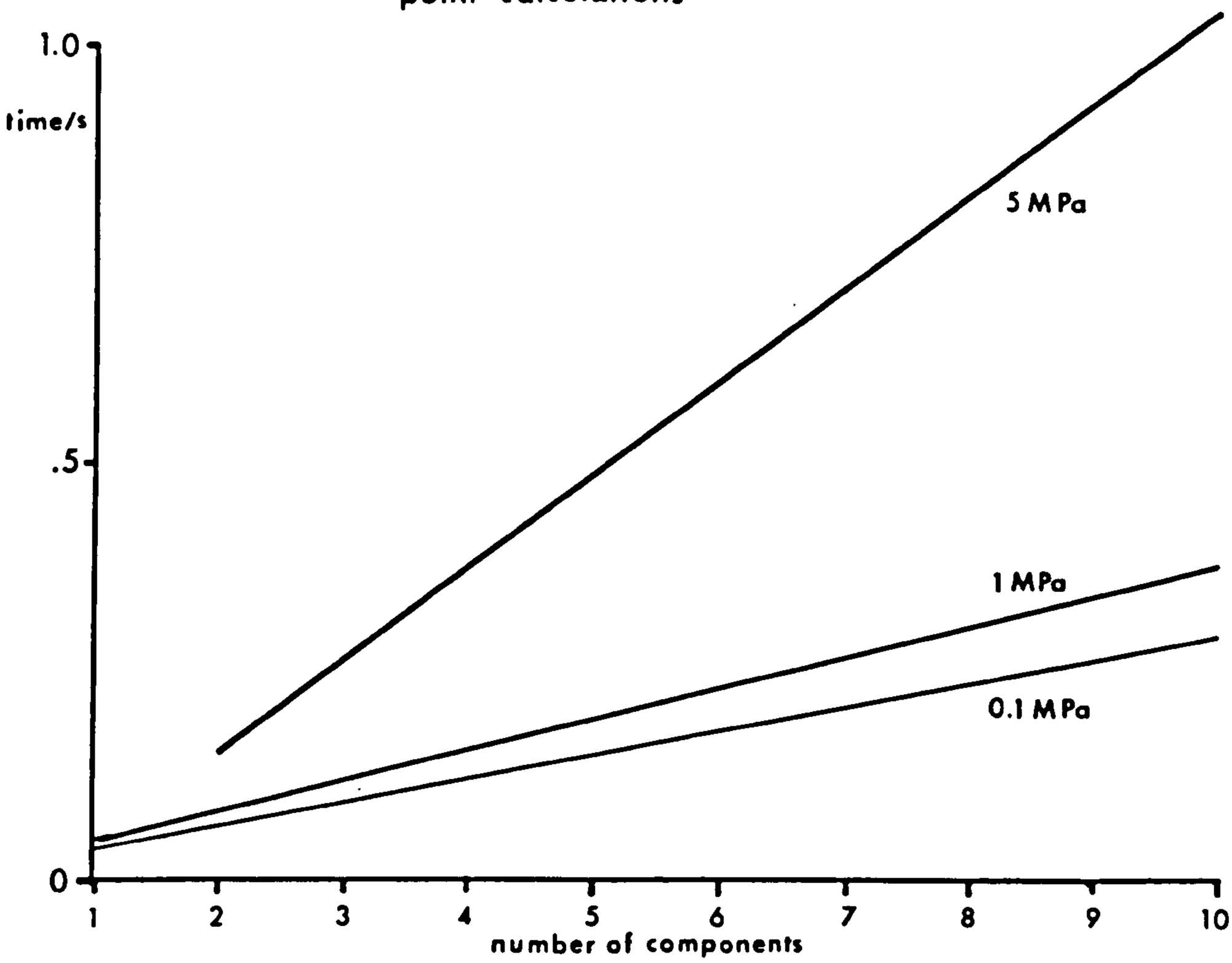
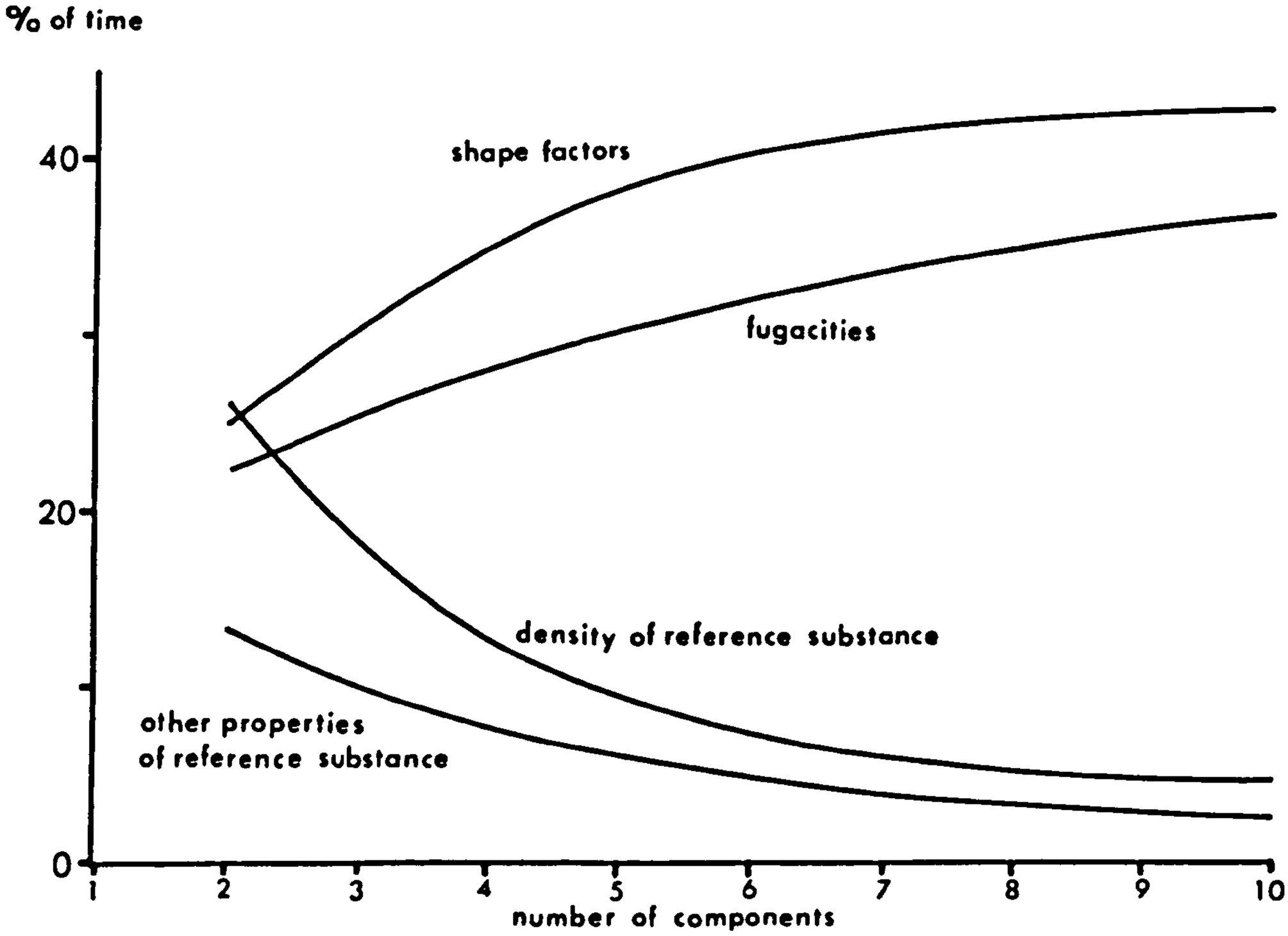


Figure 2.6 Proportion of time spent on parts of dew/bubble point calculations



The systems used for the comparisons were equimolar hydrocarbon mixtures containing 1 to 10 components from the following list: methane, ethane, ethene, propane, propene, butane, 2-methylpropane, but-1-ene, pentane, and 2-methylbutane. There was no correlation between the number of components and the ratio of calculation times for the two methods - figures in table 2.1 are the averages for all mixtures. The present version of PREPROP has reduced calculation times by a factor of 20 as compared with early versions.

For dew and bubble point calculations the time required increases with the number of components in a mixture. Figure 2.5 shows that this increase is slow and linear. At high pressures the computation time rises dramatically and this is the first indication of the eventual breakdown of calculations. This is discussed in the next section.

In Figure 2.6 the proportion of time spent in different parts of the package is shown as a function of the number of components in a mixture. The mixtures are the same as for Table 2.1 and Figure 2.5. For multi-component mixtures the time spent in calculating the properties of the reference substance is small compared to the shape factor and fugacity calculations. It is difficult to see how any further significant increase in speed can be achieved for these two parts of the procedure. The iterative calculation for the density of the reference substance could easily be eliminated by fitting two auxiliary equations for density in terms of pressure and temperature. However, the savings in computation time would be minimal. Most benefit can be expected from improved algorithms for the dew and bubble point calculations. At low and moderate pressures the number of iterations for the existing algorithm is already small (typically 3 - 6), but at high pressures near the critical region a different approach is needed.

2.3.3 Range of Vapour-Liquid Equilibrium Calculations

Calculation of vapour-liquid equilibrium in critical and retrograde regions presents considerable difficulties, not restricted to corresponding states procedures. Gunning and Rowlinson {2.14} conclude that the problems are non-trivial but not fundamental. Experience with PREPROP supports this view. Problems arise from three sources:

Figure 2.7 V – L equilibrium in the nitrogen – methane system at 171 K

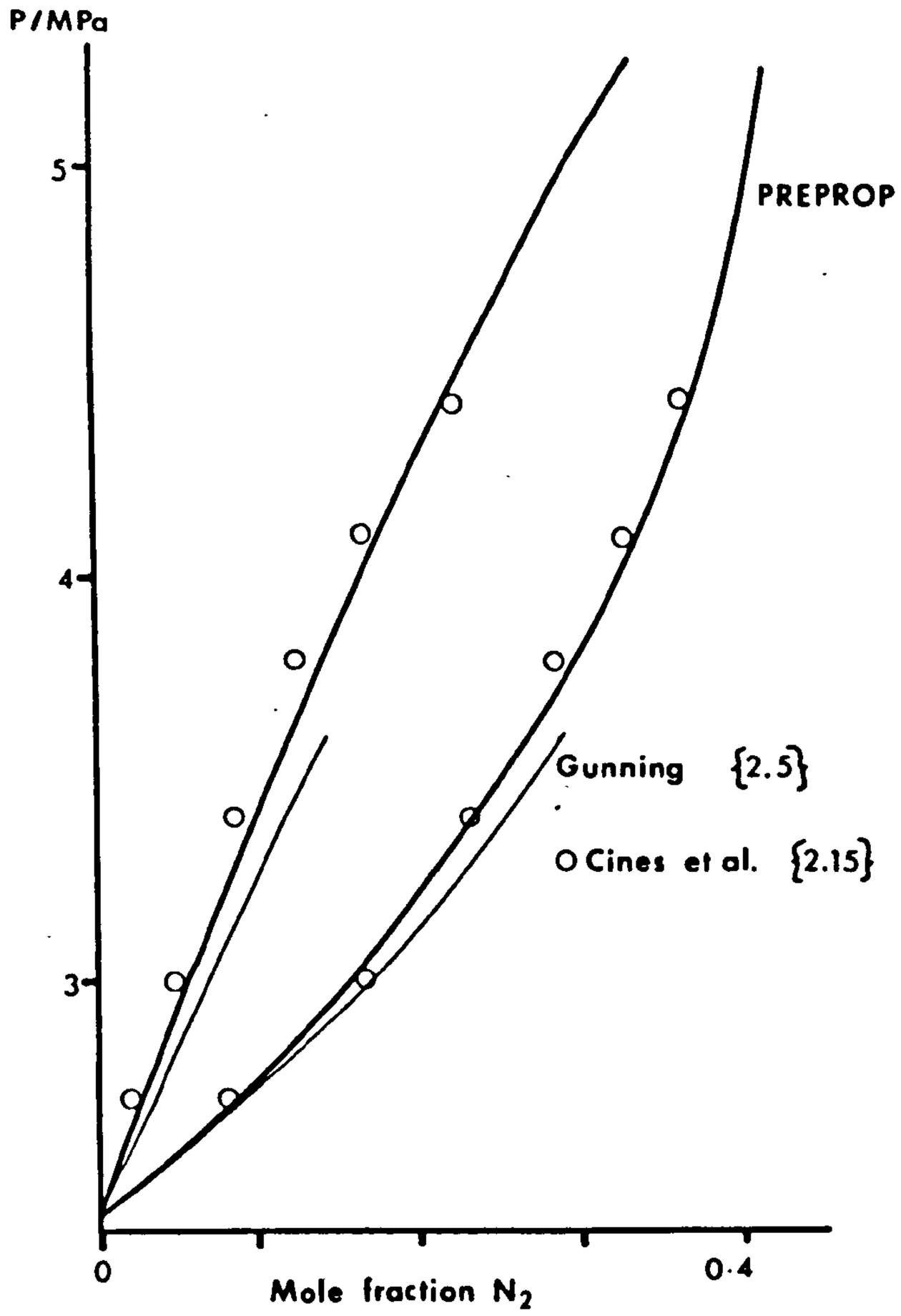
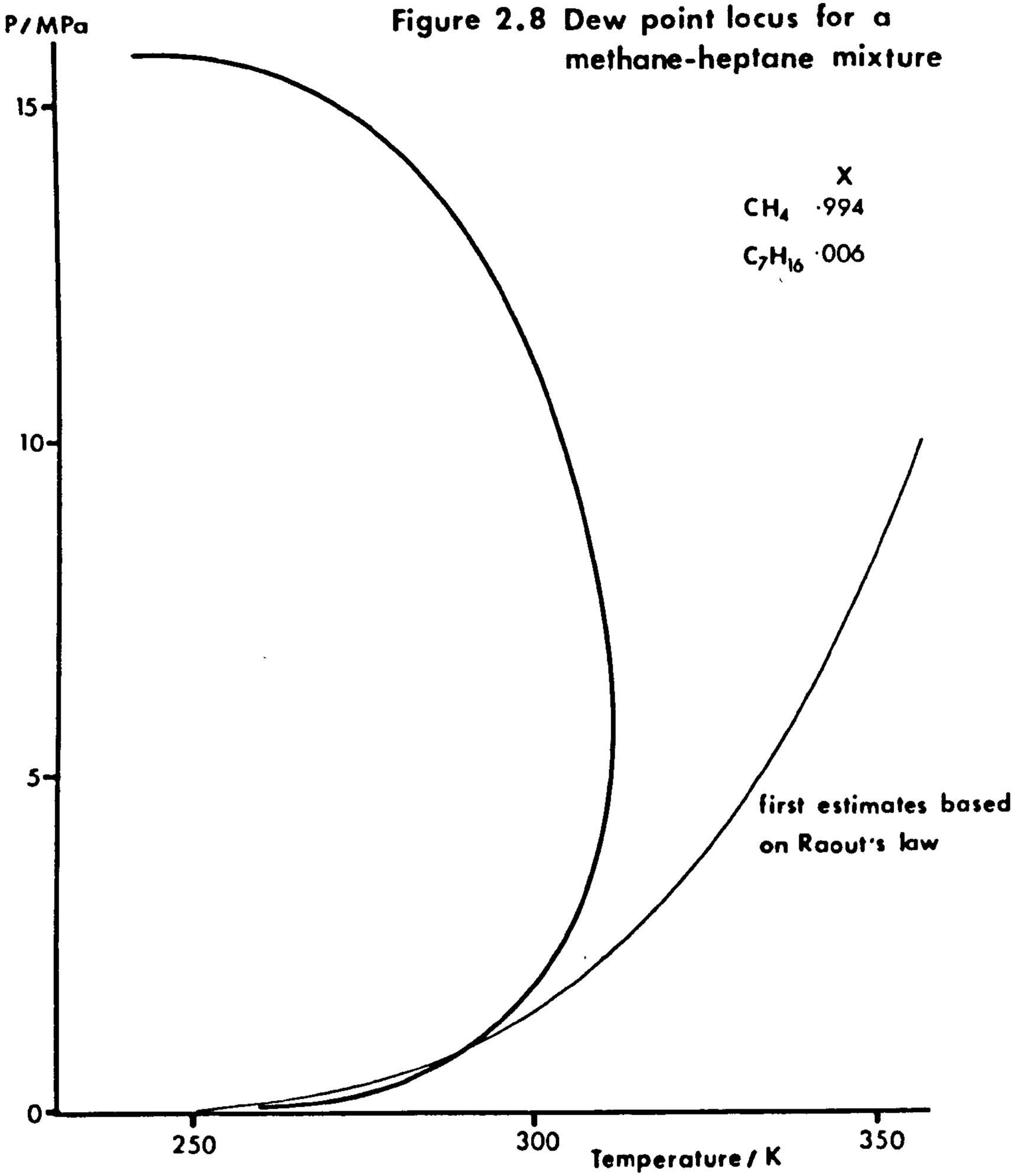


Figure 2.8 Dew point locus for a methane-heptane mixture



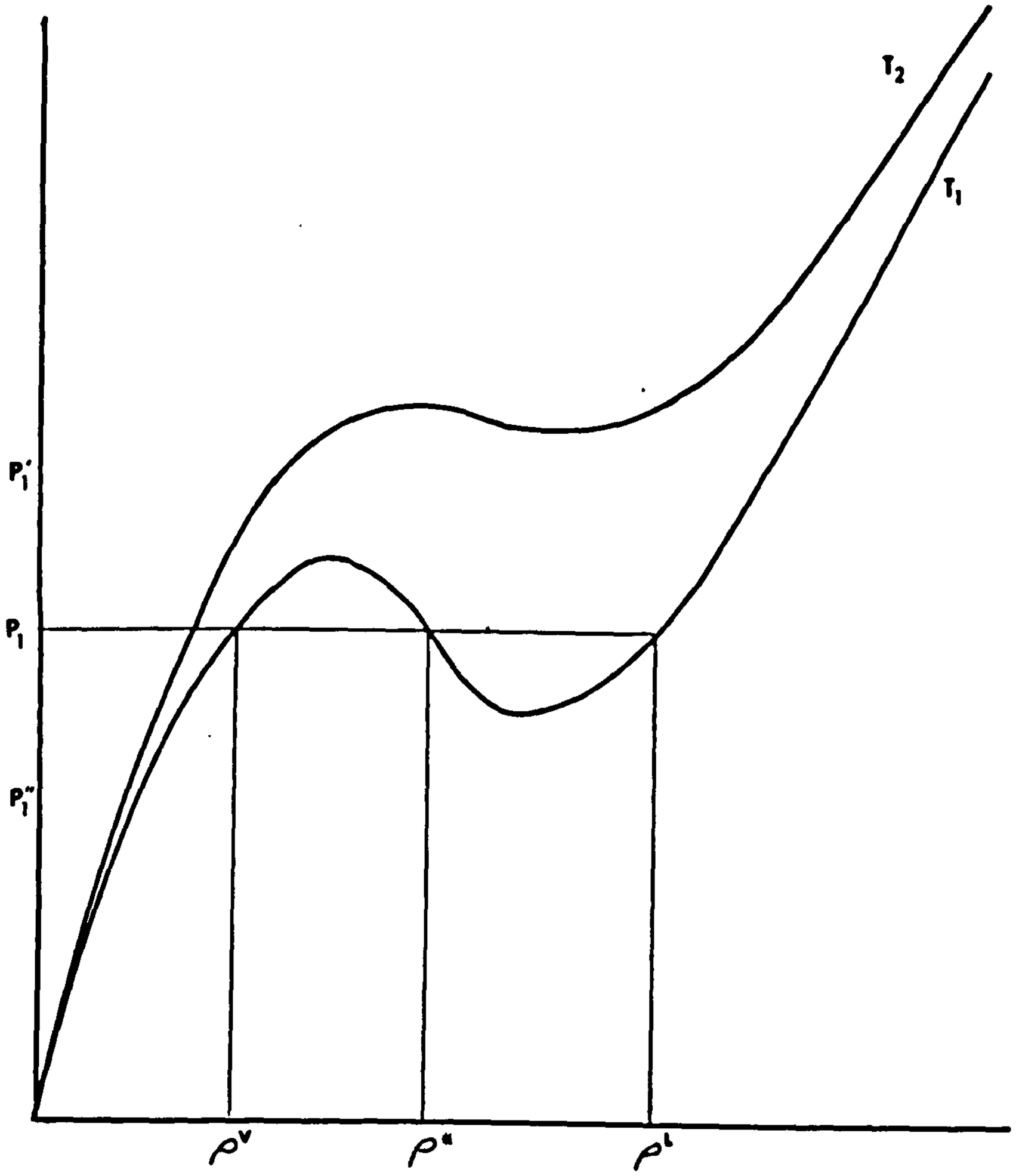
poor numerical techniques, inadequate starting estimates, and attempts to reach a solution via non-physical states of the reference substance.

Both in Gunning's work {2.5} and also in this, the iterative technique used to calculate a dew or bubble point is basically successive substitution. Significant refinements to the method are described in section 2.2.3 which have not only speeded up convergence but also produced convergence where previously no solution was found. As an example, calculations for the nitrogen-methane system are shown in Figure 2.7. Differences between the predictions are not significant since the procedures differ in detail. Figure 2.7 is typical in that, for all cases examined, the results for PREPROP extend further into the critical region.

Near to the critical point, convergence becomes slow and oscillatory, finally breaking down completely. The derivatives $(\partial x/\partial T)_P$ and $(\partial x/\partial P)_T$ along the saturation line become large near the critical point and the simple resubstitution algorithm is unable to cope with large changes in derivatives. For the Redlich-Kwong equation of state Fussell and Yanosik {2.16} overcome this problem by solving directly the set of nonlinear equations (for equality of fugacities in the two phases) using a Newton-Raphson technique. Some preliminary calculations with PREPROP, using a similar method, have proved successful where resubstitution failed, The disadvantage of such methods is that the partial derivatives $\left(\frac{\partial fug_i^L}{\partial x_j}\right)_{P,T}$, $\left(\frac{\partial fug_i^L}{\partial T}\right)_{P,x}$ and $\left(\frac{\partial fug_i^V}{\partial T}\right)_{P,y}$ must be evaluated at each iteration for all components i and j (the example is for a dew point pressure calculation). This penalty is avoided in a multidimensional equivalent of the secant method. One suitable nonlinear equation solving algorithm utilizing this technique has been described by Broydon {2.17}. Even for an equation of state as simple as the Redlich-Kwong the derivatives of component fugacities are complex. For this reason it is likely that Broydon's method will be of great value in all phase equilibrium calculations based on equations of state.

The influence of first estimates on dew point calculations in a methane-heptane mixture is shown in Figure 2.8. By supplying good initial guesses, for the temperature and composition of the liquid phase, it was

Figure 2.9 Isotherms of an equation of state



possible to extend the dew point locus through a large retrograde region up to a pressure of 15.7 MPa. First estimates based on Raoult's law are also shown in Figure 2.8. These are very poor at high pressures and do not lead to convergence above 10.0 MPa. This situation is hardly satisfactory since good first estimates are needed most when departures from Raoult's law are greatest. It is possible that convergence from poor initial points may be improved by the alternative algorithms already described. For the most difficult situations a crude, piece-meal, approach may be necessary. For example, a solution at one pressure can be used as a first estimate for a calculation at a higher pressure until the desired conditions are reached. There is an added difficulty of distinguishing between the case where no solution exists and one where the method of calculation fails, particularly for multicomponent mixtures where experimental data are scarce.

The calculation of vapour-liquid equilibrium involves solving the reference equation of state to find the density at given pressure and temperature. This step in the procedure can give problems in the critical region. Figure 2.9 shows subcritical isotherms for an equation of state. At temperature T_1 and pressure P_1 there are two physically meaningful solutions for the density, corresponding to gas and liquid phases, and at least one "unphysical" solution such as ρ^*. At a higher pressure P_1' there is no gas phase solution, and at a lower pressure P_1'' no liquid phase solution. At a higher temperature T_2, near the critical, the pressure range for two phase solutions becomes very small and the probability of stepping outside this range on an iteration in a vapour-liquid equilibrium calculation is correspondingly greater. For mixtures the equation of state is effectively different for each phase due to the composition dependence of the corresponding states parameters. At high pressures, however, the above argument still applies because the compositions of the two phases tend to equality.

There are at least two ways of dealing with this problem. Each iterative step starts from a physical state of the two-phase mixture. It must be possible to reach another such state by taking a sufficiently small step in the direction predicted by the algorithm. A strategy of reducing the step size does not guarantee convergence, however, because the step may be infinitely small. An alternative possibility

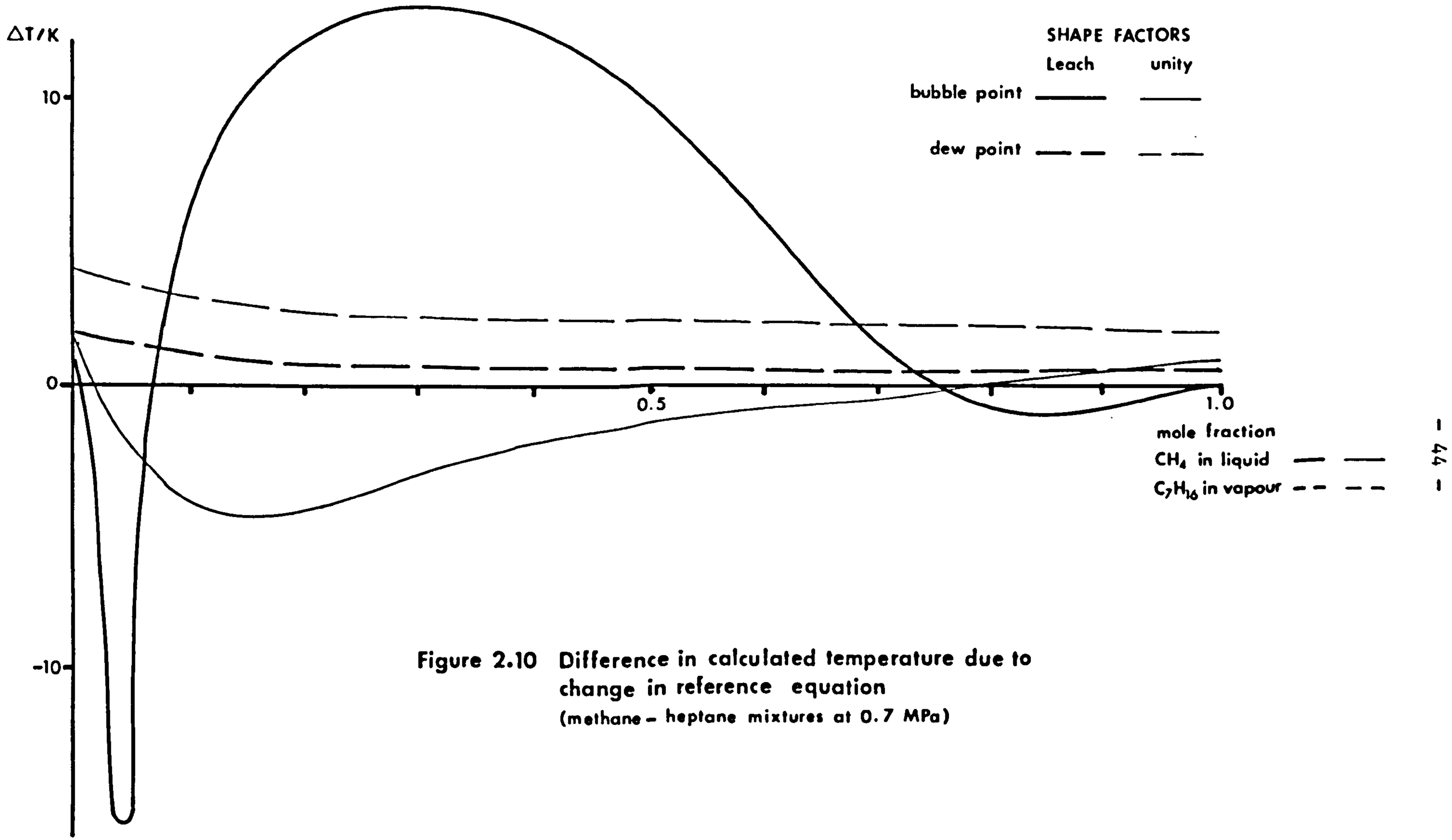


Figure 2.10 Difference in calculated temperature due to change in reference equation
(methane – heptane mixtures at 0.7 MPa)

is to use a separate equation of state for each phase giving density as a function of pressure and temperature. These equations could be extrapolated through the two phase region so that a value of the density is always available. The effect of extrapolated densities on the fugacity is not predictable and spurious solutions may result rather than forcing the iteration back to a physical region.

2.3.4 Sensitivity of Predictions

Great sensitivity of predicted values to the ingredients of a predictive procedure is most undesirable. For corresponding states the ingredients are the equation of state for the reference substance, critical parameters, and binary interaction parameters. Any undue sensitivity will be obvious in vapour-liquid equilibrium calculations since the solution depends on properties in both phases.

Work on dew and bubble points in methane-heptane mixtures showed the predicted temperatures and compositions to be sensitive on the bubble point locus but insensitive for dew points. Changing the reference equation of state from a nitrogen {2.18} to a methane {2.19} equation produces some very large changes in calculated temperatures, as shown in Figure 2.10. Similar differences are also found if binary interaction parameters are changed. At the pressure of 0.7 MPa the temperature ranges from 140 K for pure methane to 460 K for pure heptane. The influence of the shape factor equations is shown by the second set of curves in Figure 2.10 for which the shape factors were set to unity. The large differences in bubble point temperatures found originally can be attributed to shortcomings in the Leach shape factor equations (equations 2.21), which are not valid below $T^R = 0.6$ and poor above $T^R = 1.0$. This does not, however, explain the great *difference* in sensitivity between dew and bubble points.

In a dew or bubble point temperature calculation the pressure is fixed together with the composition of one phase. Any perturbation results in a change to the equivalent state of the reference substance, and hence to fugacities of components in the specified phase at any given temperature. At equilibrium the fugacities of components in both phases must be equal and so perturbations in the specified phase lead to perturbations in the unknown phase. These must be achieved by changes

in composition and temperature. The sensitivity will be determined by the relative magnitudes of the derivatives $(\partial fug_i/\partial x_i)_{P,T}$ and $(\partial fug_i/\partial T)_{P,x}$ in the two phases. For a bubble point, where the liquid composition is fixed, fugacity perturbations must be compensated for by changes in temperature and in the composition of the vapour phase. The gas phase derivatives are small compared with those in the liquid phase and so large perturbations in composition and temperature are required to match the liquid fugacities. The opposite argument implies small sensitivity for dew points.

For substances less dissimilar than methane and heptane the differences between behaviour of dew points and bubble points should be smaller. The mixtures become more ideal and the phases more similar - any perturbations due to changes in parameters contribute less to the fugacities. Manipulating the critical parameters and acentric factor for heptane to make it closer to methane does indeed reduce the differences shown in Figure 2.10.

2.3.5 Influence of uncertainty in parameters on design

In order to assess the effects of uncertainties in basic data on the design of an item of plant the distillation of an argon-oxygen mixture was chosen as an example.

The experimental vapour-liquid equilibrium data for this system is of high accuracy and is thermodynamically consistent. The data of Yorizane et al {2.20}, Wilson {2.21}, and Narinskii {2.22} were used to fit values of the binary interaction parameters. The nonlinear least squares fit minimized the residuals in temperature and composition. Two sets of parameters, obtained using different reference equations of state, are compared in Table 2.2 (for details of equations see Chapter 3).

Table 2.2 Binary interaction parameters for the argon-oxygen system

	ξ and η fitted simultaneously		η constrained to 1.0	
Equation of State	D	E	D	E
ξ	.98966	.98972	.98928	.98928
η	.99728	.99677	1.0	1.0
Sum of squares of residuals/10^{-4}	.733	.736	.734	.738

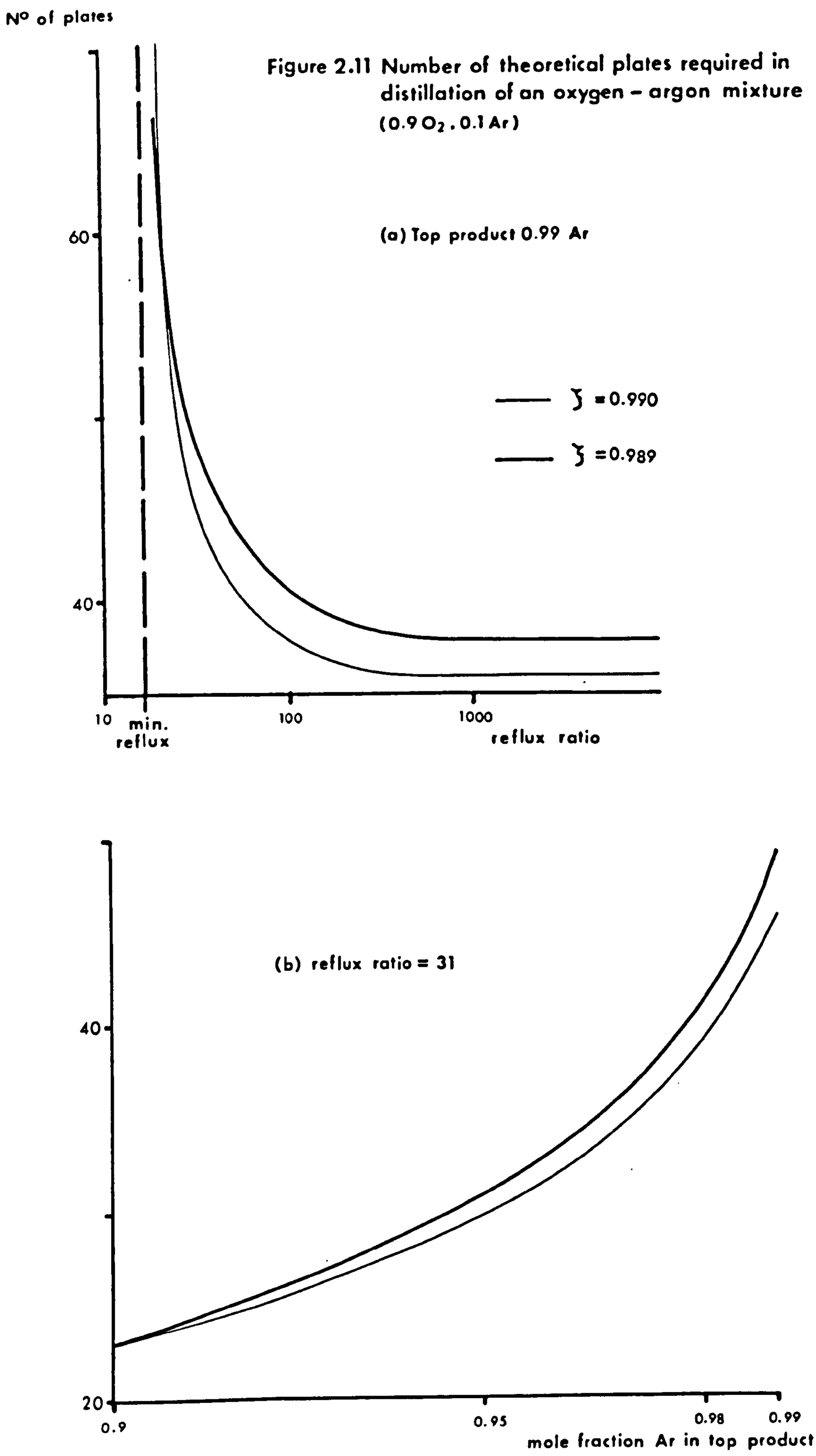


Figure 2.11 Number of theoretical plates required in distillation of an oxygen – argon mixture ($0.9\,O_2$. $0.1\,Ar$)

For each equation, results are shown for η constrained to unity and simultaneous fitting of ξ and η. There is no evidence that η differs significantly from unity and the values adopted are:

$$\xi = 0.989 \pm 0.001$$
$$\eta = 1.000 \pm 0.003$$

It must be emphasised that in general it is not possible to determine the parameters with this accuracy due to a lack of reliable and consistent data, a precision of $\pm$ 0.01 in ξ with η fixed at unity is more usual.

The model used for the distillation column is that described by Gaminibandara {2.23}. The plates are assumed ideal and a flash calculation determines the temperature on each plate. Compositions and flow rates are computed from mass and heat balances and the iterations continue until all the variables are consistent. Thermodynamic properties required are K values ($K_i = y_i \text{ fug}_i^L / x_i \text{ fug}_i^V$), and enthalpies.

Column calculations were made for a feed containing 0.1 mole fraction argon entering at its bubble point, with a top product rate of 5% of the feed at a specified purity. The operating pressure was 0.1 MPa and the feed plate was chosen to minimize the number of plates.

Figure 2.11(a) shows how the number of plates required to achieve a top product of 99% argon varies with reflux ratio and Figure 2.11(b) shows the variation with product purity at a constant reflux ratio - two values of ξ are compared in each case. The difference between $\xi = 0.989$ and $\xi = 0.990$ is not dramatic but still significant. Although ideal plates have been assumed this is not unrealistic in the air separation industry. Entrainment has, however, been ignored. The argon-oxygen system is exceptional in that the binary interaction parameters can be determined with great accuracy. In spite of this, and even though argon-oxygen mixtures are nearly ideal, the inherent incertainties in the data have significant effects on design.

There is a strong case for carrying out a sensitivity analysis in the course of any design study. This is not an expensive precaution for two reasons. Obviously, such an analysis may prevent costly design errors. Secondly, the cost of re-running a design programme is small because good estimates of all variables already exist - the calculation should converge rapidly if the design is not sensitive to small changes in the thermodynamic data.

CHAPTER 3

Equations of State for the Reference Substance

3.1 Introduction

In Chapter 2 the residual thermodynamic properties of a conformal mixture were related to the equation of state of a single "reference" substance. It is assumed in this work that the equation is of the form $P = P(\rho,T)$.

Equations (2.12) contain the implicit assumptions that the equation of state is valid for the whole fluid region and that it may be integrated through the two-phase region to give equal fugacities for the coexisting phases. These requirements are not fundamental to corresponding states predictions. Gunning and Rowlinson {3.1} used two equations and it would even be possible to use tabular data. A procedure based on a single equation has the advantage of internal consistency and is relatively simple and efficient.

The need for a very accurate representation of the properties of the reference substance has been stressed by several authors {3.1}, {3.2}. Good reproduction of P-ρ-T data is not, in itself, sufficient. All the derived properties which may be required, particularly the saturation line, must also be considered.

The fitting of an equation of state to multiple data forms was first done by Bender {3.3} and is now the standard way of correlating thermodynamic data - current methods are described by Angus {3.4}. It is now possible to produce an equation of state which will represent all the available data for a fluid to within experimental accuracies or inconsistencies. The resulting equations tend to be complex and have a large number of coefficients with no physical significance.

3.2 Choice of Reference Substance

It is not necessary to select a single reference substance for use in all cases. For greatest accuracy the reference substance should be one of the major components of the mixture. In the distillation of

air, for example, nitrogen would be an obvious choice. The constraints are that the reference must be conformal with the other components, and a sufficiently accurate equation of state must be available.

There are few substances for which a large body of accurate experimental data exist. The number of comprehensive correlating equations is fewer still - some recent examples are compared in Table 3.1.

Table 3.1 A comparison of some high-accuracy equations of state

Substance {reference}	No. of adjustable parameters	Range of applicability	
Argon {3.5}	51	84 - 300 K	$0.56 < T^R < 2.0$
		0 - 100 MPa	$0 < P^R < 20.4$
Oxygen {3.6}	47	55 - 350 K	$0.36 < T^R < 2.26$
		0 - 35 MPa	$0 < P^R < 6.9$
Water {3.7}	41	273 - 1200 K	$0.42 < T^R < 1.85$
		0 - 300 MPa	$0 < P^R < 13.6$
Methane {3.8}	33	90 - 470 K 0 - 1000 MPa	$0.47 < T^R < 2.5$ $0 < P^R < 218$
		470 - 620 K 0 - 400 MPa	$2.5 < T^R < 3.3$ $0 < P^R < 8.7$
Nitrogen {3.9}	33	64 - 650 K 0 - 1000 MPa	$0.5 < T^R < 5.1$ $0 < P^R < 294$
		650 - 1100 K 0 - 90 MPa	$5.1 < T^R < 8.5$ $0 < P^R < 26.4$

The nitrogen equation stands out as covering the greatest region of P-ρ-T space but, unfortunately, there are shortcomings in the low temperature liquid region and on the saturation line {3.9}. It would be useful

to have methane as the reference substance since it is more common than nitrogen in mixtures of industrial importance. In addition, all the properties of methane are well represented by the I.U.P.A.C. equation {3.8}.

3.3 An Extended Equation for Methane

The equations of state used by the I.U.P.A.C. Thermodynamic Tables Project Centre for both methane and nitrogen {3.8, 3.9} are of the form

$$
\begin{aligned}
P = \rho RT &+ \rho^2(A_1T + A_2T^{\frac{1}{2}} + A_3 + A_4/T + A_5/T^2) \\
&+ \rho^3(A_6T + A_7 + A_8/T + A_9/T^2) + \rho^4(A_{10}T + A_{11} + A_{12}/T) \\
&+ \rho^5A_{13} + \rho^6(A_{14}/T + A_{15}/T^2) + \rho^7A_{16}/T + \rho^8(A_{17}/T + A_{18}/T^2) \\
&+ \rho^9A_{19}/T^2 + \rho^3e^{-\gamma\rho^2}\Big[(A_{20}/T^2 + A_{21}/T^3) \\
&+ \rho^2(A_{22}/T^2 + A_{23}/T^4) + \rho^4(A_{24}/T^2 + A_{25}/T^3) \\
&+ \rho^6(A_{26}/T^2 + A_{27}/T^4) + \rho^8(A_{28}/T^2 + A_{29}/T^3) \\
&+ \rho^{10}(A_{30}/T^2 + A_{31}/T^3 + A_{32}/T^4)\Big] \qquad (3.1)
\end{aligned}
$$

In this work the methane equation was used as a basis for an extended equation of state covering a wider range of P-ρ-T space.

3.3.1 Regions of Interest

The pressure range covered by the I.U.P.A.C. equation is sufficient but the temperature range would not be adequate for predicting the properties of nitrogen above 400 K. A temperature range extending to high reduced temperature is also required to deal with highly volatile components in mixtures at normal temperatures. Although hydrogen cannot be treated in the usual way over the whole phase diagram, it behaves like a classical gas at temperatures well above the critical. The effective critical temperature is about 40 K, hence the upper limit

Table 3.2 Triple point temepratures for some common substances {3.10}

	Triple point Temperature/K	$_{T}^{R}$
Ar	83.78	.56
HBr	186.29	.50
CH_3Cl	175.44	.42
CH_4	90.68	.47
CO	68.14	.51
CO_2	216.58	.71
C_2H_2	192.6	.62
C_2H_4	103.97	.37
C_2H_6	89.28	.29
C_3H_6	87.8	.24
C_3H_8	85.47	.23
C_4H_{10}	134.86	.32
Kr	115.95	.55
N_2	63.15	.50
O_2	54.35	.35

of the nitrogen equation only corresponds to hydrogen at 340 K. In order to represent hydrogen at up to 1000 K, properties are required to a reduced temperature of 20. The strategy adopted was to use nitrogen and hydrogen data to generate pseudo-data points for methane which could be incorporated into the fitting procedure. The methods are described in the following sections.

At low temperatures the situation is not so good. The methane equation represents the data down to the triple point at $T^R = 0.47$ but this is not low enough for some substances as shown by Table 3.2. The equation must, at least, extrapolate into the low temperature region and not behave wildly. Iterative calculations on multicomponent mixtures often proceed via reduced temperatures below 0.5, even though the final solution is above 0.5. It is particularly important that the derivatives $(\partial P/\partial T)_\rho$ and $(\partial P/\partial \rho)_T$ should have the correct sign down to the very lowest temperatures so that calculations do not fail unnecessarily.

Complex equations, with many parameters, tend not to extrapolate well. The problems are most apparent in the low temperature "liquid" below $T^R = 0.4$, at which real methane is in the solid state. An equation which perfectly correlates all the experimental data is not, in itself, sufficient for predictive calculations. Some extrapolated data were included in the fitting porcedure in order to improve low temperature extrapolation.

3.3.2 The Fitting Procedure

The usual method is to adopt some functional form for the equation of state $P = P(\rho,T)$, for example equation (3.1)′, and then determine the unknown coefficients by minimizing the weighted sum of squared differences between the selected data set and calculated values. In general the equation of state may be written

$$P = P(\rho,T,a_1,a_2, \ \ldots \ , a_n) \qquad (3.2)$$

where a_1 to a_n are the unknown coefficients. For any experimental point i, the residual is

$$\phi_i = (P_i^{exp} - P(\rho_i,T_i,a_1, \ \ldots \ , a_n))$$

or $$\phi_i = (P_i^{exp} - P_i^{calc}) \qquad (3.3)$$

and the weighted sum of squares

$$\Phi = \sum_{i=1}^{m} w_i \, \phi_i^2 \tag{3.4}$$

If equation (3.2) is linear in the coefficients then (3.4) may be written as

$$\Phi = \underline{W}(\underline{C}\,\underline{a} - \underline{e})^2 \tag{3.5}$$

where

$$\underline{a} = [a_1, a_2, \ldots, a_n]^T$$

$$\underline{e} = [P_1^{exp}, P_2^{exp}, \ldots, P_m^{exp}]^T$$

$$\underline{W} = \begin{bmatrix} w_1 & & 0 \\ & \ddots & \\ 0 & & w_m \end{bmatrix}$$

$$\underline{C} = \begin{bmatrix} c_{11} \cdots\cdots & c_{1n} \\ \vdots & \\ c_{m1} & c_{mn} \end{bmatrix}$$

and $P_i^{calc} = \sum_{j=1}^{n} c_{ij} a_j$ or $c_{ij} = \left(\frac{\partial P_i^{calc}}{\partial a_j}\right)_{a_{k \neq j}}$

If Φ is a minimum with respect to all the coefficients $\underline{a}$, then $(\partial\Phi/\partial\underline{a}) = 0$. Hence

$$2\underline{C}^T\underline{W}(\underline{C}\,\underline{a} - \underline{e}) = 0 \tag{3.6}$$

or $$\underline{a} = (\underline{C}^T\underline{W}\,\underline{C})^{-1} \, (\underline{C}^T\underline{W})\underline{e} \tag{3.7}$$

Multiple Data Forms

The method is not restricted to P-ρ-T data. Any derived property which is linear in the coefficients $\underline{a}$ may be included in the fit. The equation analogous to (3.3) is

$$\phi_i = (F_i^{exp} - F_i^{calc})^2 \tag{3.8}$$

where F is any linear property, i.e.

$$F_i = \sum_{j=1}^{n} c_{F,ij} a_j \text{ or } c_{F,ij} = \left(\frac{\partial F_i}{\partial a_j}\right)_{a_{k\neq j}} \tag{3.9}$$

Suitable linear data include second virial coefficients, isochoric heat capacity

$$C_V^{res} = T\int_0^{\rho} \left(\frac{\partial^2 P}{\partial T^2}\right)_{\rho} \frac{d\rho}{\rho^2} \tag{3.10}$$

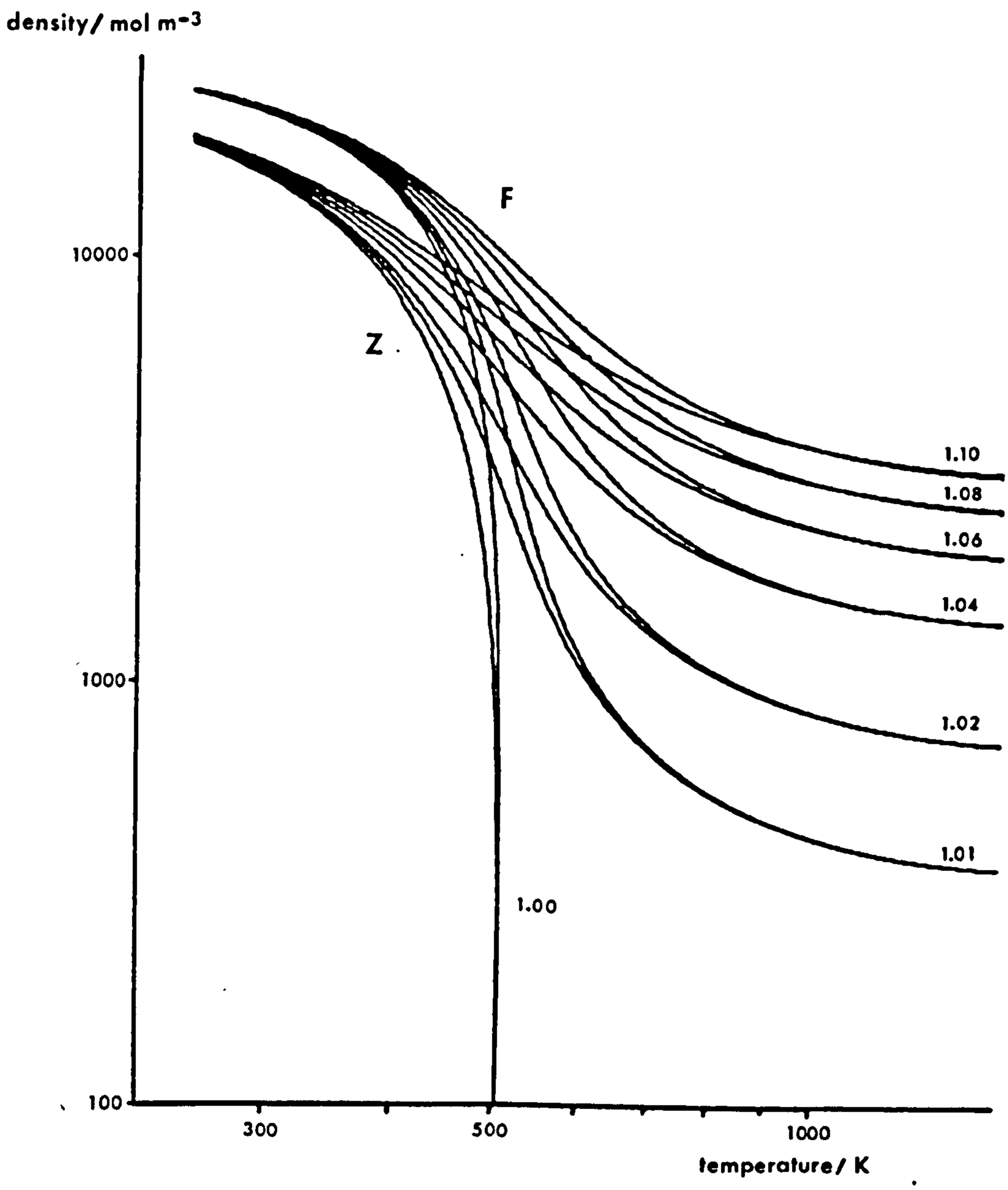
and saturation line data. The latter is incorporated using the condition of equal fugacities for coexisting phases

$$P^{\sigma}\left(\frac{1}{\rho^L} - \frac{1}{\rho^V}\right) = \int_{\rho^V}^{\rho^L} \frac{P(\rho,T^{\sigma})}{\rho^2}\, d\rho \tag{3.11}$$

The function minimized is now the weighted sum of squared residuals for all these properties

$$\begin{aligned}\Phi = &\sum_{i=1}^{m_1} w_i \left[P_i^{exp} - P(\rho_i,T_i)\right]^2 \\ &+ \sum_{j=1}^{m_2} w_j \left[B_j^{exp} - B(T_j)\right]^2 \\ &+ \sum_{k=1}^{m_3} w_k \left[C_{V,k}^{exp} - C_V(\rho_k,T_k)\right]^2 \\ &+ \sum_{\ell=1}^{m_4} w_\ell \left[P^{\sigma}\left(\frac{1}{\rho^L} - \frac{1}{\rho^V}\right) - \int_{\rho^V}^{\rho^L} \frac{P(\rho,T^{\sigma})}{\rho^2}\, d\rho\right]^2\end{aligned} \tag{3.12}$$

Figure 3.1 Lines of constant Z and F for methane



The minimum is found in the same way as before using equation (3.7) the c_{ij} are calculated from equation (3.9).

Least-squares fitting using multi-property data is standard practice at the I.U.P.A.C. Thermodynamic Tables Project Centre. The programmes developed there were used in this work.

3.3.3 Pseudo-data from Nitrogen and Hydrogen

To calculate P-ρ-T data for methane using nitrogen as a reference requires a knowledge of critical paramteres and shape factors. Corresponding states are defined as states of equal compressibility factor and fugacity/pressure ratio (this is equivalent to equations(2.19)). For substance i, relative to the reference substance k, these conditions may be written

$$\left.\begin{aligned} Z_i &= Z_k(T_i/\theta_{ik}\ T_i^c,\ V/\phi_{ik}\ V_i^c) \\ F_i &= F_k(T_i/\theta_{ik}\ T_i^c,\ V/\phi_{ik}\ V_i^c) \end{aligned}\right\} \qquad (3.13)$$

and the definitions of the shape factors follow:

$$\left.\begin{aligned} \theta_{ik}(T_i^R,\ V_i^R) &= \left(\frac{T_k^c}{T_k}\right)\left(\frac{T_i}{T_i^c}\right) = \left(\frac{T_i^R}{T_k^R}\right) \\ \phi_{ik}(T_i^R,\ V_i^R) &= \left(\frac{V_k^c}{V_k}\right)\left(\frac{V_i}{V_i^c}\right) = \left(\frac{V_i^R}{V_k^R}\right) \end{aligned}\right\} \qquad (3.14)$$

For non-spherical molecules the effective, angle-averaged, potential in equation (2.14) is a function of temperature. At high temperatures the effective potential reaches a limiting value and hence the shape factors should become constants.

Lines of constant Z and F are plotted for methane in Figure 3.1 using the I.U.P.A.C. equation {3.8}. For the nitrogen equation {3.9}

the lines are similar but in different positions. If the two substances were everywhere conformal it should be possible to superimpose the two sets of lines by shifting the axes for one substance relative to the other (on a logrithmic scale). For methane and nitrogen this can be done for high temperatures, confirming that the shape factors are constants. The distance by which each axis is shifted gives $\log(T_{CH_4}/T_{N_2})$ and $\log(\rho_{CH_4}/\rho_{N_2})$, hence θ and ϕ may be evaluated from equations (3.14).

The graphical method gives the following high temperature limits for the shape factors

$$\left.\begin{aligned} \theta_{N_2,CH_4} &= 0.967 \\ \phi_{N_2,CH_4} &= 1.041 \end{aligned}\right\} \qquad (3.15)$$

These values were compared with calculations of shape factors made directly from the two equations of state over a large grid of reduced temperatures and densities. For $T^R > 2.5$ and $V^R > 1.2$, values of θ range from 0.964 to 0.972 with most values around 0.966. For ϕ the range is 1.025 to 1.068 with most values at 1.04. The numerical results show that the shape factors remain near the graphical limits down to $V^R = 0.5$.

The high temperature shape factors were used to generate nine isotherms corresponding to methane at temperatures from 500 K to 1300 K at 100 K intervals. Above 600 K densities were from 0.1 mol m^{-3} to 32 mol m^{-3}, and at lower temperatures from 9 mol m^{-3} to 32 mol m^{-3}. The weights assigned were decreased with density to reflect the estimated reliability of the data.

A similar scheme was used to obtain scaling parameters for methane/hydrogen at high temperatures. McCarty {3.11} has fitted an equation of state of the same form as (3.1) to experimental data for hydrogen. This equation was used to plot lines of constant Z and F as before. The overlap region with methane is small and so the plot was superimposed on the curves for nitrogen to obtain the values

$$\left.\begin{aligned} \frac{\rho^c_{N_2}}{\rho^c_{H_2}\,\phi_{H_2,N_2}} &= 0.5324 \\ \text{and} \quad \frac{T^c_{H_2}\,\theta_{H_2,N_2}}{T^c_{N_2}} &= 0.3292 \end{aligned}\right\} \qquad (3.16)$$

Shape factors may be transformed according to $\theta_{ij} = \theta_{ik}/\theta_{jk}$ and $\phi_{ij} = \phi_{ik}/\phi_{jk}$. Using (3.15), (3.16) and the critical properties of methane and nitrogen gives

$$\frac{\rho^c_{CH_4}}{\rho^c_{H_2}\,\phi_{H_2,CH_4}} = 0.4997$$

$$\text{and} \quad \frac{T^c_{H_2}\,\theta_{H_2,CH_4}}{T^c_{CH_4}} = 0.2116$$

Data for methane extending to high reduced temperatures were calculated using these scaling factors and the equation of state for hydrogen. Experimental data correlated by this equation extend to 673 K ($T^R \simeq 16$) and 70 MPa ($P^R \simeq 34$), it is claimed to extrapolate to 3000 K and 70 MPa. Isotherms corresponding to methane temperatures of 1400 K to 5000 K were generated at intervals of 100 K with densities from 0.01 mol m^{-3} to the limit of the hydrogen equation. A total of 781 points were generated with weights decreasing with increasing temperature and density.

3.3.4 Results of the Fitting

Three equations were produced using the techniques described in previous sections. These equations are labelled B, C, and D in Table 3.3 and in Appendix C where numerical values of the coefficients are listed. An equation of the form (3.1) was used in all cases. The 32 linear coefficients were found by least squares fitting and the exponential constant γ was fixed at a value close to that suggested by Bender {3.3}, $\gamma = (1/\rho^c)^2$. The equations are constrained to pass through the experimental critical point of methane, where the derivatives $(\partial P/\partial\rho)_T$ and $(\partial^2 P/\partial\rho^2)_T$ are constrained to be zero. The critical point

Table 3.3 Comparison of equations of state for methane

Equation		A (IUPAC)	B	C	D	E (section 3.4)
No. of coefficients		33	33	33	33	24
P-ρ-T data (by author)	No. of data points	R.M.S. % deviation from input data			density	
					pressure	
Goodwin	555	2.894	2.185	2.293	1.675	1.587
		0.256	0.269	0.269	0.283	0.310
Douslin	374	0.071	0.064	0.067	0.071	0.075
		0.070	0.064	0.067	0.070	0.075
Cheng	318	2.096	1.802	1.908	1.903	1.936
		.336	0.229	0.229	0.225	0.228
Robertson & Babb	108	5.314*	3.091	2.826	2.535	2.861
		1.392	0.697	0.601	0.526	0.636
Deffet	228	3.587*	1.644	1.216	0.921	1.390
		1.113	0.496	0.362	0.227	0.409
Roe	78	0.100*	0.093	0.095	0.084	0.092
		0.180	0.184	0.184	0.185	0.212
Pope	140	0.086*	0.084	0.083	0.092	0.119
		0.464	0.453	0.447	0.464	0.527
Epperley	155	0.067*	0.069	0.069	0.076	0.071
		0.067	0.069	0.069	0.076	0.071
Nitrogen data	319	7.500*	2.487*	0.770	0.806	0.620
		3.543	1.098	0.327	0.347	0.272
Hydrogen data	781	1.183*	0.599*	0.143	0.266	0.149
		1.077	0.533	0.119	0.223	0.130
C_V	283	1.209	1.241	1.234	1.283	1.250
Second virial coefficient (R.M.S. mol cm^{-3})	55	2.897	2.689	2.720	2.340	2.377
Saturation Line	158					
Pressure		0.172	0.161	0.162	0.163	0.177
Liquid density		0.724	0.670	0.676	0.722	0.769
Vapour density		1.024	1.023	1.038	1.053	1.021

* data not included in fit

Note: details of data used by I.U.P.A.C. will be found in {3.8}.

parameters selected were the same as those used by I.U.P.A.C. {3.8}, namely: T^c = 190.555 K, ρ^c = 10109.5 mol m^{-3}, and P^c = 4.5950 MPa. Input data included all the P-ρ-T, C_V, saturation line, and second virial coefficient points used by I.U.P.A.C. plus the single phase P-ρ-T data of Robertson and Babb {3.12}, Deffet et al. {3.13}, Roe {3.14}, Pope {3.15}, and Epperley {3.16}.

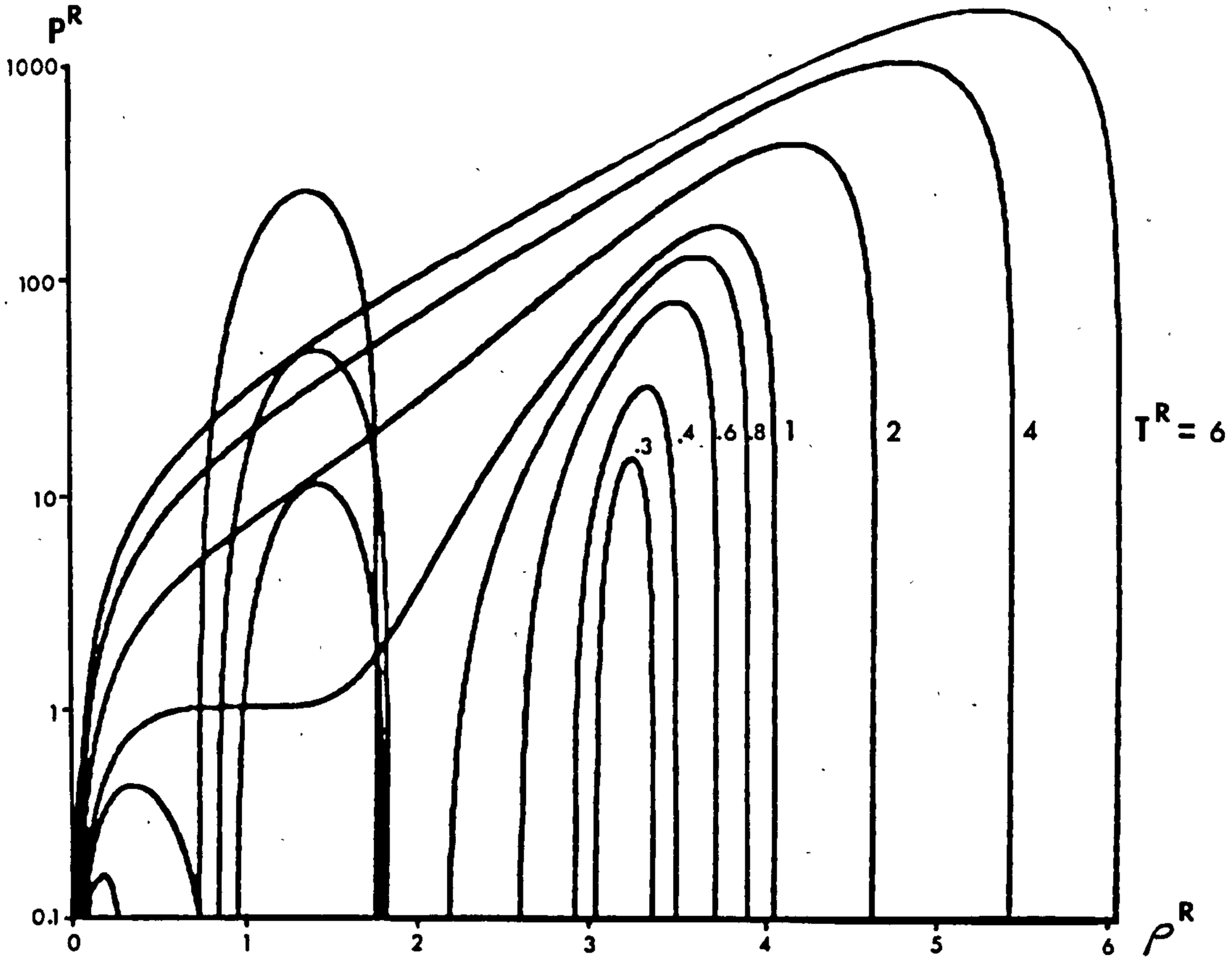
Equation B is the result of carrying out the fitting on all the methane data listed above. The weights for all the data were adjusted so that the extra data could be reasonably represented without degrading the fit to the original data selected by I.U.P.A.C. In Table 3.2 the new equations are compared with the I.U.P.A.C. equation.

Equation C includes the pseudo-data generated from nitrogen and hydrogen equations. Weights were adjusted so that the fit to real methane data was maintained. As expected, the nitrogen and hydrogen data is well represented. Where the nitrogen data overlaps with high temperature and pressure methane data (Deffet et al., Robertson and Babb), the deviations are of a similar magnitude for both data sets. An important feature observed with the hydrogen and the nitrogen data is that the deviations do not increase rapidly towards the data boundaries. Also, there are no large oscillations. This smooth behaviour means that extrapolation outside the region for which methane data exists is safe, although the accuracy may be smaller.

Isotherms for equation C are plotted in Figure 3.2. The Maxwell loops are very large at low temperatures and dominate the two phase region but do not cause any numerical difficulty. All the isotherms have the correct slope at the melting line but the sharp turning point is potentially unsatisfactory, particularly at the lowest temperatures. For the purposes of extrapolation the isotherms should, ideally, continue indefinitely with a positive slope and without intersecting. In an attempt to achieve this, the isotherms were extrapolated to give pseudo-data for the region where real methane is a solid. These data were then included in a new fitting operation.

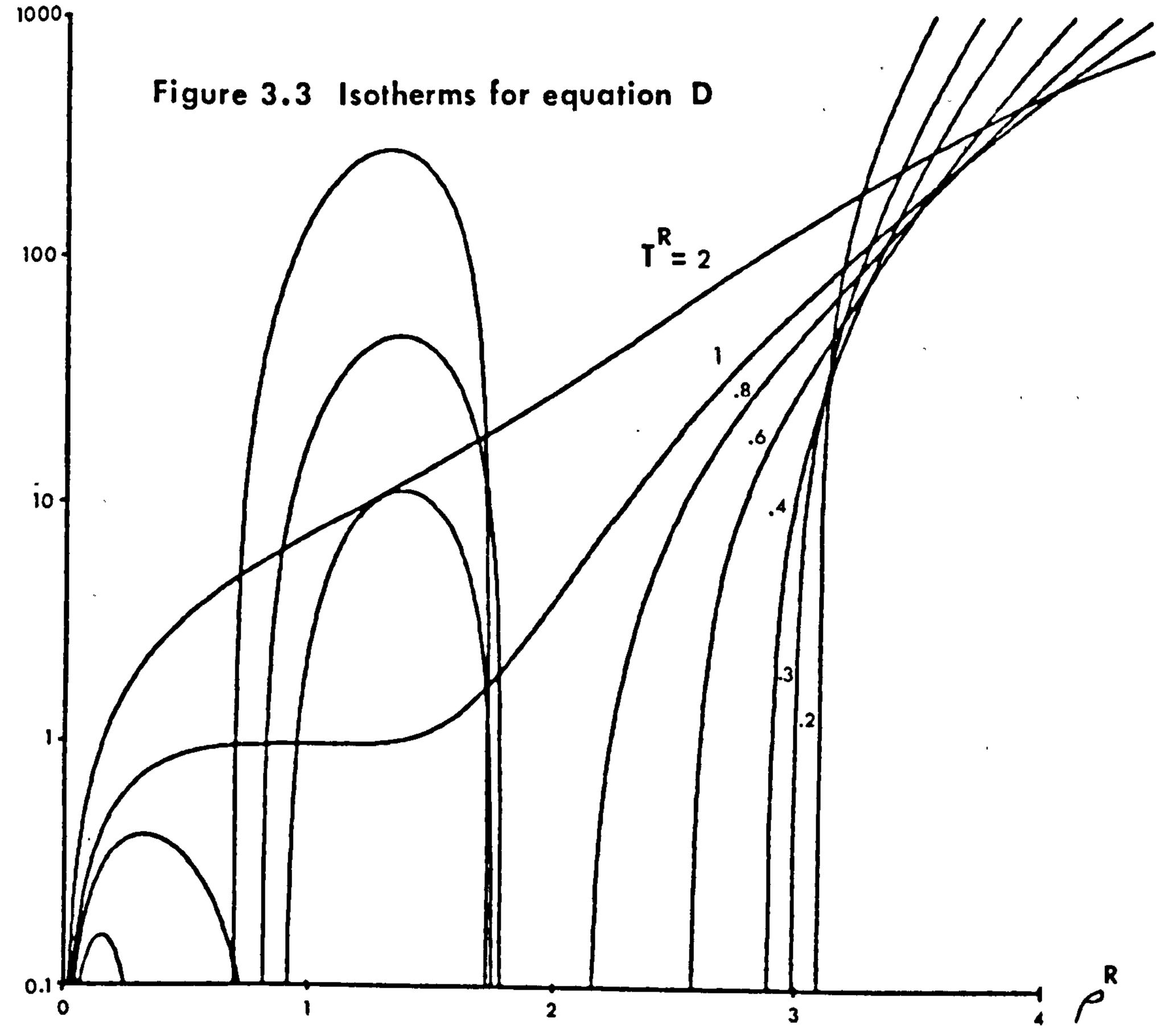
It was not possible to make the equation behave in the ideal way but some improvements were possible. Increasing the weight on the "solid"

Figure 3.2 Isotherms for methane equation C



p^R

Figure 3.3 Isotherms for equation D



phase data from zero causes the isotherms to intersect at successively higher pressures and eventually disrupts the fit to experimental data. Crossing of the isotherms can obviously cause problems but if restricted to sufficiently high pressures this phenomenon is preferable to the tight loops shown in Figure 3.2. The gradients are always of the correct sign and this is important for any iterative calculation entering the low temperature region. Equation D was selected as the best compromise between accurate reproduction of the experimental data and good extrapolating behaviour - isotherms are plotted in Figure 3.3.

3.3.5 Accuracy at Low Pressures

It is important that the equation of state be a good representation of the P-ρ-T values at low pressures if accurate fugacities are to be calculated at higher pressures. The fugacity is calculated from

$$\ln\left(\frac{fug}{\rho RT}\right) = Z - 1 + \frac{1}{RT}\int_0^{\rho}(P - \rho RT)\frac{d\rho}{\rho^2} \qquad (3.17)$$

If the pressure calculated from the equation of state is subject to an error $\Delta P(\rho)$ the calculated fugacity is

$$\ln\left(\frac{fug}{\rho RT}\right)_{calculated} = \ln\left(\frac{fug}{\rho RT}\right)_{exact} + \frac{\Delta P(\rho)}{\rho RT} + \frac{1}{RT}\int_0^{\rho}\frac{\Delta P(\rho)}{\rho^2}\,d\rho \qquad (3.18)$$

Apart from the term which depends only on the final density, the error consists of contributions to the integral in equation (3.18) from zero density upwards. Because $\Delta P(\rho)$ is divided by ρ^2 in the integral, the errors at low pressures contribute much more to cumulative errors in the fugacity than do the errors at higher pressures (and densities). At low pressures the second virial coefficient accounts for most of the non-ideal behaviour of a gas and good fugacities were therefore forced by increasing the weights used in the fitting operation for the second virial coefficients.

Another problem is incompatibility between coexistence data and single phase data close to the saturation line; this has been noted by Angus et al. {3.8} in connection with producing thermodynamically consistent tables. From the point of view of prediction, these small inconsistencies could be significant. We are not merely interested in coexisting states of the reference substance but in a larger region around the saturation line corresponding to coexisting states of other substances and mixtures. Little can be done about this until better data become available.

3.4 Application of Wagner's Regression Technique to an Equation of State for Methane

3.4.1 The Regression Method

For an empirical correlating equation, such as an equation of state, it is desirable to keep the number of adjustable parameters to a minimum. To represent a large body of experimental data with an empirical equation often requires many parameters but such equations present problems of extrapolation and the parameters have no physical meaning. Wagner's method {3.17} exploits the fact that an equation of arbitrary form is likely to have a high degree of inter-correlation between coefficients determined in a least squares fit. A smaller number of uncorrelated terms can be used to represent the data. The form of the equation is not fixed in advance but determined by an iterative procedure. Only those terms which make a statistically significant improvement in the fit are selected from a large number of possible terms.

It is not computationally practical to evaluate explicitly the weighted sum of squares of residuals for every equation which can be produced by selecting terms from a pool of, say, 50. Wagner avoids the explicit evaluation by using the Gauss algorithm to solve an augmented form of the linear equations in (3.6). The computation is guided by choosing the pivot element (corresponding to a term in the equation) which reduces the sum of squares of residuals by the largest amount. Equation (3.6) may be written

$$\underline{C}^T \underline{W} \underline{C} \underline{a} = \underline{C}^T \underline{W} \underline{e} \qquad (3.19)$$

or $\underline{N} \underline{a} = \underline{b}$

Wagner uses the two matrices

$$\underline{A} = \begin{vmatrix} \underline{N} & \underline{b} \\ \underline{b} & \Phi \end{vmatrix} \quad \text{and} \quad \underline{E} ,$$

where Φ is the weighted sum of squared residuals and $\underline{E}$ is initially the unit matrix. Row and column eliminations are carried out, pivoting on the diagonal elements of $\underline{N}$. The whole $\underline{A}$ and $\underline{E}$ matrices are transformed at each elimination. Wagner showed that the element Φ is always the sum of squares for an equation containing the terms (corresponding to pivot elements) used so far. The effect of including a new term may be assessed simply by transforming Φ rather than the whole matrix. Thus it is possible to build up an equation of state adding terms one at a time.

As each new coefficient is added, the statistical significance of all coefficients in the equation is tested. If any fall below a specified level the least significant is eliminated and the test repeated. The Gauss algorithm is again used for elimination but this time pivoting on the diagonal elements of $\underline{E}$. If all coefficients are individually significant the significance of the equation *as a whole* is tested by checking whether elimination of the least significant coefficient increases the sum of squares appreciably. If this test fails, then an "exchange of variables" is attempted. Terms already in the equation are swapped with those not included, one at a time, if the sum of squares can be reduced. When no further, significant, reduction is possible the procedure terminates.

Wagner claims that his method will select the "optimum" equation but clearly this cannot be the case. The algorithm does not consider the effect of swapping terms two, three, or more at a time. To find the "best" equation all possible swaps must be tried and we are left with the original problem. Although the equation selected may not be the unique optimum, experience with the algorithm has shown that it does enable a data set to be represented with fewer coefficients than in other regression schemes.

3.4.2 Results for the Equation of State

Wagner originally applied his technique to vapour pressure equations. Armstrong and de Reuck {3.18} extended the method to fitting equations of state and it has been used in the production of the I.U.P.A.C. propene tables {3.19}. The computer programmes written for that purpose were adapted for use with methane. Wagner's approximations to probability density integrals are not valid for over 1500 data points and thus had to be changed in view of the 3500 points for methane.

The results are generally encouraging. It was possible to fit the methane data with 20 - 24 coefficients selected from a pool of 50 possible terms of the "extended B.W.R." type used by Stewart and Jacobsen {3.6}. The relative weights on input data were kept the same as for equation D, but absolute weights and probability levels in the statistical test were varied to give different fits with different numbers of coefficients. Equation E was finally selected as the best and is compared with the other equations in Table 3.3. It has 24 coefficients and is of the form

$$
\begin{aligned}
P = \rho RT &+ \rho^2(A_1T + A_2T^{\frac{1}{2}} + A_3 + A_4/T + A_5/T^2) \\
&+ \rho^3(A_6T + A_7/T^3) + \rho^4(A_8 + A_9/T + A_{10}/T^3) \\
&+ \rho^5(A_{11}T^2 + A_{12}/T^2) + \rho^6A_{13}/T^2 \\
&+ \rho^8A_{14}/T + \rho^9A_{15}/T + \rho^{11}A_{16}/T^2 \\
&+ \rho^3e^{-\gamma\rho^2}\left[(A_{17}/T^2 + A_{18}/T^4)\right. \\
&+ \rho^2A_{19}/T^4 + \rho^4A_{20}/T^2 + \rho^6A_{21}/T^2 \\
&\left. + \rho^8(A_{22}/T^2 + A_{23}/T^4)\right] \qquad (3.20)
\end{aligned}
$$

Numerical values of the coefficients will be found in Appendix C. Although most of the residuals for equation E are larger than those

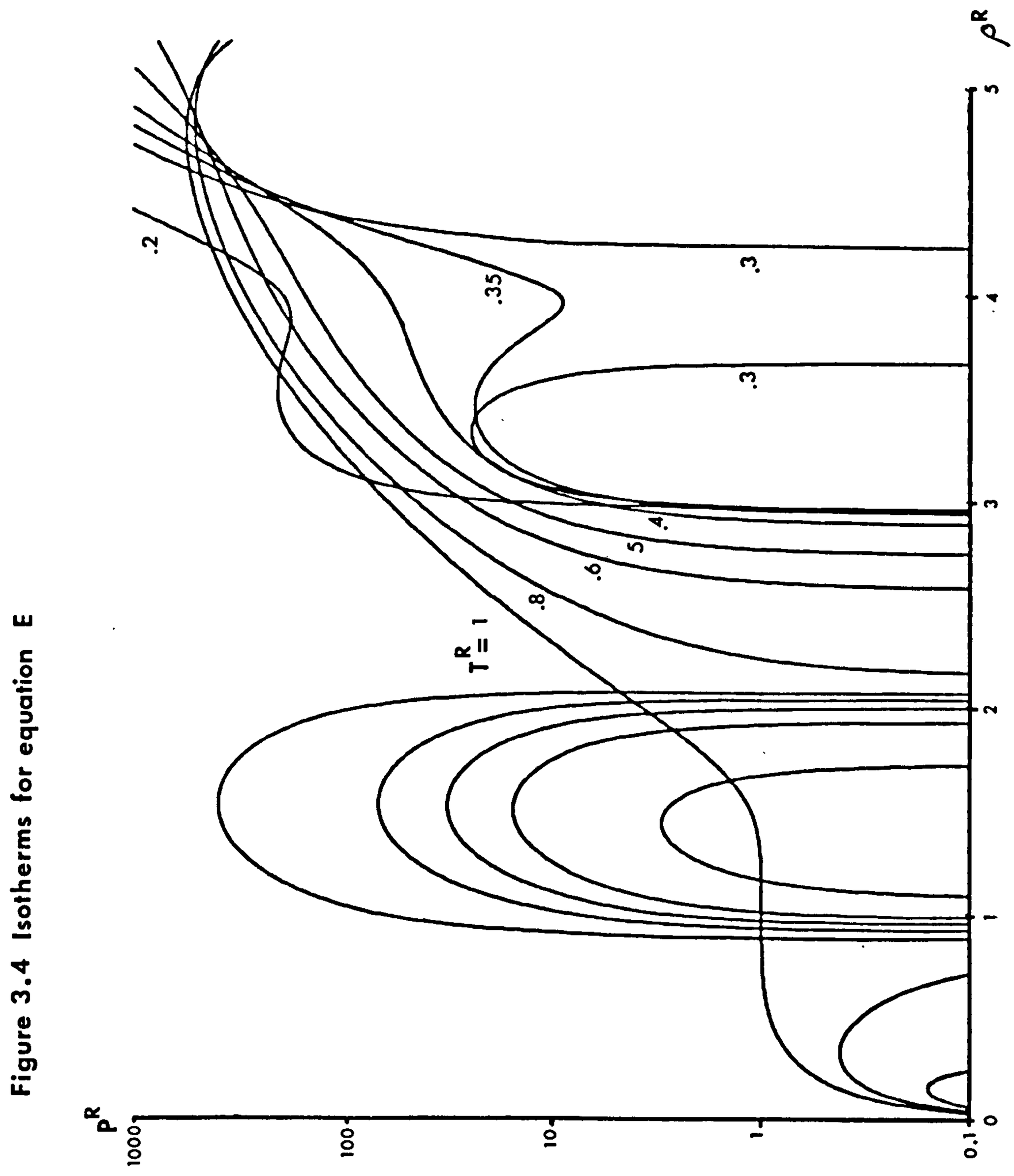


Figure 3.4 Isotherms for equation E

for the 33 coefficient equations the differences are small and the very large quantity of data is well represented. Isotherms for equation E are plotted in Figure 3.4. There could obviously be problems in using this equation below $T^R = 0.35$.

3.5 Conclusions

All the equations of state developed here, B - E, represent the experimental data for methane over the range of I.U.P.A.C. tables. Above 300 K and 40 MPa the agreement with experimental data is much better than for equation A. Equations C, D, and E include data generated from nitrogen and hydrogen equations allowing extrapolation to 1300 K at 500 MPa and to 3000 K at 150 MPa. Equation D is probably the best for predictive calculations down to the lowest temperatures, although in one trial both D and E gave reasonable predictions down to the triple point of ethane at $T^R = 0.29$.

None of the equations described in this chapter represents a satisfactory solution to the problem of formulating a single equation of state which will reproduce the properties of a variety of fluids via the corresponding states principle. The deficiencies are greatest at the lowest temperatures. The uncertainties in the extrapolation of existing data to lower temperatures cause problems. In some cases, the extrapolated data improve the equation (e.g. equation D), but in others they may be incompatible with the form of the equation (e.g. equation E). To provide low temperature data on some rational basis experimental values must be used. Good experimental data exist for ethane {3.20} and propane {3.21}, which have reduced triple point temperatures of 0.29 and 0.23 respectively. Unfortunately, the Leach shape factor equations are only valid down to $T^R = 0.6$. There is no reason to suppose that the shape factors will be constant in the low temperature region and hence the problem is not trivial. Now that a great deal of data are available in the form of correlating equations the task of extending the shape factor equations is not so formidable and would seem to be a necessary step.

CHAPTER 4

Calculation of Vapour-Liquid Equilibrium using Minimization Techniques

4.1 Introduction

Problems of chemical and/or physical equilibrium at given temperature and pressure are usually solved in one of two ways. Either the nonlinear equations describing the problem are solved directly, or the Gibbs free energy (G.F.E.) of the system is minimized. The two procedures are mathematically and thermodynamically equivalent but their practical application is quite different.

Chemical equilibrium problems are treated by both methods {4.1}, but for physical equilibrium only the nonlinear equation approach is common. Unfortunately, G.F.E. minimization is not straightforward because of the mass balance constraints which must be included. Some recent applications of G.F.E. minimization to the calculation of physical and chemical equilibria are described by Dluzniewski and Adler {4.2}, Ma and Shipman {4.3}, and George et al. {4.4}. Only Dluzniewski and Adler attempt to deal with the mass balance constraints directly, otherwise the problem of constrained minimization is avoided at the expense of complex and cumbersome algorithms. The method of George et al. is of some interest and is considered in more detail later in this chapter.

Numerical methods for constrained minimization are not as well developed as those for unconstrained problems, but powerful and efficient algorithms are now available. In this work, the Variable Metric Projection (V.M.P.) method of Sargent and Murtagh {4.5} was adapted for use in calculating flash equilibria. Nonlinear equality and inequality constraints may be handled.

Three types of flash problem are considered in this chapter. It is assumed that initial values of temperature, pressure, and overall composition are specified:

i) Simple flash - amounts and compositions of both phases at the initial conditions.

ii) Isenthalpic flash - as above, but for the final state (at given pressure) in an isenthalpic process.

iii) Isentropic flash - as ii), but for a constant entropy process.

In problem i) the pressure and temperature are fixed and hence the G.F.E. is a minimum. In problems ii) and iii) the final temperature is not known; either a succession of simple flash calculations may be used within an iteration on the temperature, or the appropriate function may be minimized subject to a nonlinear constraint of constant enthalpy or entropy. The latter is a much more efficient approach and is the one adopted here.

Thermodynamic properties were calculated using the PREPROP package. Both equation of state methods and the corresponding states method (as described in Chapter 2) have the advantage of thermodynamic consistency. This turned out to be essential if convergence was to be always obtained. The minimization method may be used with thermodynamic properties from other sources but great care is required in setting up the problems.

4.2 Criteria of Equilibrium

Gibbs {4.6} states that if an isolated system is to be at equilibrium,

> "... it is necessary and sufficient that in all possible variations of the state of the system which do not alter its energy, the variation of its entropy shall either vanish or be negative."

For an isolated system there is no work input and hence the volume is necessarily constant. Gibbs' criterion may be written

$$(\delta S)_{U,V} \leqslant 0 \qquad (4.1)$$

It is necessary to distinguish between an infinitesimal increment denoted by δ and a finite increment Δ. The much stronger criterion for *stable* equilibrium is

$$(\Delta S)_{U,V} \leqslant 0 \qquad (4.2)$$

Equation (4.1) is a first order condition and defines a local maximum of the entropy at fixed internal energy and volume. Equation (4.2) defines a global maximum, second and higher differentials are not ignored, and Δ need not be a small increment. The problem of finding global minima or maxima is non-trivial and most minimization procedures make no attempt to identify a solution as global or local. We assume that, for a physical problem, a solution satisfying (4.1) is also a stable equilibrium satisfying (4.2).

Different criteria of equilibrium apply according to which properties are held constant in the system.

Constant S and V

The internal energy is a minimum,

$$(\delta U)_{S,V} \geq 0 \tag{4.3}$$

Variations which violate (4.3) also violate (4.1) and hence these conditions are equivalent.

Constant V and T

The Helmholtz free energy is defined as

$$A = U - TS \tag{4.4}$$

For an infinitesimal change at constant temperature

$$\delta A = \delta U - T\ \delta S \tag{4.5}$$

The change in internal energy at constant volume and temperature may be written

$$(\delta U)_{V,T} = (\delta U)_{V,S} + \left(\frac{\partial U}{\partial S}\right)_V (\delta S)_{T,V}$$

or

$$(\delta U)_{V,T} = (\delta U)_{V,S} + T\ (\delta S)_{T,V} \tag{4.6}$$

hence from (4.3)

$$(\delta U)_{V,T} \geq T(\delta S)_{T,V} \tag{4.7}$$

For constant volume (4.5) becomes

$$(\delta A)_{V,T} = (\delta U)_{V,T} - T(\delta S)_{V,T} \tag{4.8}$$

Substituting (4.7) in (4.8) gives the required inequality

$$(\delta A)_{V,T} \geq 0 \tag{4.9}$$

It follows that the Helmholtz free energy is a minimum at constant volume and temperature.

By similar arguments we have the following conditions:

Constant P and T

$$(\delta G)_{P,T} \geq 0 \tag{4.10}$$

The Gibbs free energy is a minimum.

Constant P and S

$$(\delta H)_{P,S} \geq 0 \tag{4.11}$$

The enthalpy is a minimum.

Constant P and H

$$(\delta S)_{P,H} \leq 0 \tag{4.12}$$

The entropy is a maximum.

4.3 The Variable Metric Projection Method for Minimization

In this section the V.M.P. method is outlined for unconstrained and constrained minimization. For a full description of numerical optimization techniques and V.M.P. see {4.5}, {4.7 - 4.9}.

4.3.1 Unconstrained Minimization

For a function of n variables the point $\hat{x} = [\hat{x}_1, \hat{x}_2, \ldots, \hat{x}_n]^T$ is a local minimum if there exists a constant $\epsilon > 0$ such that

$$f(\hat{x}) < f(\hat{x} + \Delta x),\ 0 < \| \Delta x \| < \epsilon \tag{4.13}$$

where Δx represents a step in the n dimensional space and $\| \Delta x \|$ is the Euclidean norm defined by $\| \Delta x \| = \left[\sum_{i=1}^{n} (\Delta x_i)^2\right]^{\frac{1}{2}}$.

In the following, all functions are considered to be continuous and twice differentiable. Under these conditions we can expand f(x) in a Taylor series about $\hat{x}$

$$f(\hat{x} + \Delta x) - f(\hat{x}) = \Delta x^T g(\hat{x}) + \tfrac{1}{2}\Delta x^T H(\hat{x})\ \Delta x + \ldots.$$

where g(x) is the gradient vector $\left[(\partial f/\partial x_1), (\partial f/\partial x_2), \ldots, (\partial f/\partial x_n)\right]^T$ and H(x) is the Hessian matrix, a square n x n matrix of second derivatives

$$\begin{bmatrix} \left(\frac{\partial^2 f}{\partial x_1^2}\right) & \frac{\partial^2 f}{\partial x_1 x_2} & \cdots\cdots \\ \cdot & & \\ & \cdot & \\ \left(\frac{\partial^2 f}{\partial x_1 x_2}\right) & \cdot & \\ \cdot & & \\ \cdot & & \left(\frac{\partial^2 f}{\partial x_n^2}\right) \\ \cdot & & \end{bmatrix}$$

At a stationary point $g(\hat{x}) = 0$ and a sufficient condition for its being a minimum is that $H(\hat{x})$ is positive definite (for a function of a single variable the equivalent condition is $(d^2f/dx^2) > 0$).

Determining the Minimum

The general quadric has the form

$$f(x) = a + b^T x + \tfrac{1}{2} x^T H x \qquad (4.14)$$

where a and b are constant vectors and H is a constant matrix. The gradient vector is given by

$$g(x) = b + Hx \qquad (4.15)$$

where H is the Hessian matrix. From (4.15) we have

$$g(x + p) - g(x) = Hp \qquad (4.16)$$

where p is a step in n-space. If the function has a minimum at (x + p), g(x + p) = 0, giving

$$g(x) + Hp = 0 \qquad (4.17)$$

Provided H is non-singular this set of linear equations may be solved for p, hence giving the co-ordinates of the minimum

$$H^{-1} g(x) + p = 0$$

or

$$p = - S\ g(x) \qquad (4.18)$$

where $S \equiv H^{-1}$.

For a function which is not a quadric, equation (4.18) will not give a step to the minimum and the Hessian matrix is no longer constant. If it is assumed that a *local* quadratic approximation applies, equation (4.18) can still be used to generate a step which, it is hoped, will give a function decrease. By applying this scheme recursively the aim is to produce a sequence of steps converging to the minimum. If we are at a point x_k the next step is generated by

$$p_{k+1} = (x_{k+1} - x_k) = -S(x_k)\ g(x_k)$$

or

$$p_{k+1} = -S_k\ g_k \qquad (4.19)$$

In order to ensure a function decrease for this step its magnitude may have to be reduced and so we take a scalar multiple of it, giving

$$p_{k+1} = - \alpha_k S_k g_k \qquad (4.20)$$

Secant Methods

To use equation (4.20) as it stands requires the evaluation of $n(n + 1)/2$ second derivatives (H is symmetric), and a matrix inversion on each step. This is time consuming, particularly if analytic expressions are not availbale. As an alternative, it is possible to use the information from successive steps to construct an approximation to S, the inverse Hessian. This approach is used by *secant* methods and avoids the matrix inversion as well as the evaluation of second derivatives.

For a quadric we have, from equation (4.16),

$$g_k - g_{k-1} = Hp_k$$

Writing the gradient difference as q_k we obtain

$$q_k = Hp_k$$

$$\text{or} \quad S\, q_k = p_k \qquad (4.21)$$

If the approximation to the inverse Hessian after k steps is S_k, we require that S_k satisfies the exact equation, (4.21), for all steps so far

$$S_k\, q_j = p_j \qquad j \leqslant k \qquad (4.22)$$

Setting $p_{k+1} = S_k\, q_{k+1}$ and assuming the step reaches the minimum gives equation (4.19). In general $p_{k+1} \neq S_k\, q_{k+1}$ and $g_{k+1} \neq 0$, even for a quadric, although the assumptions improve as the solution is approached. As before, equation (4.20) is used to ensure a function decrease

$$p_{k+1} = - \alpha_k S_k g_k$$

BIBL
LONDN
UNIV.

Matrix Recursion Formulae

We presume that we have a matrix S_k which satisfies (4.22) and that p_{k+1} has been generated according to (4.20). The gradient g_{k+1} will be non-zero (unless a solution has been found) and so we wish to update S_k to S_{k+1}, so that

$$S_{k+1}\, q_{k+1} = p_{k+1} \tag{4.23}$$

$$\text{and} \quad S_{k+1}\, q_j = p_j \qquad j \leqslant k \tag{4.24}$$

We write

$$S_{k+1} = S_k + C_k \tag{4.25}$$

Inserting (4.25) in (4.23) gives

$$(S_k + C_k)\, q_{k+1} = p_{k+1} \tag{4.26}$$

$$\text{or} \quad C_k\, q_{k+1} = p_{k+1} - S_k\, q_{k+1} \tag{4.27}$$

Since S, the true inverse Hessian, is symmetric we presume that S_k, S_{k+1}, and C_k are symmetric and write

$$C_k = \frac{z_k z_k^T}{c_k} \tag{4.28}$$

where z_k is an n x r matrix of rank r, and c_k is a scalar. In equation (4.27) $C_k\, q_{k+1}$ is an n-vector and we may choose r = 1, making z_k a column vector. Substituting (4.28) in (4.27) gives

$$\frac{z_k z_k^T}{c_k}\, q_{k+1} = p_{k+1} - S_k\, q_{k+1} \tag{4.28}$$

Since the magnitudes of c_k and z_k are arbitrary we choose

$$c_k = z_k^T\, q_{k+1} \tag{4.29}$$

giving

$$z_k = p_{k+1} - S_k\, q_{k+1} \tag{4.30}$$

Substituting (4.25) and (4.28) in (4.24) gives

$$\left(S_k + \frac{z_k z_k^T}{c_k}\right) q_j = p_j \qquad j \leq k \tag{4.31}$$

If (4.22) holds for steps up to and including k, equation (4.31) requires that

$$\frac{z_k z_k^T}{c_k}\, q_j = 0 \qquad j \leq k$$

and hence

$$z_k^T\, q_j = 0 \qquad j \leq k \tag{4.32}$$

This may be proved as follows, from (4.30)

$$z_k^T\, q_j = p_{k+1}^T - q_{k+1}^T\, S_k\, q_j \tag{4.33}$$

For a quadric

$$q_j = Hp_j \quad \text{for all } j \tag{4.34}$$

where H is the true Hessian. Hence

$$z_k^T\, q_j = p_{k+1}^T\, Hp_j - q_{k+1}^T\, p_j \tag{4.35}$$

Taking the transpose of $z_k^T\, q_j$ leaves the value unchanged since it is a scalar,

$$z_k^T\, q_j = p_j^T\, Hp_{k+1} - p_j^T\, q_{k+1}$$

and from (4.34) $Hp_{k+1} = q_{k+1}$, hence

$$z_k^T q_j = 0 \quad j \leq k$$

in accordance with (4.32). It should be noted that (4.31) can only be satisfied for a quadric function. For a general function we assume a local quadratic approximation is valid at each step, but (4.31) does not hold for all previous steps.

The minimization procedure may be summarized as follows:

i) Take a step according to

$$p_{k+1} = - \alpha_k S_k g_k \qquad (4.36)\ (a)$$

ii) Calculate the new gradient g_{k+1} and the gradient change

$$q_{k+1} = g_{k+1} - g_k \qquad (4.36)\ (b)$$

iii) Update the approximation to the inverse Hessian

$$z_k = p_{k+1} - S_k q_{k+1} \qquad (4.36)\ (c)$$

$$c_k = q_{k+1}^T z_k \qquad (4.36)\ (d)$$

$$S_{k+1} = S_k + \frac{z_k z_k^T}{c_k} \qquad (4.36)\ (e)$$

4.3.2 Constrained Minimization

We consider first the case of equality constraints. The problem is to minimize the objective function $f^o(x)$ subject to the constraints

$$f^i(x) = 0, \ i=1, 2, \ldots, m < n \qquad (4.37)$$

where n is the number of variables. A necessary condition for $f^o(x)$ to have a constrained minimum at $\hat{x}$ is that there exists an m-vector $\hat{\lambda}$ such that

$$g^o(\hat{x}) + G(\hat{x})\hat{\lambda} = 0 \qquad (4.38)$$

where $g^o(x)$ is the gradient vector of $f^o(x)$, $G(x)$ is the matrix $[g^1(x), g^2(x), \ldots, g^m(x)]$, and $g^i(x)$ is the gradient vector of the contraint function $f^i(x)$. The elements of $\hat{\lambda}$ are the Lagrange multipliers.

We presume we are at a point x_k and wish to generate a step p_{k+1}, which brings us closer to the solution at $\hat{x}$. Expanding the objective and constraint gradients about x_k gives

$$g^o_{k+1} + G_{k+1}\ \lambda_{k+1} = g^o_k + G_k\ \lambda_{k+1} + (H^o_k + \sum_{i=1}^{m} \lambda^i_{k+1}\ H^i_k)\ p_{k+1} \qquad (4.39)$$

where terms of higher order in p_{k+1} have been neglected, H^o_k and H^i_k are the current approximations to the Hessian matrices of the objective function and constraint functions. Equation (4.39) may be rewritten in terms of the constrained gradient and constrained Hessian

$$g^c_{k+1} - g^c_k = H^c_k\ p_{k+1} \qquad (4.40)$$

or $$q^c_{k+1} = H^c_k\ p_{k+1} \qquad (4.41)$$

where $$g^c_k = g^o_k + G_k\ \lambda_{k+1} \qquad (4.42)$$

and $$H^c_k = H^o_k + \sum_{i=1}^{m} \lambda^i_{k+1}\ H^i_k \qquad (4.43)$$

If equation (4.38) is to be satisfied on the next step g^c_{k+1} must be zero and hence the step p_{k+1} may be calculated from (4.40) as

$$p_{k+1} = -(H^c_k)^{-1}\ g^c_k \qquad (4.44)$$

As in the unconstrained case, it is preferable to use an approximation to the inverse Hessian. To ensure a function decrease we take a scalar multiple of the step, giving

$$p_{k+1} = -\alpha_k\ S^c_k\ g^c_k \qquad (4.45)$$

Equation (4.45) has the same form as (4.20) and the updating of S^c_k S^c_{k+1} is done in an exactly analogous way.

In the constrained case there is the extra, non-trivial, difficulty of evaluating the Lagrange multipliers in equation (4.42). If the constraints are to be satisfied at x_{k+1}, then

$$f(x_{k+1}) = f_{k+1} = 0 \tag{4.45}$$

where f(x) is the vector of constraint function values $[f^1(x), f^2(x), \ldots, f^m(x)]^T$. Expanding the constraint equations in a linear approximation about x_k gives

$$f_{k+1} = f_k + G_k^T p_{k+1} = 0 \tag{4.46}$$

From (4.45) and (4.42)

$$p_{k+1} = - \alpha_k S_k^c (g_k^o + G_k \lambda_{k+1}) \tag{4.47}$$

hence

$$(G_k^T S_k^c G_k) \lambda_{k+1} = \frac{f_k}{\alpha_k} - G_k^T S_k^c g_k^o \tag{4.48}$$

or

$$\lambda_{k+1} = (G_k^T S_k^c G_k)^{-1} \left(\frac{f_k}{\alpha_k} - G_k^T S_k^c g_k^o \right) \tag{4.49}$$

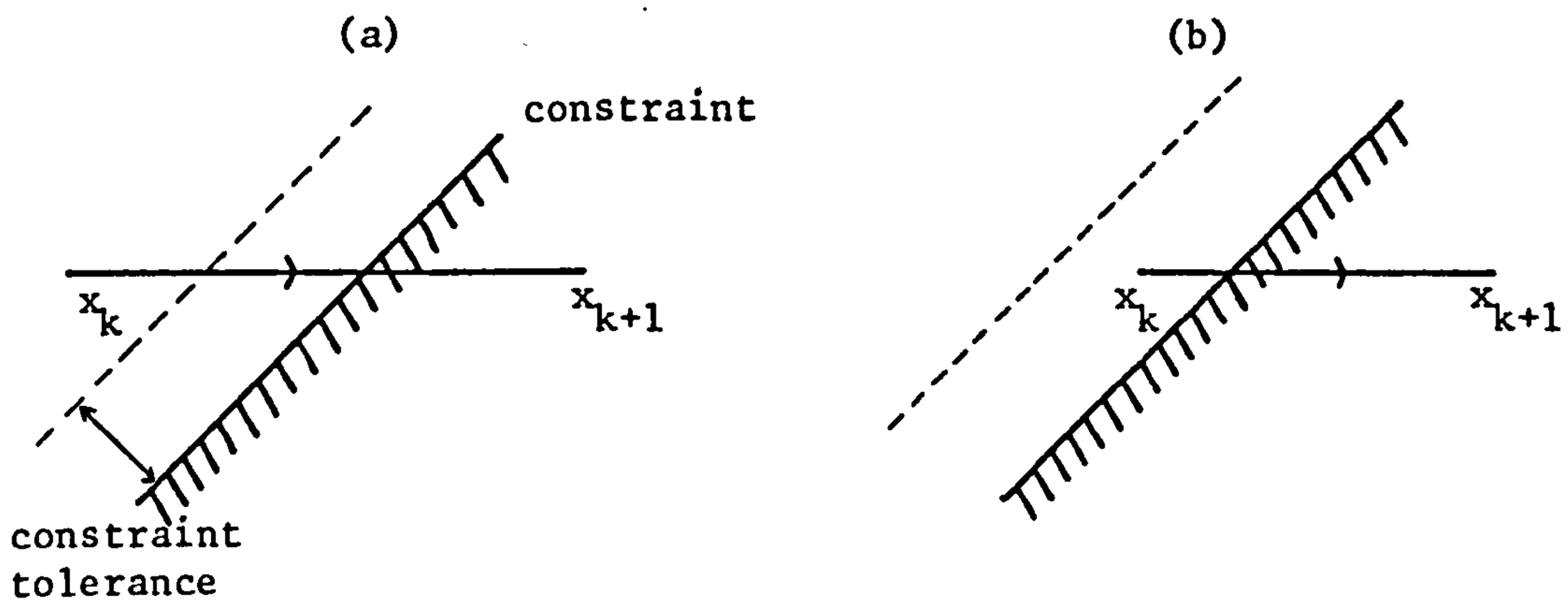
However, if the constraints are nonlinear equation (4.46) will not hold and p_{k+1} generated from (4.47) and (4.49) will not satisfy (4.45). Equations (4.47) and (4.49) are therefore solved iteratively by evaluating the non-linear constraint function f_{k+1} at x_{k+1} at the end of each cycle and then replacing f_k in (4.49) by $(f_{k+1} - G_k^T p_{k+1})$ in the following cycle.

Inequality constraints

To deal with inequality constraints we can apply the procedure for equality constraints, coupled with a strategy for selecting a set of "active" constraints to be treated as equalities. The active set strategy outlined below is described in detail by Sargent and Murtagh {4.5}, and Gaminibandara {4.9}.

Any equality constraints must always be included in the active set. In making the step from x_k to x_{k+1} several situations can arise for an inequality constraint. It both x_k and x_{k+1} are feasible (ie. do not violate the constraint) then the constraint remains inactive. If x_{k+1} is infeasible the action depends on x_k.

Figure 4.1 Infeasible Steps



In Figure 4.1 (a) x_k is outside the constraint tolerance and the step is restricted by adjusting the value of α_k so that it terminates on the constraint, or its linear approximation in the case of a nonlinear constraint. In either case, the constraint remains inactive. If more than one constraint is violated in this way the step with the smallest α_k is selected. For x_k close to the constraint boundary, as in Figure 4.1 (b), the constraint is added to the active set. Adding a constraint causes the step to be projected along the constraint and thus changes the step direction.

Constraints are tested one by one. If one is added to the active set all previously found active inequality constraints are tested to see whether they can be dropped. Dropping a constraint changes the step direction and the Lagrange multipliers, hence constraints must be dropped one at a time followed by recalculation of the multipliers. A constraint may be dropped if this causes an objective function decrease while satisfying the feasibility conditions. An estimate of the objective

function decrease on dropping a constraint may be calculated and the constraint giving the maximum decrease is the one dropped.

4.3.3 Modifications to the V.M.P. Algorithm

The algorithm used originally was that published in {4.9}. To achieve the greatest reliability some modifications were found to be necessary.

Stability Condition

Convergence properties of the V.M.P. algorithm are discussed in {4.5} and {4.10}. In order to prove convergence it is required that the iterations on nonlinear constraints satisfy the constraints exactly, and that a sufficiently large function decrease is obtained on each step. The latter is the so called *stability condition*,

$$f_k^o - f_{k+1}^o > \delta (g_k^o)^T \, p_{k+1} \qquad (4.50)$$

for some $0 < \delta < 1$.

In this work the objective function, constraint functions, and all gradients are themselves the results of iterative calculations. This means that all values are subject to non-zero arithmetic rounding errors and to random errors, or "noise", arising from the way accuracy criteria are applied in the thermodynamic routines. In V.M.P. itself, the nonlinear constraints cannot be satisfied exactly without an infinite number of iterations, finite termination introduces more noise. For the above reasons the modified algorithm permits small *increases* in the objective function, on the assumption that the intended step will decrease the gradients. To avoid degrading the algorithm too far the allowable increase must be just larger than the expected noise level. A limit on the number of function increases is also provided.

Error Criteria

The original has one error criterion for constraint violations, and another for convergence of the whole procedure. The conditions for termination of the algorithm are that the changes in variables, gradients, and objective function values between consecutive steps all fall below

the specified error. The constraint tolerance is used in the active set strategy and for termination of nonlinear constraint corrections.

The functions and variables for the present application are of widely differing magnitudes and, more importantly, the relative errors which can be tolerated are also very different. The number of error criteria has been increased so that each variable and gradient has a separate value specified. The termination test has been modified so that the change in each variable and gradient is tested against its tolerance, but the test on the objective function has been abandoned since increases may be allowed. The constraint tolerance is used as before, but a separate value may now be specified for each constraint function.

Positive - definiteness Failures

A further condition for convergence is that the approximation to the inverse Hessian, S_k, is positive-definite for all k. It may be shown {4.10} that if

$$S_{k+1} = S_k + \frac{z_k z_k^T}{c_k} \qquad (4.51)\ (a)$$

$$\det(S_{k+1}) = \det(S_k)(1 + z_k^T\ S_k^{-1}\ z_k/c_k) \qquad (4.51)\ (b)$$

If S_k is positive-definite it follows that S_{k+1} is positive-definite for any positive c_k. In the original algorithm c_k is set to an arbitrary positive value $(z_k^T\ z_k)$ if the normal rule (4.36) (d) gives a negative value. Although S_{k+1} is positive-definite, the direction of the update to S_k in equation (4.51) (a) is reversed.

Numerical experience has shown that a better strategy is to apply the update with a negative value of c_k but to restrict the magnitude so that S_{k+1} is still positive-definite. As an arbitrary choice we set

$$\det(S_{k+1}) = 0.5\ \det(S_k) \qquad (4.52)$$

From (4.51) (b) and (4.52) we obtain

$$c_k = -2\ z_k^T\ S_k^{-1}\ z_k \tag{4.53}$$

Substituting (4.36) (a), (b), (c) into (4.53) gives

$$c_k = 2(z_k^T\ q_{k+1} + \alpha_k\ z_k^T\ g_k) \tag{4.54}$$

Unfortunately this tends to reduce the magnitude of the next step by a factor of 2. Scaling up S_{k+1} for this step by a factor of 2 overcomes the problem. The updating rule for the determinant becomes

$$\det(S_{k+1}) = \det(S_k)\ 2^{n-1} \tag{4.55}$$

where n is the number of variables. The use of equations (4.54) and (4.55) has proved to be a very effective way of dealing with positive definiteness failures.

Infeasible Starting Points

Convergence can only be proved for a feasible starting point. In {4.9} a feasible point is first found by minimizing the sum of squared constraint violations. Numerical experience has shown that it is much more efficient to apply the normal algorithm immediately, with the provisos that:

i) objective function increases of any magnitude are permitted
ii) there are no iterations on nonlinear constraints
iii) if the current point is still infeasible after 6 steps minimize the sum of constraint violations.

The modified procedure has been used extensively and condition iii) has only been invoked once.

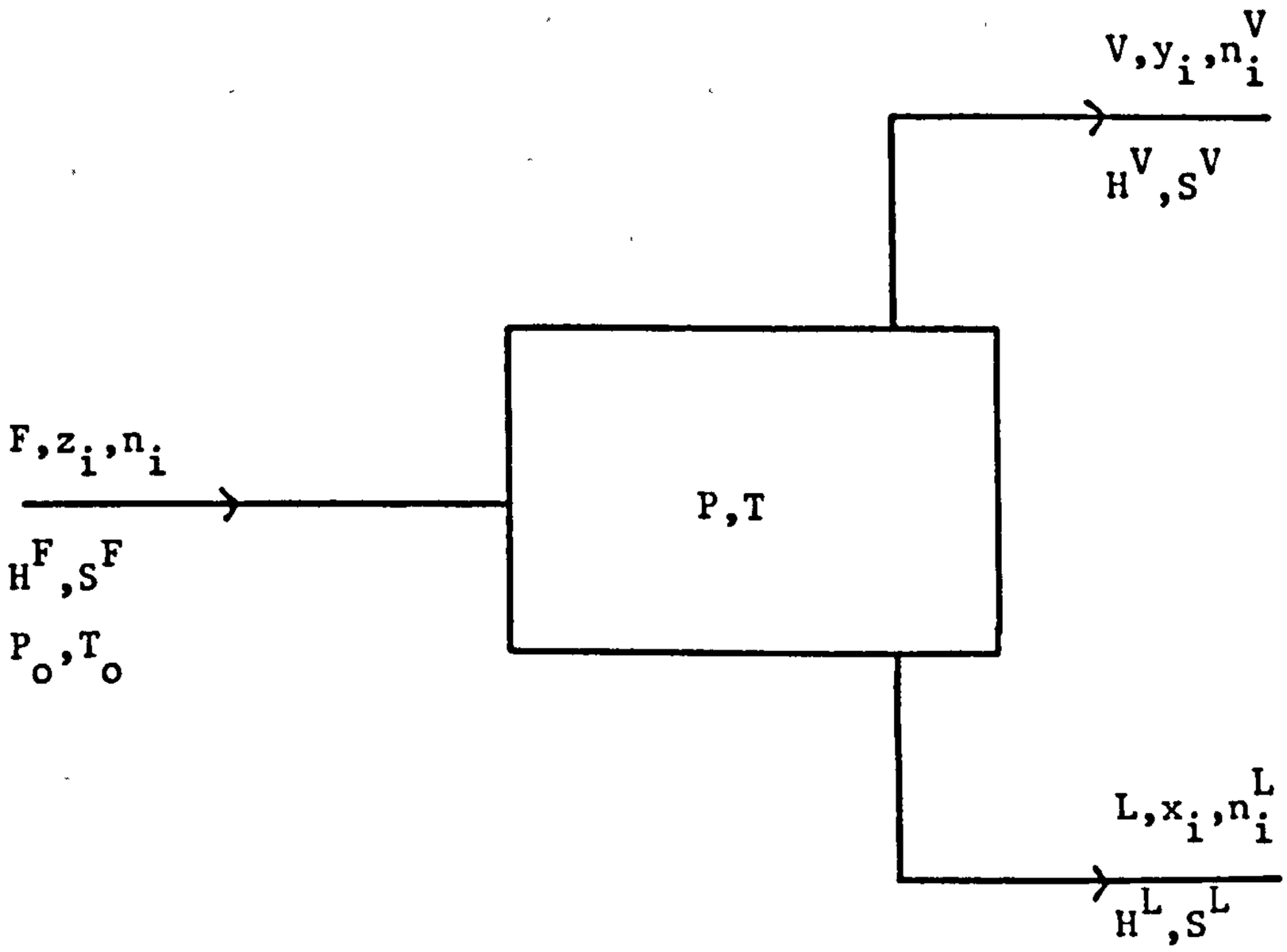
4.4 Formulation of Flash Problems for Minimization

Flash problems in this chapter are formulated in terms of the hypothetical process illustrated in Figure 4.2.

4.4.1 Choice of Minimization Variables

The criteria for equilibrium in section 4.2 determine which function should be minimized according to the conditions imposed. In principle,

Fig. 4.2 Flash process



	Feed	Vapour	Liquid
flow rate	F	V	L
mole fraction of component i	z_i	y_i	x_i
number of moles of component i	n_i	n_i^V	n_i^L
enthalpy	H^F	H^V	H^L
entropy	S^F	S^V	S^L
temperature	T_o	T	T
pressure	P_o	P	P

Basis: one time unit

for a system containing c components, any set of c + 2 independent variables may be selected. For the problems considered in section 4.1 the system pressure is always fixed. The natural choices for the remaining variables are the mole fractions and temperature. In the cases of isenthalpic or isentropic flash calculations the temperature is not known directly and the conditions of constant enthalpy or entropy must be included as constraints.

Composition Variables

A mass balance on the system in Figure 4.2 gives the following:

$$F = V + L \tag{4.56}$$

$$n_i = n_i^V + n_i^L \quad , \quad i = 1,c \tag{4.57}$$

$$z_i = \varepsilon y_i + (1 - \varepsilon)\, x_i \quad , \quad i = 1,c \tag{4.58}$$

where ε is the vapour fraction, defined as

$$\varepsilon = V/F = \Sigma n_i^V \;/\; \Sigma n_i \tag{4.59}$$

$$\left.\begin{aligned} &\Sigma z_i = \Sigma y_i = \Sigma x_i = 1 \\ &z_i = n_i/F \\ &y_i = n_i^V/V \\ &x_i = n_i^L/L \end{aligned}\right\} \tag{4.60}$$

One possible choice for composition variables is (c - 1) mole fractions (say, vapour phase) and the vapour fraction. These variables are subject to the bounds

$$0 \leq y_i \leq 1 \qquad i = 1,c-1$$

$$0 \leq \varepsilon \leq 1$$

From (4.60) we have the linear constraint

$$0 \leq \sum_{i=1}^{c-1} y_i \leq 1$$

and from (4.58) and (4.60) the nonlinear constraints

$$0 \leq \left(\frac{z_i - \varepsilon y_i}{1 - \varepsilon}\right) \leq 1 \qquad i = 1,c-1$$

These constraints are all required if the mole fractions in both phases are to sum to unity and remain in the interval $[0,1]$.

It is much simpler to use mole numbers instead of mole fractions. Again selecting the vapour phase, we have the bounds

$$0 \leq n_i^V \leq n_i \qquad i = 1,c$$

From (4.57) and (4.59) this ensures that

$$0 \leq n_i^L \leq n_i \qquad i = 1,c$$

and $0 < \varepsilon < 1$

No constraint functions are involved. Both sets of composition variables just mentioned are based on the vapour phase. Problems might be anticipated near the bubble point where the amount of vapour phase becomes negligible. In practice, single precision arithmetic on a C.D.C. computer (12 significant figures) is quite adequate to cope with these difficult regions.

4.4.2 Objective Functions, Constraint Functions, and Derivatives

I. Simple Flash - P, T, z specified, calculate x, y, ε

At equilibrium the Gibbs free energy of the system is a minimum. The total Gibbs free energy is made up of contributions from the vapour and liquid phases

$$G = G^V + G^L \tag{4.61}$$

or

$$Fg = Vg^V + Lg^L \tag{4.62}$$

where lower case letters represent molar quantities. From (4.59) we can write the objective function as

$$g = \varepsilon g^V + (1 - \varepsilon)\, g^L \tag{4.63}$$

and $g^V = h^V - T\, s^V$, etc.

For any single phase

$$\left(\frac{\partial G}{\partial n_i}\right)_{P,T,n_j} = \mu_i \tag{4.64}$$

where μ_i is the chemical potential of component i. For our system

$$dG = \sum_{i=1}^{c} \left[\left(\frac{\partial G}{\partial n_i^V}\right)_{n_j^V} dn_i^V\right]_{P,T,n_k} \qquad \begin{matrix} k = 1,c \\ i \neq j \\ j = 1,c \end{matrix} \tag{4.65}$$

From (4.57)

$$dn_i^V + dn_i^L = 0 \tag{4.66}$$

combining (4.65), (4.66) and (4.61), gives

$$\left(\frac{\partial G}{\partial n_i^V}\right)_{P,T,n_j^V} = \left(\frac{\partial G^V}{\partial n_i^V}\right)_{P,T,n_j^V} - \left(\frac{\partial G^L}{\partial n_i^L}\right)_{P,T,n_j^L} \tag{4.67}$$

The chemical potential may be expressed in terms of the fugacity as

$$\mu_i = \mu_i^{\ominus}(T) + RT\, \ln(fug_i/P^{\ominus}) \tag{4.68}$$

where $\mu_i^{\ominus}$ is the standard potential of component i (a function only of temperature), and $P^{\ominus}$ is the standard pressure. From (4.64), (4.67), and (4.68) we obtain

$$\left(\frac{\partial G}{\partial n_i^V}\right)_{P,T,n_j^V} = RT\, \ln\left(\frac{fug_i^V}{fug_i^L}\right) \tag{4.69}$$

In the following discussion feed flow rate is taken as unity and hence $n_i = z_i$.

Formulation of Problem I

variables: n_i^V, i = 1,c

bounds: $0 \leq n_i^V \leq n_i$, i = 1,c

objective function: $g = \varepsilon g^V + (1 - \varepsilon)\, g^L$

objective gradients: $$\left(\frac{\partial g}{\partial n_i^V}\right)_{P,T,n_j^V} = RT \ln\left(\frac{fug_i^V}{fug_i^L}\right)$$

constraints: none

II. Isenthalpic Flash - P_o, T_o, z, P specified, calculate x, y, ε, T

Allowing for an enthalpy change H, the relationship between initial and final states is

$$H^F - \Delta H = H^V + H^L \qquad (4.70)$$

To evaluate H^F, the enthalpy of the initial state, requires a preliminary type I calculation to determine the compositions and amounts of each phase present in the feed. In a truly isenthalpic process ΔH would be set to zero.

At equilibrium the entropy of the system is a maximum, and hence (- entropy) is a minimum.

$$S = S^V + S^L \qquad (4.71)$$

or $s = \varepsilon s^V + (1 - \varepsilon)\, s^L$

For any single phase

$$\left(\frac{\partial S}{\partial n_i}\right)_{P,n_j} = -\left(\frac{\partial \mu_i}{\partial T}\right)_{P,n_k} \qquad \begin{matrix} k = 1,c \\ j \neq i \end{matrix} \qquad (4.72)$$

From (4.66), (4.71) and (4.72), we have

$$\left(\frac{\partial S}{\partial n_i^V}\right)_{P,T,n_j^V} = \left[\left(\frac{\partial \mu_i^L}{\partial T}\right) - \left(\frac{\partial \mu_i^V}{\partial T}\right)\right]_{P,n_k} \tag{4.73}$$

and introducing (4.68) into (4.73) gives

$$\left(\frac{\partial S}{\partial n_i^V}\right)_{P,T,n_j^V} = R\left[\ln\left(\frac{fug_i^L}{fug_i^V}\right) + T\left(\frac{\partial \ln(fug_i^L/fug_i^V)}{\partial T}\right)_{P,n_k}\right] \tag{4.74}$$

The constraint function follows directly from (4.70). Let c_1 be the function defined by

$$c_1 = H^V + H^L \tag{4.75}$$

In general

$$\left(\frac{\partial H}{\partial n_i}\right)_{P,T,n_j} = \mu_i - T\left(\frac{\partial \mu_i}{\partial T}\right)_{P,n_k}$$

$$= -T^2 \left(\frac{\partial \mu_i/T}{\partial T}\right)_{P,n_k} \tag{4.76}$$

Hence from (4.75), (4.76), (4.66), and (4.68)

$$\left(\frac{\partial c_1}{\partial n_i^V}\right)_{P,T,n_j^V} = -RT^2\left(\frac{\partial \ln(fug_i^V/fug_i^L)}{\partial T}\right)_{P,n_k} \tag{4.77}$$

Formulation of Problem II

variables: n_i^V , $i = 1,c$

T

bounds: $0 \leq n_i^V \leq n_i \qquad i = 1,c$

$$T_{\text{bubble point}} \leq T \leq T_{\text{dew point}}$$

objective function: $(-s) = (\epsilon - 1)\, s^L - \epsilon s^V$

gradients: $$-\left(\frac{\partial s}{\partial n_i^V}\right)_{P,T,n_j^V} = R\left[\ln\left(\frac{fug_i^V}{fug_i^L}\right) + T\left(\frac{\partial \ln(fug_i^V/fug_i^L)}{\partial T}\right)_{P,n_k}\right]$$

$$-\left(\frac{\partial s}{\partial T}\right)_{P,n_k}$$

constraint function: $c_1 = \epsilon h^V + (1 - \epsilon)\, h^L$

bounds: $(h^F - \Delta h) \leq c_1 \leq (h^F - \Delta h)$

gradients: $$\left(\frac{\partial c_1}{\partial n_i^V}\right)_{P,T,n_j^V} = -RT^2\left(\frac{\partial \ln(fug_i^V/fug_i^L)}{\partial T}\right)_{P,n_k}$$

$$\left(\frac{\partial c_1}{\partial T}\right)_{P,n_k}$$

III. Isentropic Flash - P_o, T_o, z, P specified, calculate x, y, ϵ, T

Allowing for an entropy change ΔS, the initial and final states are related by

$$S^F - \Delta S = S^V + S^L$$

As in problem II a simple flash is required to calculate the entropy of the feed. The equilibrium condition is a minimum in the system enthalpy.

$$H = H^V + H^L$$

This is identical to (4.75) and the derivatives follow from (4.77). Let the constraint function be defined by

$$c_2 = S^V + S^L$$

and gradients follow from (4.71) and (4.74).

Formulation of Problem III

variables: n_i^V, $i = 1,c$

T

bounds: $0 \leqslant n_i^V \leqslant n_i$ $\quad i = 1,c$

$T_{\text{bubble point}} \leqslant T \leqslant T_{\text{dew point}}$

objective function: $h = \varepsilon h^V + (1 - \varepsilon)h^L$

gradients: $\left(\frac{\partial h}{\partial n_i^V}\right)_{P,T,n_j^V} = -RT^2\left(\frac{\partial \ln(fug_i^V/fug_i^L)}{\partial T}\right)_{P,n_k}$

$\left(\frac{\partial h}{\partial T}\right)_{P,n_k}$

constraint function: $c_2 = \varepsilon s^V + (1 - \varepsilon)\, s^L$

bounds: $(s^F - \Delta s) \leqslant c_2 \leqslant (s^F - \Delta s)$

gradients: $\left(\frac{\partial c_2}{\partial n_i^V}\right)_{P,T,n_j^V} = -R\left[\ln\left(\frac{fug_i^V}{fug_i^L}\right) + T\left(\frac{\partial \ln(fug_i^V/fug_i^L)}{\partial T}\right)_{P,n_k}\right]$

$\left(\frac{\partial c_1}{\partial T}\right)_{P,n_k}$

4.4.3 Zeros of Entropy and Enthalpy

The choice of zeros for both the enthalpy and entropy may be quite arbitrary since only differences in these quantities are measurable. If chemical reactions are to be considered the zeros for all substances must be consistent, but even this is unnecessary for purely physical equilibrium calculations.

In fact, a consistent set of energy zeros *was* used in this work. The PREPROP package described in Chapter 2 uses the following conventions:

> the entropy of a pure substance in its crystalline state at 0 K is taken as zero,
>
> the enthalpy of the elements in their standard states at 298.15 K is taken as zero.

The entropies are conventional in that they exclude contributions from nuclear spin or isotopic mixing. The enthalpy convention gives large numerical values for both enthalpy and free energy. This could cause problems in minimization calculations if large numbers are compared on computers with a small word length.

4.4.4 Minimization in terms of an Allocation Function

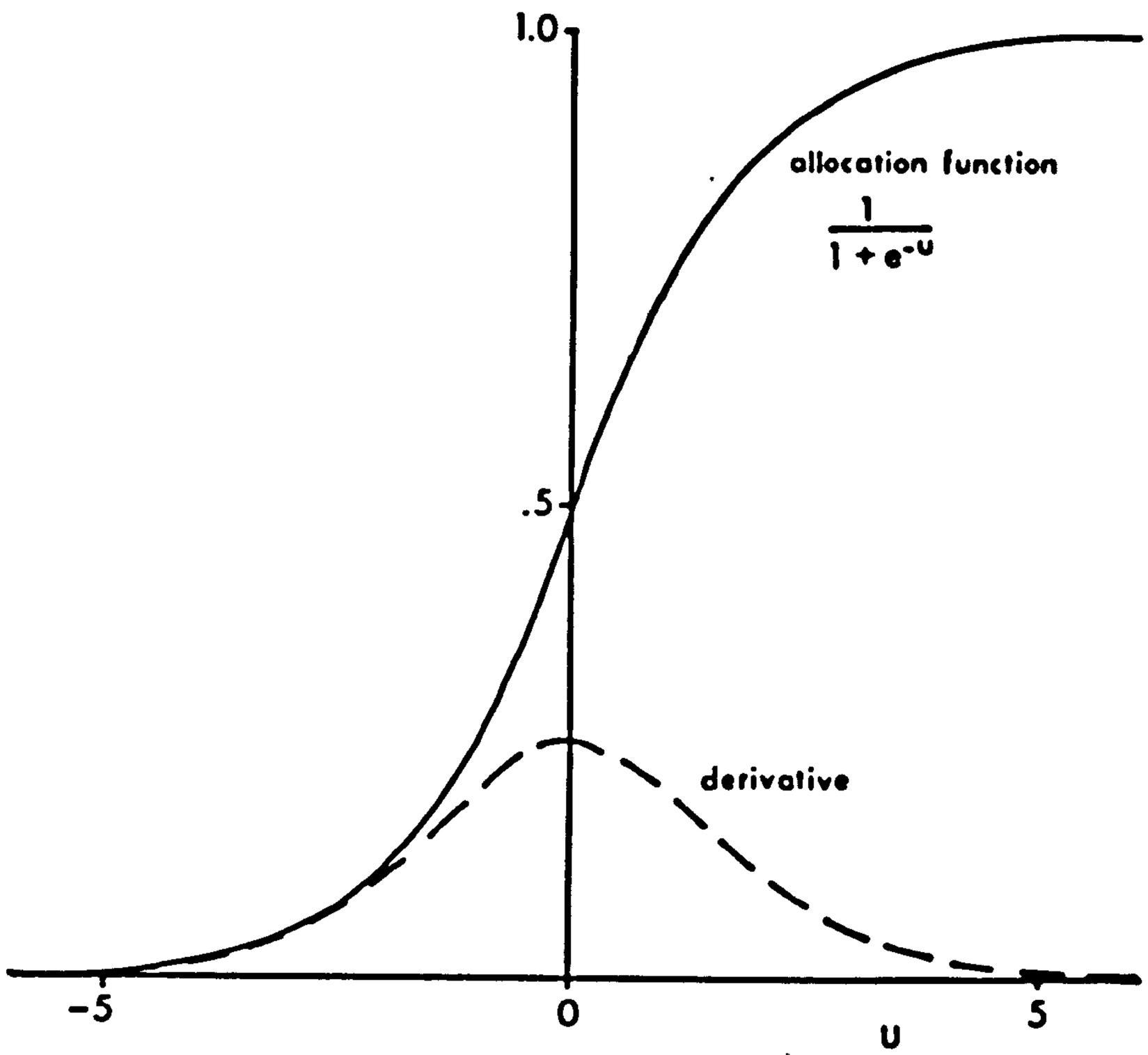
George et al {4.4} have described a method of transforming the Gibbs free energy minimization into an unconstrained problem by using an "allocation function." The allocation function maps an unbounded domain onto a bounded codomain. In particular, the following behaviour is useful

$$\left.\begin{aligned} &0 < \psi(u) < 1 \\ &-\infty < u < +\infty \end{aligned}\right\} \qquad (4.78)$$

where ψ is the allocation function. We can re-write the bounds

$$\left.\begin{aligned} &0 \leq n_i^V \leq n_i && i = 1,c \\ \text{as} \quad &n_i^V = \psi(u_i)\, n_i && i = 1,c \\ \text{or} \quad &u_i = \psi^{-1}(n_i^V/n_i) \end{aligned}\right\} \qquad (4.79)$$

Figure 4.3 ALLOCATION FUNCTION AND DERIVATIVE



If we regard the Gibbs free energy as a function of the unbounded variables u_i we can apply one of the methods for unconstrained minimization. George et al. used the following function,

$$\psi(u) = \frac{1}{1 + \exp(-u)} \tag{4.80}$$

From (4.69), (4.79), and (4.80) we have

$$\left(\frac{\partial g}{\partial u_i}\right)_{P,T,u_j} = \frac{e^{-u_i}}{(1 + e^{-u_i})^2} \, n_i \, RT \, \ln\left(\frac{fug_i^V}{fug_i^L}\right) \tag{4.81}$$

The functions $1/(1 + e^{-u})$ and $e^{-u}/(1 + e^{-u})^2$ are illustrated in Figure 4.3.

Although an allocation function can be used to transform the Gibbs free energy minimization we are still left with a nonlinear constraint in the isenthalpic or isentropic flash problems. A method for dealing with constraints is thus required in any case. This makes the transformation less worth while in a general computational scheme which must deal with all the problems. The performance of the allocation function approach is examined in the next section.

4.5 Computational Procedures

4.5.1 First Estimates

Finding first estimates of the unknown quantities in a vapour-liquid equilibrium calculation can be a difficult problem. In the simulation of an existing plant or when experimental values are being compared with calculations, first estimates are naturally available. In design work, however, this is usually not so and some automatic method for making an estimate must be provided. In this work Raoult's law has been used and provides adequate estimates away from critical and retrograde regions.

Simple Flash

We require an estimate of the compositions and amounts of each phase. According to Raoult's law

$$Py_i = P_i^{\sigma}(T) \, x_i \tag{4.82}$$

Using (4.82) to eliminate the liquid phase mole fractions from (4.58) gives

$$y_i = \frac{z_i}{\varepsilon + \frac{P}{P_i^{\sigma}(T)}(1 - \varepsilon)} \tag{4.83}$$

The vapour pressure of the pure component can be estimated from the equation

$$\ln P^{\sigma} = A - B/T \tag{4.84}$$

The constants in (4.84) can be determined from the definition of the acentric factor in equation (2.22) and a knowledge of the critical properties, hence

$$\ln\left(\frac{P^c}{P^{\sigma}}\right) = \frac{7}{3}\ln(10)(1 + \omega)\left(\frac{T^c}{T} - 1\right) \tag{4.85}$$

This equation gives a reasonable extrapolation for $T > T^c$ and can thus be used for all components including supercritical ones.

The mole fractions calculated from equation (4.83) must sum to unity

$$\sum_i y_i = \sum_i \frac{z_i}{\varepsilon + \frac{P}{P_i^{\sigma}(T)}(1 - \varepsilon)} = 1 \tag{4.86}$$

Equation (4.86) is not usually monotonic in ε. The PREPROP equation solving routine (section 2.2.8) is designed not to pass turning points and hence it cannot be used directly. The procedure used is to guess ε and solve (4.86) for T, this temperature will not in general be equal to the system temperature. The value of ε is adjusted until the temperatures are consistent. Alternatively, the bisection method could be used to solve (4.86) directly for ε. The value of ε calculated on the basis of Raoult's law is restricted to the interval $[0.1, 0.9]$ in an attempt to ensure that the minimization always starts from within the two-phase region.

Isenthalpic or Isentropic Flash

In these problems the temperature, composition, and amounts of each phase must be estimated. The pressure is fixed and hence the dew and bubble point temperatures may be calculated. For any system at fixed pressure and overall composition the enthalpy and entropy always increase with temperature. The enthalpies (or entropies) of the dew and bubble point are bounds on the enthalpy (or entropy) of any two-phase mixture. If a mixture is found to be single phase, its composition is known and the temperature may be solved for by starting at the dew or bubble point and making adjustments until the calculated enthalpy (or entropy) is equal to that specified.

In a two-phase mixture the vapour fraction can be estimated by assuming a linear variation in ethalpy (or entropy) between the dew and bubble points. Using this value of ε equation (4.86) can be solved for the temperature. It is possible that the temperature calculated in this way will not be between the dew and bubble point values. Some correction must be made and one simple method is to use the same linear interpolation as for the vapour fraction. The steps in the procedure are set out in section 4.5.4.

4.5.2 Scaling

There is an implicit assumption in general minimization procedures that all the variables, functions, and gradients are of a similar magnitude. If some gradients are much larger than others the problem is transformed into a multidimensional equivalent of a steep-sided valley, a notoriously difficult case in minimization.

In the simple flash problem all variables are moles of components in the vapour phase. The variables are in the interval $[0,1]$ and the gradients are similar unless a very small amount of a substance is present. In the isenthalpic or isentropic flash problems the variables are compositions and temperature. The temperature derivatives are a factor of $10^2 - 10^3$ times smaller than the composition derivatives. When constraints are present it is the *projected gradient* in equation (4.42) which is important. Again, the objective function gradient and constraint gradients should be similar.

Practical experinece has shown that the simple flash calculation usually performs well without any scaling whilst convergence is slow or non-existent for the more complex problems if scaling is not used. The principle of scaling variables and functions is demonstrated as follows, if we have a function

$$f = f(x_1, x_2, \ldots, x_n)$$

and gradients

$$g_i = (\partial f/\partial x_i)$$

the variables x may be transformed to scaled variables x' by

$$x_i' = x_i/s_i$$

where s_i is a scalar constant. We must have

$$f(x_1, x_2, \ldots) = f'(x_1', x_2', \ldots)$$

and hence

$$g_i' = (\partial f'/\partial x_i') = s_i\, g_i$$

If the function is also scaled so that

$$f' = f/s_f$$

then $g_i' = s_i\, g_i/s_f$

In this way it is possible to scale all the variables and functions in order to adjust the gradients. Although, in general, there are more gradients than scale factors no problem occurs in practice since all the composition gradients tend to be of a similar magnitude.

The procedure used in this work was to calculate scaling factors based on gradients at the starting point. A simpler method using fixed scaling factors works reasonably well but there is no computational penalty involved in evaluating the gradients since they can be used in the first step of the minimization procedure. Scaling is carried

out so that all the gradients of the contraint function are in the interval [0,1] with the temperature derivative of constraint and objective functions equal to unity. In practice this ensures that all the objective function gradients are also in a similar interval.

Scaling Algorithm

1. Evaluate objective function gradients and constraint function gradients at the starting point.

2. Set CSCALE, the constraint function scale factor, to the maximum of the absolute constraint gradients:

$$\text{CSCALE} = \max |g_i|$$

3. Set TSCALE, the temperature scale factor, to make the temperature derivative of the constraint equal to unity:

$$\text{TSCALE} = |\text{CSCALE}/(\partial f/\partial T)|$$

4. Set OSCALE, the objective function scale factor, to make the temperature derivative of the objective function equal to unity:

$$\text{OSCALE} = |\text{TSCALE}(\partial f^{o}/\partial T)|$$

4.5.3 Derivatives

The flash problems are formulated for a minimization approach in section 4.4.2. In the case of the simple flash the gradients are expressed in terms of fugacities, which are relatively simple to calculate. The remaining problems require, in addition, the following derivatives

$$\left(\frac{\partial s}{\partial T}\right)_{P,n_k} , \quad \left(\frac{\partial h}{\partial T}\right)_{P,n_k} , \quad \left(\frac{\partial \ln(fug_i^V/fug_i^L)}{\partial T}\right)_{P,n_k}$$

Analytic expressions for these quantities are complex and the computational effort is probably not worth while. In this work a simple forward difference approximation was used for the derivatives, e.g.

$$\left(\frac{\partial s}{\partial T}\right) \approx \frac{s(T + \delta T) - s(T)}{\delta T} , \text{ etc.}$$

where δT is a temperature increment.

With the PREPROP package very little extra work is involved in evaluating the derivatives. The entropy, enthalpy, and fugacities are all calculated in any case whenever an objective function or constraint function value is required. Both objective function and constraint function gradients are needed at the same conditions and only once per iteration in V.M.P. Hence, only one extra function evaluation is required for a full set of derivatives. A temperature increment of 0.001 K has proved satisfactory. Larger values may be used at the start of a minimization, but accurate gradients are required in the neighbourhood of a minimum. Clearly, a minimum cannot be located to an accuracy greater than the finite difference increment.

4.5.4 Complete Algorithms

The algorithms in this section correspond to the computer routines VLEQM and FLASH which will be found in Appendix A.

I. Simple Flash

Given pressure, temperature, number of components, component identifiers, and overall composition.

1. Set initial values for thermodynamics routines, e.g. number of components, pressure, etc.
   If input phase is unknown, go to step 2., if input is two-phase, go to step 3., otherwise go to step 4.

2. Calculate dew and bubble point temperatures and compare with input temperature. If input is single phase go to step 4.

3. Make first estimates of vapour fraction and composition of the two-phase mixture (see section 4.5.1).

4. Set initial values of shape factors etc.
   If input is single phase go to step 8.

5. Set optimization parameters: bounds on variables, maximum number of function evaluations, termination and error criteria, etc.
   Go to step 7.

6. Starting point when user-supplied first estimates are available.

7. Minimize Gibbs free energy using V.M.P..
   If calculation was successful, go to step 9., otherwise set error flag and stop.

8. Calculate enthalpy, entropy, etc. of the single phase.

9. Calculate all mole fractions and the vapour fraction from mole numbers, put all values into the correct locations, stop.

II. Isenthalpic or Isentropic Flash

The procedure for either case is exactly analogous, the isenthalpic flash is described bleow. Given the overall composition, final pressure, and either the temperature and pressure of the initial state, or its enthalpy h*. A non-zero value for Δh, the enthalpy change in the process, may also be set.

1. If the enthalpy of the input stream is specified go to step 2(b).

2(a) Do a "simple flash" calculation to determine the enthalpy.

(b) Set the constraint value, cl = h* - Δh.

3. Determine the phases present in the final state

(a) Calculate dew point temperature T_{dew}, and enthalpy H_{dew}. If cl > H_{dew}, go to step 3(c).

(b) Calculate bubble point temperature T_{bub}, and enthalpy H_{bub}. If cl > H_{bub}, go to step 4(a).

(c) Final state is single phase, iterate on temperature until calculated enthalpy is equal to cl, stop.

4. First estimates for the two-phase mixture.

(a) Estimate vapour fraction assuming linear variation of enthalpy across the two-phase region

$$\varepsilon = (cl - H_{bub})/(H_{dew} - H_{bub})$$

(b) Estimate temperature and composition by solving equation (4.86) for T.

(c) If the estimated temperature is outside the two-phase region apply a correction

$$T = T_{bub} + \varepsilon(T_{dew} - T_{bub})$$

(d) Set bounds on composition variables.

5. Scale the temperature, enthalpy, and entropy (see section 4.5.2), set bounds on temperature.

6. Set optimization parameters.

7. Minimize (- entropy) using V.M.P.
If calculation was successful, go to step 8., otherwise set error flag and stop.

8. Calculate mole fractions, vapour fraction, etc., stop.

4.6 Computational Performance

No calculated results in terms of temperatures, compositions, etc., are given here. Whether calculated values agree with experimental results is a test of the particular method of generating the thermodynamic data and not of the computational procedure. A calculation is considered "successful" if fugacities of components in the two phases are equal to within a specified tolerance (10^{-5} of the fugacity in the tests reported below).

4.6.1 Comparison of performance

The computational efficiency may be best compared on the basis of "function evaluations". A function evaluation is defined as a complete calculation of fugacities, enthalpy, and entropy for both phases. Not all of these properties may be required, but in the corresponding states procedure all are evaluated simultaneously at no extra cost. Each evaluation of the objective function, constraint function or gradients requires one function evaluation.

Table 4.1 Number of function evaluations required for vapour-liquid equilibrium calculations

Number of Components	Dew/Bubble	Simple Flash	Isenthalpic/ isentropic flash
2	5 - 6	8 - 13	13 - 24
4	5 - 6	24 - 26	24 - 26
5	6 - 8	13 - 25	26 - 40
8	5 - 9	30 - 50	30 - 60

Table 4.1 shows the performance measured for several mixtures. The number of function evaluations dependes very much on the conditions, compositions, and types of substances in the mixture. A great number of iterations are required when the mixture contains only a trace amount of gas or liquid. The calculations are more difficult if the components of a mixture are of widely differing volatilities.

In all cases the minimum in the objective function is very shallow. In the isenthalpic and isentropic calculations the temperature and amounts of each phase are correlated; many combinations of temperature

and composition can give very nearly the same energy. The finite difference increment in temperature must therefore be small enough to give accurate gradients.

A sensitivity analysis was carried out by perturbing various constants in the thermodynamics package. Although the positions of the minima were affected the changes were not large. The problem of locating the minimum seems to be a numerical one rather than a feature of the thermodynamics.

The influence of first estimates on the number of function evaluations required was investigated for the simple flash. For mixtures containing components of similar volatility the quality of first estimates had a strong influence on claculation times. As expected, for better estimates fewer evaluations were necessary. When the components were of widely differing volatility better first estimates sometimes increased the number of evaluations; only when the estimate was very close to the solution was a substantial decrease observed. For such mixtures it seems that a unit matrix is not a very good approximation to the inverse Hessian and the initial steps generated by V.M.P. must be very small in order to obtain an objective function decrease.

4.6.2 Allocation function method

The implementation of the allocation function discussed in section 4.4.4 requires trivial changes to the algorithms given. Some trials were made on the simple flash problem. The method performed well in some cases and badly in others, requiring from one half to twice the number of function evaluations required by direct minimization. The reliability tended to be low, often no solution could be found or an incorrect solution was accepted.

The allocation function and its derivative are illustrated in Figure 4.3 and it is evident how automatic bad scaling can occur. If any component is present in large or small amount, the value of u is numerically large and the gradient $(\partial\psi/\partial u)$ is small. Components with smaller values of u will have much larger gradients and hence there is little chance of ever having gradients of similar magnitudes. The

gradients of the Gibbs free energy in equation (4.81) are multiplied by $(\partial\psi/\partial u)$ and so the product may be small even if fugacities are not equal. Spurious solutions are thus possible.

The allocation function introduces some fundamental problems of reliability and offers little advantage, particularly if any additional constraints are introduced. The use of such methods cannot be recomended on the basis of computational experience in this work.

Table 5.1 Classical critical constants for hydrogen

T^c/K	ρ^c/mol m^{-3}	Z^c	Reference
36.92	19390	.291*	This work
43.6	19417	.291*	Gunn et al. {5.5}
46.9	21335	.284	de Boer {5.2}

* Arbitrary choice.

CHAPTER 5

HYDROGEN AND HYDROGEN-CONTAINING MIXTURES

5.1 Introduction

The quantum fluids hydrogen, helium, and neon form an important class of substances excluded from the simple corresponding states treatment outlined in Chapter 2. Due to weak intermolecular forces these substances remain in the fluid state at very low temperatures. The small molecular masses mean that a classical approximation to the partition function is not valid down to the triple point, as is the case for most other substances.

It is not the intention here to include all the fluid states of quantum gases in a corresponding states treatment. A series of papers by de Boer and co-workers {5.1, 5.2, 5.3, 5.4} covers the fundamentals. In the chemical and petroleum industries it is common to find hydrogen as part of a mixture at temperatures well above the critical temperature of pure hydrogen. In these cases classical behaviour can be expected and the mixture should conform to the simple corresponding states principle. in both liquid and vapour phases.

As pointed out by de Boer {5.2} the experimentally determined critical parameters cannot legitimately be used to give reduced quantities for quantum fluids at high temperatures since the phase transitions are also influenced by quantal effects. Effective, or "classical", pseudo-critical parameters for quantum fluids have been suggested before and those developed here for hydrogen are compared with two other sets in Table 5.1.

Gunn et al. {5.5} fitted temperature dependent parameters to compressibility factor data and the table shows the high temperature limits. The values credited to de Boer are implied by his reduced critical values based on intermolecular potential parameters.

Since this work is concerned with conditions for which the classical limiting values of the critical parameters should apply, no temperature dependence was included. The region of interest was restricted to temperatures exceeding 50K and the pseudo-critical parameters were fitted

Table 5.2 Numerical values for coefficients in equation (5.1)

Coefficient	
C_1	$.207366566000099 \times 10^{2}$
C_2	$.418461204975099 \times 10^{-2}$
C_3	$-.754099517852711 \times 10^{-4}$
C_4	$.192804503191338 \times 10^{-6}$
C_5	$-.221012317954670 \times 10^{-9}$
C_6	$.123950006389127 \times 10^{-12}$
C_7	$-.273671864804350 \times 10^{-16}$
C_{11}	1.515
C_{14}	512.

Values are for heat capacity in J mol $^{-1}$ K^{-1} and temperature in K.

to data for pure hydrogen. The resulting critical parameters were then used to predict properties in hydrogen-hydrocarbon mixtures for one phase conditions and for vapour-liquid equilibrium.

5.2 Perfect Gas Heat Capacity for Hydrogen

To calculate thermal properties by the corresponding states principle requires values of the properties in the perfect gas state (see section 2.2.5). A convenient representation is an equation for the isobaric heat capacity of the perfect gas as a function of temperature. An equation of the form

$$C_p^o = C_1 + C_2T + C_3T^2 + C_4T^3 + C_5T^4 + C_6T^5 + C_7T^6 + \frac{C_{11}x^2e^x}{(e^x - 1)^2} \qquad (5.1)$$

where $x = C_{14}/T$, was fitted to the data tabulated by Hilsenrath et al. {5.6}. The coefficients in equation (5.1) are given in Table 5.2. The data is represented to within the accuracy of the tables over the range 10 - 1000 K. Up to 1400 K the maximum deviation is 0.7%.

5.3 Effective Critical Parameters for Hydrogen

5.3.1 Fitting Strategy

The parameters needed for a corresponding states representation of hydrogen are the critical density ρ^c, critical temperature T^c, critical compressibility factor Z^c, and acentric factor ω. From the point of view of fitting experimental data ρ^c and Z^c cannot be varied independently since they both have a direct influence on the calculated density of the reference substance, through the shape factor equations (2.21) and (2.20), and equation (2.18). The critical compressibility was fixed at the "normal fluid" value of 0.291.

The three independent parameters, ρ^c, T^c, and ω, were fitted to P-V-T data for pure hydrogen. The data used were taken from the review by Wooley et al. {5.7} and the experimental work of Michels et al. {5.8}, totalling 2100 points covering temperatures from 50 K to 600 K and densities up to 38000 mol m^{-3} (pressures to 90 MPa).

The fitting was done by minimizing a sum of squares defined by

$$S = \sum_{i=1}^{N} (Z_i^{cal} - Z_i^{exp})^2 = S(T^c, \rho^c, \omega)$$

where N is the number of data points and the difference is between the calculated and experimental compressibility factor at given density and temperature. S is a non-linear function of the parameters and the minimization procedure used was the modified variable metric projection method described in Chapter 4. The calculation is ill-conditioned, with a near singular Hessian matrix, but converges rapidly with the new procedure for maintaining positive definiteness.

5.3.2 Results

The results presented here were obtained using the corresponding states procedure and equations of state described in Chapters 2 and 3. Equations C, D, and E developed in Chapter 3 produced essentially identical values for the critical parameters and acentric factor, in fact the numbers in Table 5.3 are based on equation (D) of Chapter 3.

Table 5.3 Critical parameters and acentric factor for hydrogen

Set	T^c/K	ρ^c/mol m^{-3}	Z^c	ω	RMS % deviation in Z*	Bias**
I	37.49	19125	.291	.131	0.89	-5.8
II	36.52	19304	.291	.04	0.90	-7.8
III	36.92	19490	.291	.04	0.99	0.

* RMS % deviation = $100 \times \sqrt{\dfrac{\sum_{i=1}^{N} [(Z_i^{exp} - Z_i^{cal})/Z_i^{exp}]^2}{N}}$

** Bias = $\sum_{i=1}^{N} (Z_i^{exp} - Z_i^{cal})$

Three sets of parameters are shown. Set (I) corresponds to an unconstrained minimum, but on physical grounds the acentric factor is unreasonably large. The acentric factor of nitrogen is 0.04 and setting this as an upper bound in the minimisation gives the parameter sets (II) and (III).

Set (II) gives a smaller sum of squares but the calculated compressibility factors are mostly larger than the experimental ones. Set (III) parameters were constrained to give a zero bias and, since the goodness of fit was hardly affected, this set was chosen for subsequent use.

The fit to within 1% is considered satisfactory in view of the very wide range of data used, the error is up to 10% at the lowest temperatures and highest densities but is otherwise generally below 0.5%. As a first check on how well the pseudo-critical parameters would represent hydrogen in mixtures the compressibility factor data of Mihara et al. {5.9} were compared with predictions, results are shown in Table 5.4.

Table 5.4 Comparison of predicted and experimental compressibility factors in hydrogen-hydrocarbon mixtures

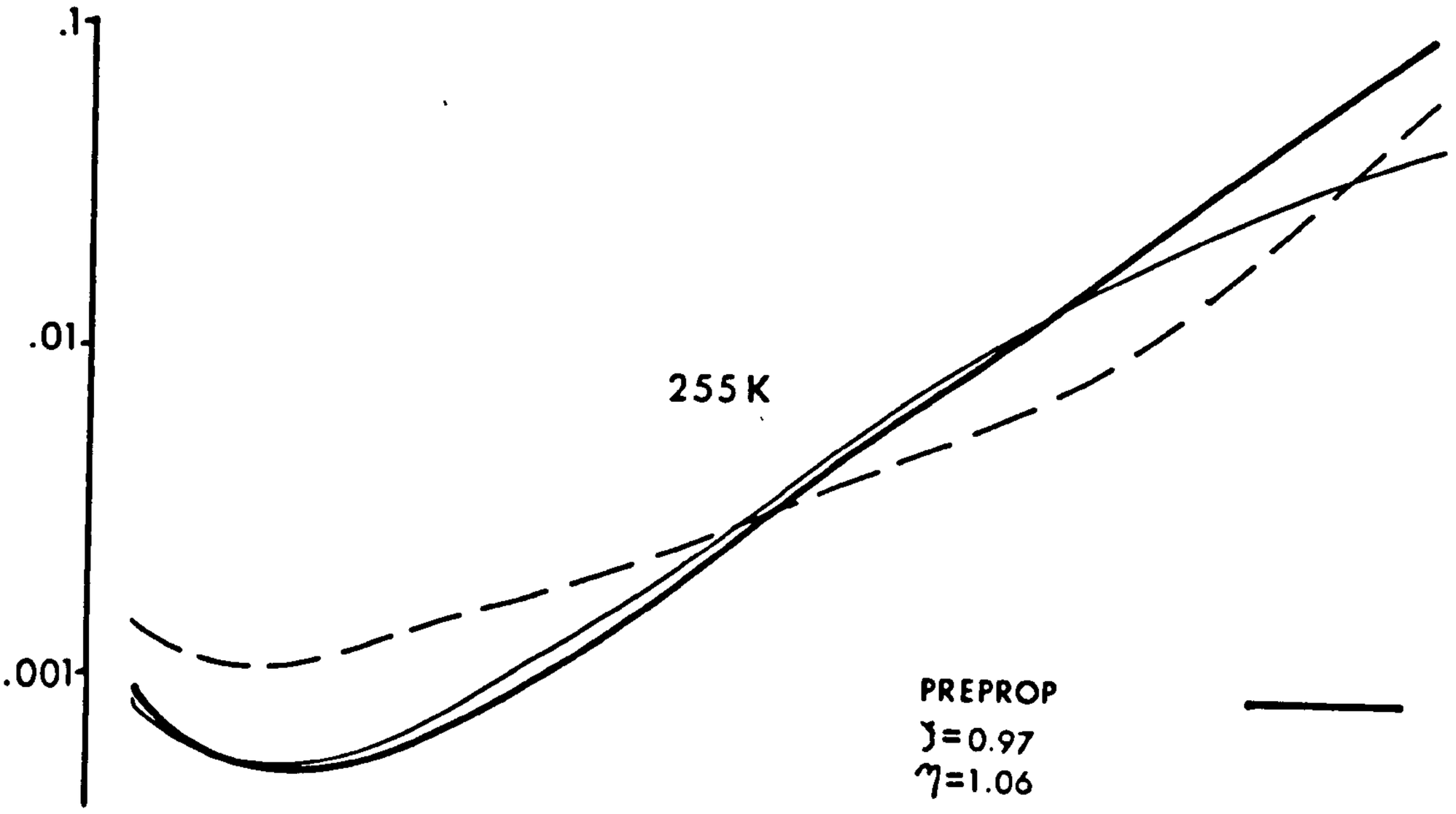
(Temperature range 298K - 348K)

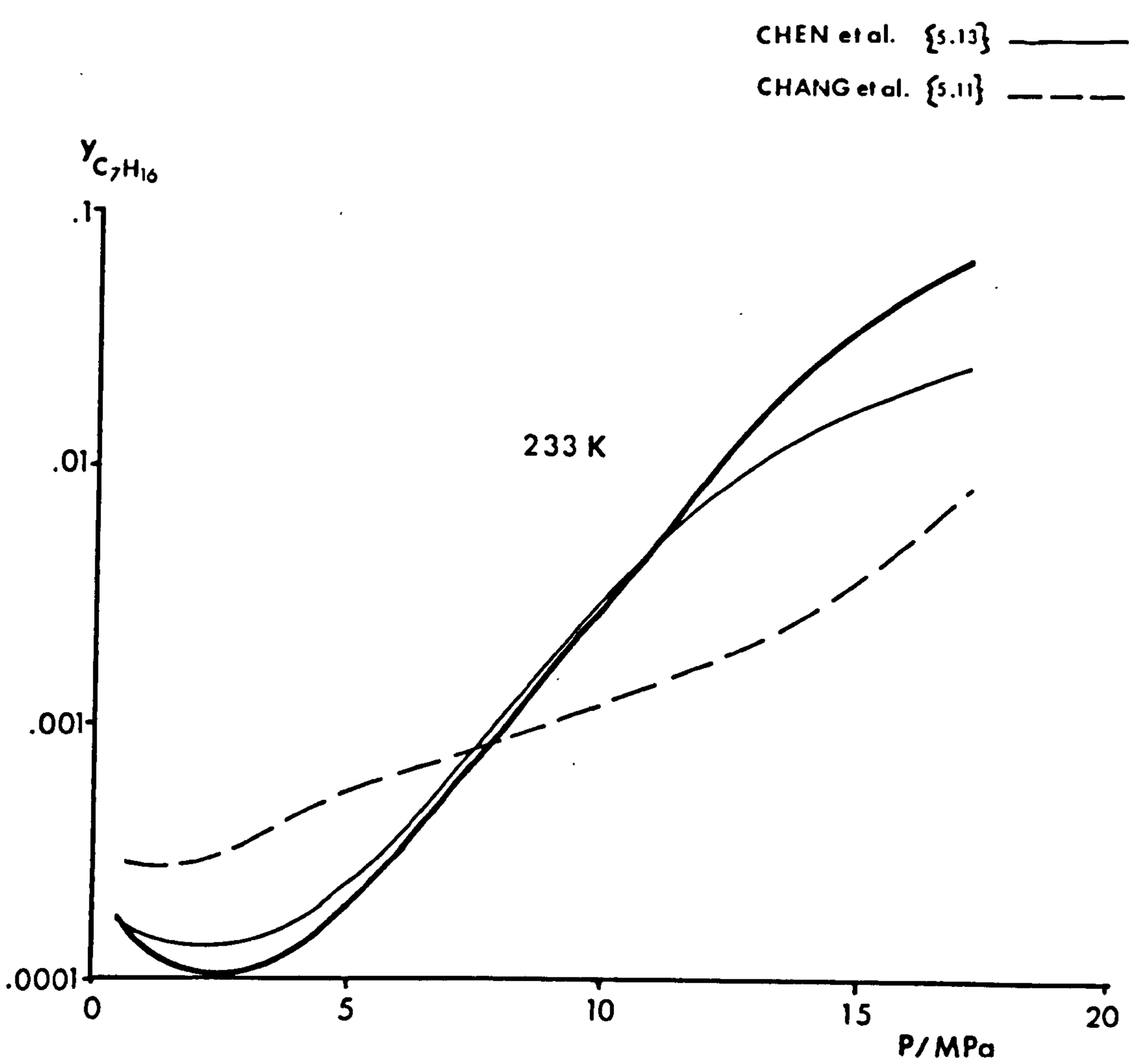
System	P range/MPa	No. Points	R.M.S. % deviation in Z (a)	(b)
Pure H_2	.3 - 8.5	45	0.10	0.10
Pure CH_4	.3 - 8.6	47	0.10	0.10
H_2-CH_4	.2 - 9.2	153	0.20	0.11
H_2-C_2H_6	.3 - 9.3	154	0.83	0.54
H_2-C_3H_8	.3 - 5.1	72	0.48	0.34

Interaction parameters: (a) unity (b) see Table 5.8

Calculated compressibility factors are not sensitive to the binary interaction parameters (for definition see equations (2.24)) and no attempt was made to fit "best" values to volumetric data. The experimental uncertainty is about 0.1% and the agreement shown in Table 5.4 is quite satisfactory.

Figure 5.1 DEW POINT COMPOSITIONS FOR METHANE - HEPTANE MIXTURES





5.4 Vapour-Liquid Equilibrium in Hydrogen-Hydrocarbon Mixtures

5.4.1 Introduction

Hydrogen-hydrocarbon mixtures are examples of systems containing a heavy and a very light component. Experimental difficulties in carrying out vapour-liquid equilibrium measurements on these systems are considerable since the amount of heavy component in the vapour phase is very small. Even small errors in the measurement of vapour composition may represent 100% of the amount of heavy component present. The experimental problems are discussed in some detail by Gunn et al. {5.10}.

In the following sections a system which ought to be well represented by the corresponding states principle (methane-heptane) is first examined to give some idea of the accuracy which can be expected in mixtures of light and heavy components. The available data for hydrogen-hydrocarbon systems is then compared with predictions.

5.4.2 Vapour-Liquid Equilibria in the Methane-Heptane System

The only experimental work in which the temperature, pressure, and compositions of both phases were measured simultaneously is that of Chang, Hurt, and Kobayashi {5.11}. They give 69 experimental points at temperatures from 200K to 255K and pressures from 0.7 MPa to 20.7 MPa. These data were compared with predictions and agreement can only be described as extremely poor. Using the "accepted" values {5.12} for the binary interaction parameters, $\xi = 0.90$ and $\eta = 1.0$, solutions to bubble point calculations could only be obtained for 32 points and composition deviations averaged nearly 200%. Other values of interaction parameters gave only minor improvements. It is interesting to note that Chang et al. quote mole fractions to five decimal places and claim a maximum error of 5% of the amount present.

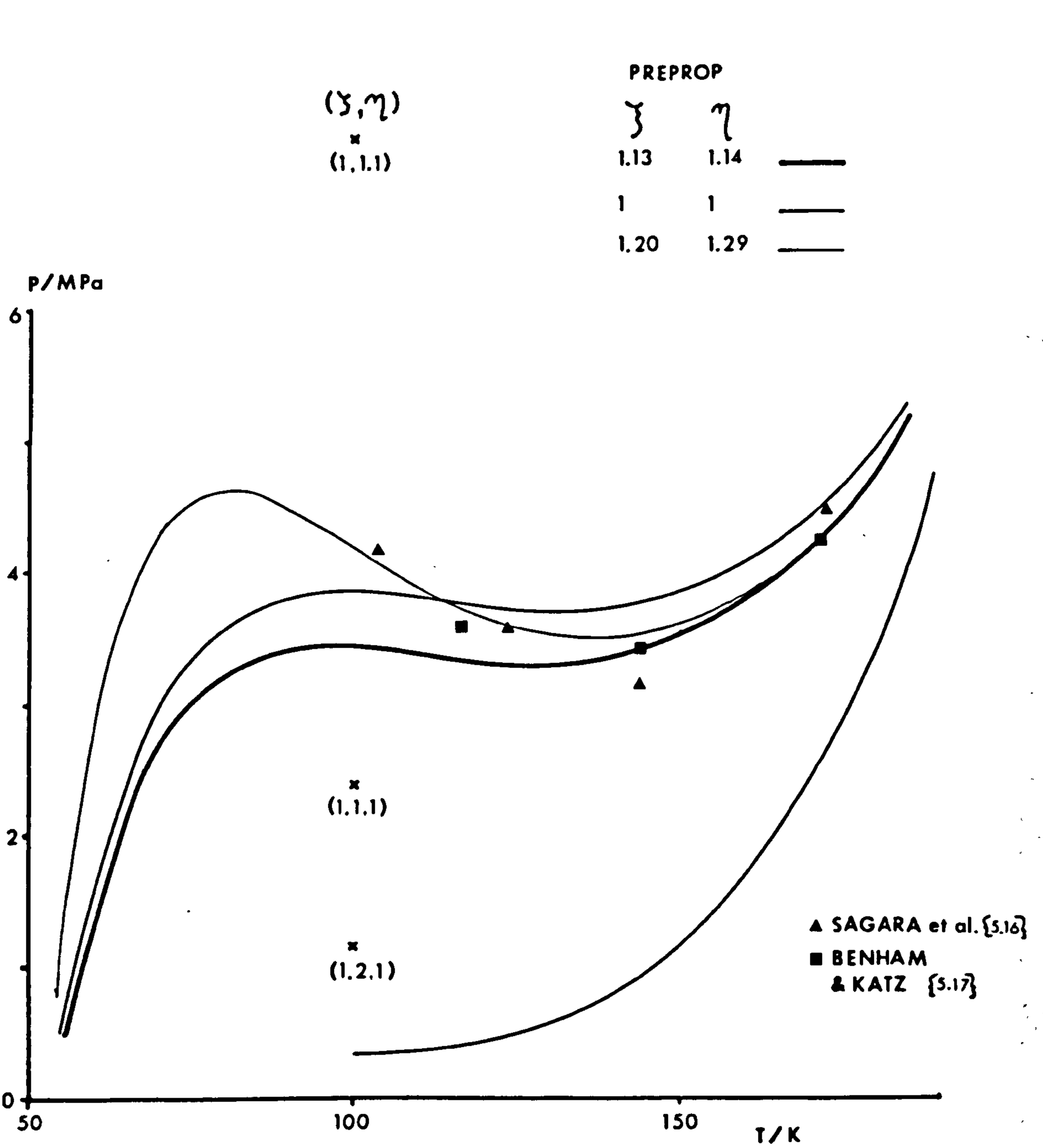
In a more recent paper Chen et al. {5.13}, of the same laboratory, state that the earlier work was erroneous. The new dew point compositions are compared with the original values in Figure 5.1. The difference is up to 90% at 255K and up to 440% at 233K, again a high accuracy of 2% or 0.00001 mole fraction is claimed. Combining the new vapour phase compositions with the original liquid phase data for the two isotherms in common gives better agreement with predictions, as shown in Table 5.5 and Figure 5.1.

Table 5.5 Pressure and composition deviations in bubble point calculations for methane-heptane mixtures

(Isotherms at 233K and 255K, 26 experimental points {5.11}, {5.13})

Interaction Parameters		No. of Solutions found	R.M.S. % deviation	
ξ	η		Pressure	Heptane composition
1.0	1.0	25	37	60
0.9	1.0	14	190	1455
0.97	1.0	26	23	33
0.97	1.06	26	7	17

Figure 5.2 Experimental and predicted V–L equilibria for a $CH_4 - H_2$ mixture (0.9663, 0.0337)



A further indication of possible accuracies in data for such systems is provided by Lin et al. {5.14} who compare the data of Chen et al. {5.13} for methane-hexane dew points with compositions measured by chromatography. The agreement is not better than ± 0.001 in mole fraction. The mean absolute deviation in composition for the best parameters in Table 5.5 is 0.00008 mole fraction.

It seems that uncertainties in the data make meaningful comparisons of experimental and predicted results difficult, at least for the methane-heptane system. There is no reason to suppose that the experimental problems are any less severe for hydrogen-hydrocarbon mixtures as under most conditions there will be little of the heavy component in the vapour phase. The results in Table 5.5 provide a context for similar comparisons in the case of hydrogen containing mixtures.

5.4.3 Hydrogen-Hydrocarbon Mixtures

The problem of how experimental data and predictions of vapour-liquid equilibrium can best be compared is discussed by Clark and Koppany {5.15}. A flash calculation at specified temperature and pressure would be the ideal since both can be measured with good accuracy. Unfortunately, almost no experimental values of overall composition and vapour fraction are available. To generate such data by picking an arbitrary vapour fraction and doing a mass balance is unsatisfactory because it leads to a comparison based on uncertainties in both the liquid *and* vapour phase data. The experimental data is reported on isotherms and vapour phase compositions are subject to the greatest error, therfore the comparisons here are all on the basis of bubble point pressure calculations. The data used are summarised in Table 5.6.

Some predictions for the methane-hydrogen system are shown on P-T co-ordinates in Figure 5.2 together with the interpolated experimental data. Even with interaction parameters set to unity retrograde behaviour is observed at conditions far removed from the critical. This strange phenomenon was first pointed out by Kay {5.25} for hydrogen-naphtha mixtures, and he also showed it to be present in the ammonia-hydrogen and ammonia-nitrogen systems. At certain pressures up to three bubble points are shown in Figure 5.2 but in practice the maximum in the bubble point curve is not observed because the mixture freezes.

Table 5.6 Experimental data for hydrogen-hydrocarbon systems

System	T/K	P/MPa	No. of points	Reference
H_2-CH_4	103 - 174	2.0 - 10.8	28	5.16
	116 - 172	3.4 - 27.5	13	5.17
	88	1.7 - 16.9	11	5.18
H_2-C_2H_4	123 - 248	2.0 - 8.0	22	5.16
	158 - 255	1.7 - 13.8	22	5.19
H_2-C_2H_6	148 - 223	2.0 - 8.0	16	5.16
	144 - 283	1.7 - 13.8	23	5.19
H_2-C_3H_6	198 - 248	2.0 - 8.0	12	5.20
	200 - 297	1.7 - 13.8	20	5.19
H_2-C_3H_8	173 - 348	1.7 - 13.8	32	5.21
	172 - 297	1.7 - 13.8	24	5.19
H_2-n-C_4H_{10}	200 - 302	2.2 - 16.5	18	5.22
	328 - 394	2.8 - 16.8	60	5.23
CH_4-C_2H_4	198 - 248	1.0 - 6.1	12	5.16
CH_4 -C_3H_6	173 - 248	2.0 - 8.1	9	5.20
H_2-CH_4-C_2H_4	123 - 248	2.0 - 8.1	97	5.16
H_2-C_2H_4-C_3H_6	148 - 223	2.0 - 8.1	80	5.16
H_2-CH_4-C_3H_6	198 - 248	2.0 - 8.1	48	5.20
	200	3.4	2	5.17
H_2-C_2H_4-C_3H_8	173 - 248	2.0 - 8.1	37	5.20
H_2-C_3H_6-C_3H_8	173 - 248	2.0 - 8.1	49	5.20
H_2-CH_4-C_2H_6	144, 200	3.4, 6.9	15	5.24
H_2-CH_4-C_3H_8	144 - 255	3.4 - 6.9	28	5.17

Table 5.7 Comparison of calculated and experimental bubble point data for binary systems

System	Reference	R.M.S. % deviations ($\xi = \eta = 1.0$) P	y_1	y_2	Best values for interaction parameters ξ	η	R.M.S. % deviation (for best parameters) P	y_1	y_2
H_2-CH_4	5.16	23	23	27	1.20	1.29	8	3	9
	5.17	37	17	25	1.13	1.14	8	8	8
	5.18	59	1	53	*				
H_2-C_2H_4	5.16	21	9	36	1.08	1.01	24	5	25
	5.19	26	14	29	1.08	1.01	14	9	19
H_2-C_2H_6	5.16	25	4	41	1.11	1.01	22	2	25
	5.19	32	15	30	1.11	1.01	16	10	17
H_2-C_3H_6	5.20	14	1	65	*				
	5.19	32	11	30	1.11	1.0	18	5	16
H_2-C_3H_8	5.21	29	20	27	1.1	1.01	22	15	27
	5.19	23	5	29	1.1	1.01	23	3	16
H_2-n-C_4H_{10}	5.22	23	1	43	1.1	1.0	21	.5	31
	5.23	47	21	40	1.18	0.97	12	13	23
CH_4-C_2H_4	5.16	6	5	8	.975	1.00	3	3	5
CH_4-C_3H_6	5.20	8	2	53	*				
CH_4-C_7H_{16}	5.11,5.13	37	0	60	.97	1.06	7	0	17

* no parameters improve fit, data probably in error.

Great sensitivity to the binary interaction parameters is seen on the bubble point locus, the dew points are hardly affected since a trace of hydrogen in the vapour phase implies an essentially one component system. Sensitivity of dew point calculations may be observed in Figure 5.3 when the system contains more hydrogen. Three points plotted in Figure 5.2 for a temperature of 100K show calculated bubble points for pairs of interaction parameters (ξ, η). Values of $\eta > 1$ are required to reproduce the degree of retrograde behaviour found experimentally. The two parameters have opposite effects and unusual values are required to fit all the experimental data. In the case of hydrogen-methane the parameters (1.20, 1.29) fit the data of Sagara et al. {5.16} very well (see Figure 5.3), but not the data of Benham and Katz {5.17}. The two sets of data are not entirely consistent (see Figure 5.2) but the parameters (1.13, 1.14) fit both sets of binary data and also the data for ternary systems.

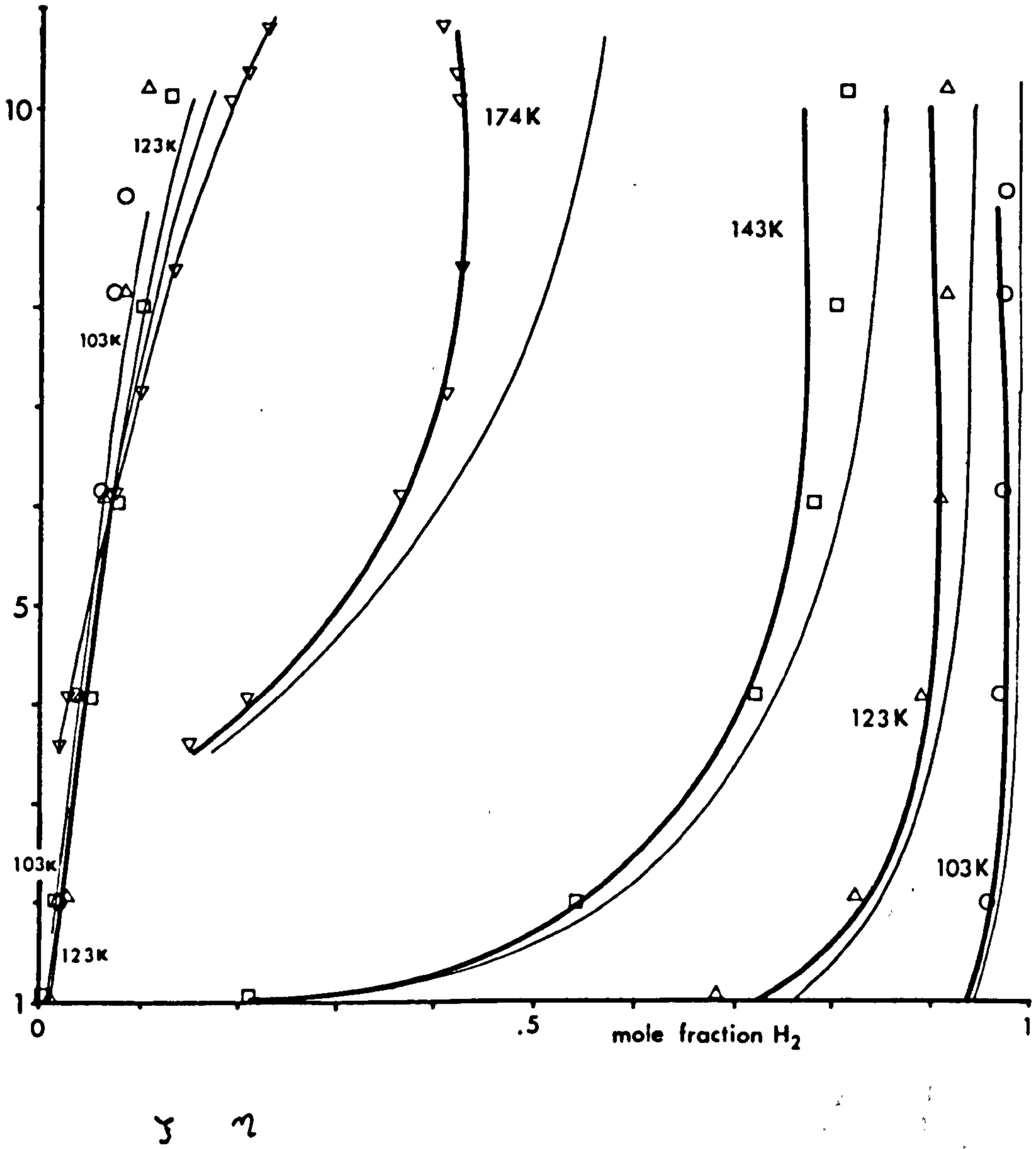
Hydrogen-propane is an example of a system for which no parameters fit the data well. Some of the vapour phase data are compared with calculations in Figure 5.4. The parameters (1.1, 1.01) are not significantly better than unity for the binary system but are better for the ternaries.

Comparisons of calculated and experimental data for binary systems are summarised in Table 5.7 and the binary interaction parameters used in the ternary systems are listed in Table 5.8. A comparison of predicted and experimental data for the ternary systems is in Table 5.9. General

Table 5.8 Binary interaction parameters used in ternary systems

System	ξ	η
H_2-CH_4	1.13	1.14
H_2-C_2H_4	1.08	1.01
H_2-C_2H_6	1.11	1.01
H_2-C_3H_6	1.11	1.0
H_2-C_3H_8	1.10	1.01
CH_4-C_2H_4	0.975	1.0
CH_4-C_2H_6	1.0	1.0
CH_4-C_3H_6	0.99	1.0
CH_4-C_3H_8	0.99	1.0
C_2H_4-C_2H_6	0.99	1.0
C_2H_4-C_3H_6	0.99	1.0
C_3H_6-C_3H_8	1.0	1.0

Figure 5.3 V-L EQUILIBRIUM IN THE HYDROGEN-METHANE SYSTEM



	γ	η	
PREPROP	1	1	———
	1.2	1.29	———

Sagara et al. {5.16} ○△□▽

Figure 5.4 DEW POINTS FOR HYDROGEN – PROPANE MIXTURES

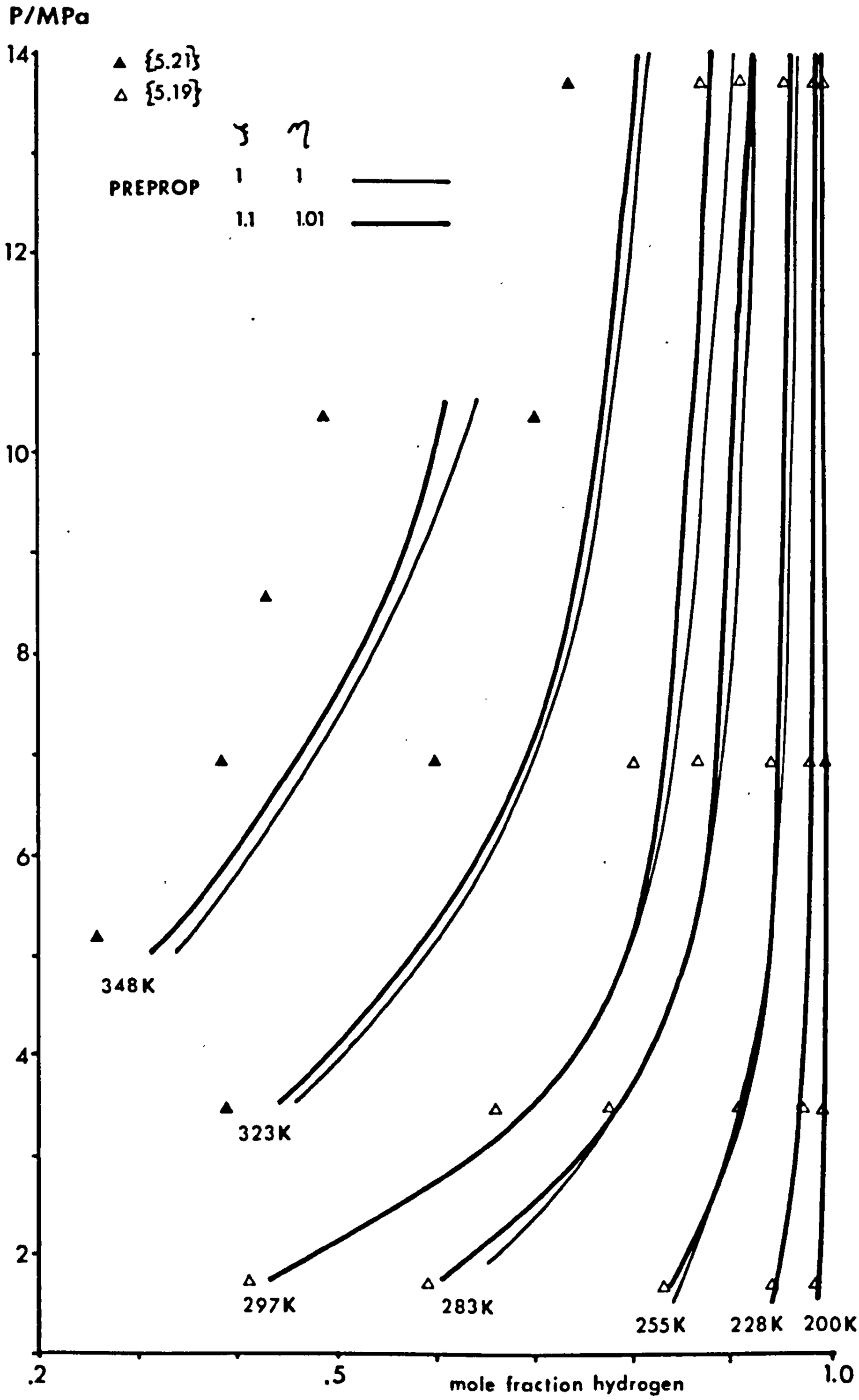


Table 5.9 Comparison of Predicted and Experimental bubble point data of ternary systems

System	Reference	P	R.M.S. % deviation y_1	y_2	y_3
H_2-CH_4-C_2H_6	5.16	13	11	11	27
H_2-C_2H_4-C_3H_6	5.16	22	4	16	27
H_2-CH_4-C_3H_6	5.20	51	17	14	64
	5.17	28	26	5	31
H_2-C_2H_4-C_3H_8	5.20	14	4	13	19
H_2-C_3H_6-C_3H_8	5.20	28	0.5	28	24
H_2-CH_4-C_2H_6	5.24	10	7	15	29
H_2-CH_4-C_3H_8	5.17	12	13	15	27 *

* Excluding 2 points for which the data are in error.

comments on the results are included in the next section but two details should be disposed of immediately.

The data of Freeth and Verschoyle {5.18} on the hydrogen-methane system does not fit in with the other data. The measurements were carried out at 88K in an apparatus designed for P-V-T work and hence the accuracy is probably not equal to that of the later work.

Both binary and ternary systems containing propene show poor agreement between experiment and calculations. The methane-propene system in particular should be well represented by the corresponding states principle and the discrepancy here must be due to poor measurements. Unfortunately no other data for this system could be found. The data of Sagara et al. {5.20} for propene containing systems should be treated with caution.

5.5 Discussion

It is clear that the experimental P-V-T data for hydrogen can be adequately represented over a wide range of conditions using pseudo-critical parameters and the corresponding states principle. Under most conditions the predictions are well within the accuracy required for engineering purposes. The same is true for mixture P-V-T data.

The results are not so good for vapour-liquid equilibrium. Standards for comparison are provided by the methane-ethene and methane-heptane systems for which results are included in Table 5.7. For the hydrogen-methane system the predictions are probably within experimental errors and inconsistencies but this is less likely to be so for the other data. Although the absolute accuracy of the experimental data is not known - for compositions the claims usually made refer to reproducibility - it seems unlikely that the uncertainties can account for all the poor results.

The unusually high values for the binary interaction parameters found in the fitting exercise require some comment. There is no fundamental reason why the interaction parameters should not be substantially different for hydrogen containing mixtures and hydrocarbon mixtures. What is disturbing is the lack of a trend from substance to substance and the generally poor fit, which indicate that the parameters are merely compensating for shortcomings elsewhere in the theory. During the course of the work described in Chapter 3 some doubts arose as to the validity of the Leach shape factor equations (equations (2.21)) at high reduced temperatures. Most of the data for hydrogen is at reduced temperatures above 1.5 and any anomalous behaviour would clearly influence the results here.

An indication that shape factors *are* causing problems comes from the need to constrain the fitted value of the acentric factor to keep it physically reasonable. According to the Leach equations the shape factors are nearly constant for reduced temperatures exceeding 2.0, the limiting values being related to the acentric factor. If these limiting values are incorrect then this would be compensated for in the fitted acentric factor.

Saville {5.26} has compared shape factors from Leach's equations with values calculated from pure component data on methane and several other substances. At high temperatures the Leach shape factors are poor, in particular the volume correction ϕ has the wrong deviation from unity. Above a reduced temperature of 1.3 and below 3.0 the following equations represent the shape factors of nitrogen relative to a methane reference

$$\theta_{io} = 1 + (\omega_i - \omega_o)\left[\frac{2.472}{T^R} - 2.210\right] \qquad (5.2)$$

$$\phi_{io} = \frac{Z_o^c}{Z_i^c}\left[1 + (\omega_i - \omega_o)\left(2.884 - \frac{3.858}{T^R}\right)\right] \qquad (5.3)$$

Assuming that these equations may be extrapolated to higher temperatures, and repeating the unconstrained fit of pseudo-critical parameters to the pure hydrogen data, gives the following results (results from Table 5.3 are in parentheses):

T^c/K	35.045	(36.92)
ρ^c/mol m^{-3}	16208	(19490)
ω	-0.067	(0.04)
R.M.S. deviation in Z	0.5	(0.99)

The results of vapour-liquid equilibrium calculations for some binary mixtures, using these parameters and the modified shape factors, are presented in Table 5.10.

Table 5.10 Comparison of calculated and experimental bubble point data for some binary systems - using modified shape factors

System	Reference	Best values for interaction parameters		R.M.S. % deviation		
		ξ	η	P	y_1	y_2
H_2-CH_4	5.16	1.25	1.11	7	5	7
	5.17	1.23	1.06	11	5	12
H_2-C_2H_6	5.16	1.42	1.12	7	1	24
	5.19	1.37	1.07	3	6	8
H_2-C_3H_8	5.21	1.41	1.09	7	11	17
	5.19	1.46	1.13	3	1	13
H_2-C_4H_{10}	5.22	1.45	1.07	12	.5	30
	5.23	1.53	1.09	6	9	13

Both sets of data for each system could be well represented by a single pair of parameters, except hydrogen-butane where the data are not consistent. The values of the interaction parameters are large but the trend is reassuring.

Although agreement is considerably improved, the results here can only be treated as provisional since it is becoming clear that a much more detailed investigation of the shape factor equations is really required. Something intermediate between Leach's equations and equations (5.2) and (5.3) would presumably give a more realistic acentric factor for hydrogen and provide a better starting point for looking at the vapour-liquid equilibria.

CHAPTER 6

Conclusions

The corresponding states procedure developed in this work represents a considerable advance in terms of reliability, accuracy, range of predictions, and efficiency. The components of the procedure, as it stands, have been extended to their limits and some basic problems are becoming obvious.

For small molecules and their mixtures the corresponding states principle is very accurate and reliable. It must be emphasised, however, that values of the binary interaction parameters are required for any practical application. The precision may be lower for mixtures of large and small molecules. There is some doubt as to the quality of experimental results but even more uncertainty is associated with the van der Waals one-fluid theory of mixtures. There is good theoretical and experimental evidence {6.1, 6.2} to support the theory when the molecular size differences are not large. But the computer simulation results only extend to a diameter ratio of 1.15, corresponding to a volume ratio of about 1.5. This value may be compared with a critical volume ratio of about 4.4:1 for heptane:methane. More experimental data are required to determine whether the existing theory is applicable in such cases. Computer simulations are the most useful source of data since exact results can be obtained for any given model.

The validity of the Leach shape factor equations (2.21) has been questioned repeatedly in this work. It is clear that the present correlations are inadequate at both high and low temperatures. Experimental data of exceedingly high accuracy are required to determine values of shape factors with reasonable precision. These data do not exist for molecules which are appreciably non-spherical. Improved shape factor equations are urgently required and once again it seems that the necessary data must be obtained from computer simulations. Work is continuing in this area.

It was stated in the introduction that theoretically based methods are not yet in a position to deal with all substances of industrial interest. Polar molecules are an obvious example. These have been treated with some success recently by applying a perturbation theory {6.3, 6.4}. In the case of polar mixtures the perturbation is applied to a mixture of non-polar molecules which is itself handled by corresponding states. It is therefore a relatively simple matter to incorporate the perturbations into the existing procedures. However, even without these perturbations and by assuming that polarity has the same effect on the vapour pressure curve as does a non-spherical molecular shape, the results are often surprisingly accurate, particularly at high temperatures. In general, however, molecular shape and polarity both make separate contributions to "shape" factors. It is logical to try and find shape factors as functions of shape and polarity but there remains the problem of disentangling the two effects on bulk properties. Some good results have been obtained for several ammonia containing mixtures {6.5} but a general correlation is required. An obvious way of separating the shape and polarity effects is by simulation experiments.

Although the computation times for corresponding states calculations have been reduced dramatically it is unlikely that times can be further reduced by more than a factor of two. The shape factor calculations are very time consuming and any new formulation should be chosen to increase the efficiency of this step. It is probable that the corresponding states procedure will always be slower than a simple correlation such as the Chao-Seader, but at least the two are comparable and the greater reliability of corresponding states will often be more important.

The use of minimization procedures to calculate vapour-liquid equilibrium has produced some encouraging results. The reliability and efficiency of the existing algorithms is already high, but the method and its implementation are still under active development. Suggestions were made in section 2.3.3 for extending the range of vapour-liquid equilibrium calculations to the critical point and it is hoped to include the modifications in future versions of the thermodynamic package.

References

Chapter 1

1.1 Redlich, O., and J.N.S. Kwong, Chem. Rev., 44, 233 (1949).

1.2 Benedict, M., G.B. Webb, and L.C. Rubin, J. Chem. Phys., 8, 334 (1940).

1.3 Bender, E., The calculation of phase equilibria from a thermal equation of state, Müller, Karlsruhe (1973).

1.4 Wilson, G.M., J. Am. Chem. Soc., 86, 127 (1964).

1.5 Renon, H. and J.M. Prausnitz, A.I.Ch.E. Journal, 14, 135 (1968).

1.6 Pitzer, K.S., J. Chem. Phys., 7, 583 (1939).

1.7 Rowlinson, J.S., Trans. Faraday Soc., 50, 647 (1954).

Chapter 2

2.1 Bett, K.E., J.S. Rowlinson, and G. Saville, Thermodynamics for Chemical Engineers, Ch.9, Athlone Press, London (1975).

2.2 Rowlinson, J.S. and I.D. Watson, Chem. Engng. Sci, 24, 1565 (1969).

2.3 Leach, J.W., P.S. Chappelear and T.W. Leland, A.I.Ch.E. Journal, 14, 568 (1968).

2.4 Leland, T.W., J.S. Rowlinson and G.A. Sather, Trans. Faraday Soc., 64, 1447 (1968).

2.5 Gunning, A.J., Ph.D. Thesis, University of London (1972).

2.6 Watson, I.D. and J.S. Rowlinson, Chem. Engng. Sci., 24, 1575 (1969).

2.7 Hastings, C.(Jr.), Approximations for digital computers, Princeton Univ. Press, Princeton, N.J. (1955).

2.8 Lees, B., Computer Aided Design Centre, Cambridge, private communication (1978).

2.9 Thompson, P.A., J. Chem. Eng. Data, 22, 431 (1977).

2.10 Mollerup, J., Advan. Cryog. Eng., 20, 172 (1975).

2.11 Saville, G., Department of Chemical Engineering, Imperial College, London, S.W.7., private communication (1978).

2.12 Chao, K.C. and J.D. Seader, A.I.Ch.E. Journal, 7, 598 (1961).

2.13 Motard, R.L., H.M. Lee and R.W. Barkely, CHESS (Chemical Engineering Simulation System) Users' Guide, Unive. of Houston, Dept. of Chem. Eng., Report RE9-69 (1969).

2.14 Gunning, A.J. and J.S. Rowlinson, Chem. Engng. Sci., 28, 521 (1973).

2.15 Cines, M.R., J.T. Roach, R.J. Hogan and C.H. Roland, Chem. Eng. Prog. Sym. Series, 49, 4 (1953).

2.16 Fussell, D.D. and J.L. Yanosik, paper presented at the 51st Annual Fall Technical Conference of the Society of Petroleum Engineers of A.I.M.E., New Orleans (1976).

2.17 Broydon, C.G., Math. Comp., 19, 577 (1965).

2.18 Angus, S., B. Armstrong and K.M. de Reuck, International Thermodynamic Tables of the fluid state - 6. Nitrogen, Pergamon Press, Oxford (in press).

2.19 Angus, S., B. Armstrong and K.M. de Reuck, International Thermodynamic Tables of the fluid state - 5. Methane, Pergamon Press, Oxford (1978).

2.20 Yorizane, M., S. Yoshimura, H. Masuoka, A. Toyama, Y Nakako and I. Funada, Chem. Engng. Sci., 33, 641 (1978).

2.21 Wilson, G.M., P.M. Silverberg and M.G. Zellner, Advan, Cryog. Eng., 10, 192 (1965).

2.22 Narinskii, G.B., Kislorod, 10, 9 (1957).

2.23 Gaminibandara, G.G.K.K., Ph.D. Thesis, University of London (1976).

2.24 Howath, A.L., Physical properties of inorganic compounds, Edward Arnold, London (1975).

Chapter 3

3.1 Gunning, A.J. and J.S. Rowlinson, Chem. Engng. Sci., 2, 521 (1973).

3.2 Leach, J.W., P.S. Chappelear and T.W. Leland, A.I.Ch.E. Journal, 14, 568 (1968).

3.3 Bender, E., The calculation of phase equilibria from a thermal equation of state, Müller, Karlsruhe (1973).

3.4 Angus, S., Guide to the correlation of experimental thermodynamic data on fluids, I.U.P.A.C. Thermodynamics Tables Project Centre, Imperial College, London, S.W.7. (1978).

3.5 Siebe, D.A., An equation of state representing the P-ρ-T properties of argon as tabulated by the International Union of Pure and Applied Chemistry, University of Idaho College of Engineering (1975).

3.6 Stewart, R.B. and R.T. Jacobsen, Preliminary thermodynamic property formulation for oxygen, Centre for Applied Thermodynamic Studies Report No. 76-5, University of Idaho (1976).

3.7 Pollak, R., The thermodynamic properties of water, I.U.P.A.C. Thermodynamic Tables Project Centre, London (1976).

3.8 Angus, S., B. Armstrong and K.M. de Reuck, International Thermodynamic Tables of the fluid state - 5. Methane, Pergamon Press, Oxford (1978).

3.9 Angus, S., B. Armstong and K.M. de Reuck, Internation Thermodynamic Tables of the fluid state - 6. Nitrogen, Pergamon Press, Oxford (in press).

3.10 Encyclopedie Des Gaz, L'Air Liquide, Division Scientifique, Elsevier Scientific Publishing Co., Amsterdam (1976).

3.11 McCarty, R.D., A modified Benedict - Webb - Rubin equation of state for parahydrogen, NBSIR 74 - 357 (1974).

3.12 Robertson, S.L. and S.E. Babb, J. Chem. Phys, 51, 1357 (1969).

3.13 Deffet, L., L. Lialine and F. Ficks, Industrie chim. belge, 9, 879 (1964).

3.14 Roe, D.R., Ph.D. Thesis, University of London (1972).

3.15 Pope, G.A., Ph.D. Thesis, Rice University, Houston, Texas (1972).

3.16 Epperley, A.D., Ph.D. Thesis, University of Missouri, Colombia (1970).

3.17 Wagner, W., A new correlation method for thermodynamic data applied to the vapour-pressure curve of argon, nitrogen and water, I.U.P.A.C. Thermodynamic Tables Project Centre, London (1977).

3.18 Armstrong, B. and K.M. de Reuck, to be published.

3.19 Angus, S., B. Armstrong and K.M. de Reuck, International Thermodynamic Tables of the fluid state - 7. Propene (in preparation).

3.20 Goodwin, R.D., H.M. Roder and G.C. Straty, Thermophysical peoperties of ethane from 90 to 600 K at pressures to 700 bar, N.B.S. Technical Note 684, Boulder, Colorado (1976).

3.21 Goodwin, R.D., Summary of the nonanalytic equation of state for propane, Cryogenics Division, N.B.S.,Boulder, Colorado (1977).

Chapter 4

4.1 Van Zeggeren, F. and S.H. Storey, The Computation of Chemical Equilibria, Cambridge University Press, Cambridge (1970).

4.2 Dluzniewski, J.H. and S.B. Adler, I. Chem. E. Symposium series No. 35, Instn. Chem. Engrs., London (1972).

4.3 Ma, Y.H. and C.W. Shipman, A.I.Ch.E. Journal, 18, 299 (1972).

4.4 George, B., L.P. Brown, C.H. Farmer, P. Buthod, and F.S. Manning, Ind. Eng. Chem. Process Des. Dev., 15, 372 (1976).

4.5 Sargent, R.W.H., and B.A.Murtagh, Mathematical Programming, 4, 245 (1973).

4.6 The Collected Works of J. Willard Gibbs, Vol. 1, P. 56, Longmans, New York (1928).

4.7 Sargent, R.W.H., Numerical Optimization Techniques, Department of Chemical Engineering, Imperial College, London, 3rd Ed. (1975).

4.8 Sargent, R.W.H., Reduced-gradient Methods for Nonlinear Programming, in P.E. Gill and W. Murray (Eds.), Numerical Methods for Constrained Optimization, Academic Press, London (1974).

4.9 Gaminibandara, G.G.K.K., Ph.D. Thesis, University of London (1976).

4.10 Murtagh, B.A., and R.W.H. Sargent, The Computer Journal, 13, 185 (1970).

Chapter 5

5.1 de Boer, J. and A. Michels, Physica, 5, 945 (1938).

5.2 de Boer, J., Physica, 14, 139 (1948).

5.3 de Boer, J. and B.S. Blaisse, Physica, 14, 149 (1948).

5.4 de Boer, J. and R.J. Lunbeck, Physica, 14, 520 (1948).

5.5 Gunn, R.D., P.L. Chueh and J.M. Prausnitz, A.I.Ch.E. Journal, 12, 937 (1966).

5.6 Hilsenrath, J. et al., National Bureau of Standards Circular 564, Washington (1955).

5.7 Wooley, W., R.B. Scott and R.G. Brickwedde, J. Research N.B.S., 41, 379 (1948).

5.8 Michels, A., W. de Graaff, T. Wassenaar, J.M.H. Levelt and P Louwerse, Physica, 25, 25 (1959).

5.9 Mihara, S. and H. Sagara, J. Chem. Eng. Japan, 10, 395 (1977).

5.10 Gunn, R.D., J.J. McKetta and A. Nassar, A.I.Ch.E. Journal, 20, 347 (1974).

5.11 Chang, H.L., L.J. Hurt and R. Kobayashi, A.I.Ch.E. Journal, 12, 1212 (1966).

5.12 Teja, A.S., Chem.Engng. Sci., 33, 609 (1978).

5.13 Chen, J.J., P.S. Chappelear and R. Kobayashi, J. Chem. Eng. Data, 21, 213 (1976).

5.14 Lin, Y., R.J.J. Chen, P.S. Chappelear and R. Kobayashi, J. Chem. Eng. Data, 22, 404 (1977).

5.15 Clark, F.G. and C.R. Koppany, Hydrocarbon Processing, Nov. (1978).

5.16 Sagara, H., Y. Arai and S. Saito, J. Chem. Eng. Japan, 5, 339 (1972).

5.17 Bneham, A.L. and D.L. Katz, A.I.Ch.E. Journal, 3, 33 (1957).

5.18 Freeth, F.A. and T.T.H. Verschoyle, Proc. Royal Soc. (London), 130A, 453 (1931).

5.19 Williams, R.B. and D.L. Katz, Ind. Eng. Chem., 46, 2512 (1954).

5.20 Sagara, H., S. Mihara, Y. Arai and S. Saito, J. Chem. Eng. Japan, 8, 98 (1975).

5.21 Trust, D.B. and F. Kurata, A.I.Ch.E. Journal, 17, 86 (1971).

5.22 Aroyan, H.J. and D.L. Katz, Ind. Eng. Chem., 43, 185 (1951).

5.23 Klink, A.E., H.Y. Cheh and E.H. Amick (Jr.), A.I.Ch.E. Journal, 21, 1142 (1975).

5.24 Cosway, H.F. and D.L. Katz, A.I.Ch.E. Journal, 5, 46 (1959).

5.25 Kay, W.B., Chem. Revs., 29, 501 (1941).

5.26 Saville, G., Dept. of Chem. Eng., Imperial College, London, S.W.7., private communication (1979).

Chapter 6

6.1 Leland, T.W., J.S. Rowlinson, and G.A.Sather, Trans. Faraday Soc., 64, 1447 (1968).

6.2 McDonald, I.R., in K. Singer (ed.), Sataistical Mechanics Volume 1., Specialist Periodical Report, The Chemical Society, London (1973).

6.3 Gubbins, K.E., and C.H.Twu, Chem. Engng. Sci, 33, 863 (1978).

6.4 Twu, C.H., and K.E. Gubbins, Chem. Engng. Sci, 33, 879 (1978).

6.5 Sarashina, E., Y. Arai, and S. Saito, J. Chem. Eng. Japan, 7, 421 (1974).

APPENDIX B

Derivatives of Corresponding States Parameters for the van der Waals one-fluid model

In Chapter 2 the corresponding states principle is developed in terms of the van der Waals one-fluid model of mixtures. Equation (2.27) for the component fugacities involves the derivatives $\Delta_i h_x$ and $\Delta_i f_x$, where Δ_i is the differential operator

$$\left(\frac{D}{Dx_i} - \sum_j x_j \frac{D}{Dx_j}\right)_{V,T}$$

and (D/Dx_i) denotes differentiation with respect to x_i in which all other mole fractions are treated as independent variables. Equations (2.29) and (2.30) for the enthalpy and entropy involve the derivatives $(\partial f_x/\partial T)_V$ and $(\partial h_x/\partial T)_V$. The relevant equations are (2.20), (2.23), (2.24), and (2.25).

$$h_x = \sum_k \sum_\ell x_k \, x_\ell \, h_{k\ell} \tag{B.1}$$

$$f_x = \frac{\sum_k \sum_\ell x_k \, x_\ell \, f_{k\ell} \, h_{k\ell}}{h_x} \tag{B.2}$$

$$h_{k\ell} = \eta_{k\ell}\left(\frac{h_{kk}^{1/3}}{2} + \frac{h_{\ell\ell}^{1/3}}{2}\right)^3 \tag{B.3}$$

$$f_{k\ell} = \xi_{k\ell} \, (f_{kk} \, f_{\ell\ell})^{\frac{1}{2}} \tag{B.4}$$

$$h_{kk} = \left(\frac{V_k^c}{V_o^c}\right) \phi_k \, (V_k^R, \, T_k^R) \tag{B.5}$$

$$f_{kk} = \left(\frac{T_k^c}{T_o^c}\right) \theta_k \ (V_k^R, \ T_k^R) \tag{B.6}$$

$$T_k^R = \frac{\theta_k \ T}{T_o^c f_x} \tag{B.7}$$

$$V_k^R = \frac{\phi_k \ V}{V_o^c h_x} \tag{B.8}$$

Generalised Derivatives

We define a general linear differential operator $\underset{\sim}{D}$, which may represent Δ_i or $(\partial/\partial T)_V$. Applying the operator to equation (B.1) gives

$$\underset{\sim}{D}h_x = \sum_k \sum_\ell h_{k\ell} \underset{\sim}{D} x_k \ x_\ell + \sum_k \sum_\ell x_k \ x_\ell \ \underset{\sim}{D} \ h_{k\ell} \tag{B.9}$$

from (B.3)

$$\sum_k \sum_\ell x_k \ x_\ell \ \underset{\sim}{D} \ h_{k\ell} = \sum_k \sum_\ell x_k \ x_\ell \ \frac{\eta_{k\ell}}{8} \underset{\sim}{D} \ (h_{kk}^{1/3} + h_{\ell\ell}^{1/3})^3$$

$$= \sum_k \sum_\ell x_k \ x_\ell \ \frac{\eta_{k\ell}}{8} \ (h_{kk}^{1/3} + h_{\ell\ell}^{1/3})^2 (h_{kk}^{-2/3} \underset{\sim}{D} h_{kk} + h_{\ell\ell}^{-2/3} \underset{\sim}{D} h_{\ell\ell})$$

since the sum is over all k and ℓ the last two terms make an identical contribution. Hence

$$\sum_k \sum_\ell x_k \ x_\ell \ \underset{\sim}{D} \ h_{k\ell} = \sum_k \sum_\ell x_k \ x_\ell \ \frac{\eta_{k\ell}}{4} \ (h_{kk}^{1/3} + h_{\ell\ell}^{1/3})^2 h_{kk}^{1/3} \ \frac{\underset{\sim}{D} \ h_{kk}}{h_{kk}} \tag{B.10}$$

Substituting in (B.9) gives

$$\underset{\sim}{D}\, h_x = \sum_k \sum_\ell h_{k\ell}\, \underset{\sim}{D}\, x_k\, x_\ell + \sum_k \sum_\ell x_k\, x_\ell \frac{\eta_{k\ell}}{4} \left(h_{kk}^{1/3} + h_{\ell\ell}^{1/3}\right)^2 h_{kk}^{1/3} \frac{\underset{\sim}{D}\, h_{kk}}{h_{kk}} \tag{B.11}$$

By definition

$$\underset{\sim}{D}\, h_x\, f_x = h_x\, \underset{\sim}{D}\, f_x + f_x\, \underset{\sim}{D}\, h_x$$

giving

$$\underset{\sim}{D}\, f_x = \frac{\underset{\sim}{D}\, h_x\, f_x - f_x\, \underset{\sim}{D}\, h_x}{h_x} \tag{B.12}$$

From equation (B.2)

$$h_x\, f_x = \sum_k \sum_\ell x_k\, x_\ell\, f_{k\ell}\, h_{k\ell} \tag{B.13}$$

Applying the differential operator to (B.13)

$$\begin{aligned} \underset{\sim}{D}\, h_x\, f_x = & \sum_k \sum_\ell f_{k\ell}\, h_{k\ell}\, \underset{\sim}{D}\, x_k\, x_\ell + \\ & \sum_k \sum_\ell x_k\, x_\ell\, f_{k\ell}\, \underset{\sim}{D}\, h_{k\ell} + \\ & \sum_k \sum_\ell x_k\, x_\ell\, h_{k\ell}\, \underset{\sim}{D}\, f_{k\ell} \end{aligned} \tag{B.14}$$

From (B.4)

$$\underset{\sim}{D}\, f_{k\ell} = \frac{\xi_{k\ell}}{2(f_{kk} f_{\ell\ell})^{\frac{1}{2}}} \left(f_{kk}\, \underset{\sim}{D}\, f_{\ell\ell} + f_{\ell\ell}\, \underset{\sim}{D}\, f_{kk}\right)$$

$$= \frac{f_{k\ell}}{2} \left(\frac{\underset{\sim}{D}\, f_{kk}}{f_{kk}} + \frac{\underset{\sim}{D}\, f_{\ell\ell}}{f_{\ell\ell}}\right)$$

hence

$$\sum_k \sum_\ell x_k\, x_\ell\, h_{k\ell}\, \underset{\sim}{D}\, f_{k\ell} = \sum_k \sum_\ell x_k\, x_\ell\, h_{k\ell}\, f_{k\ell}\, \frac{\underset{\sim}{D}\, f_{kk}}{f_{kk}} \qquad \text{(B.15)}$$

From (B.12), B.14), (B.15) and (B.10)

$$\underset{\sim}{D}\, f_x = \Bigg[\sum_k \sum_\ell f_{k\ell}\, h_{k\ell}\, \underset{\sim}{D}\, x_k\, x_\ell +$$

$$\sum_k \sum_\ell x_k\, x_\ell\, f_{k\ell}\, \frac{n_{k\ell}}{4}\, (h_{kk}^{1/3} + h_{\ell\ell}^{1/3})^2\, h_{kk}^{1/3}\, \frac{\underset{\sim}{D}\, h_{kk}}{h_{kk}} +$$

$$\sum_k \sum_\ell x_k\, x_\ell\, h_{k\ell}\, f_{k\ell}\, \frac{\underset{\sim}{D}\, f_{kk}}{f_{kk}} - f_x\, \underset{\sim}{D}\, h_x \Bigg] \Big/ h_x \qquad \text{(B.16)}$$

Derivatives of mole fractions

Terms of the type $\underset{\sim}{D}\, x_k\, x_\ell$ arise in equations (B.11) and (B.16). When $\underset{\sim}{D}$ represents $(\partial/\partial T)_V$, these terms disappear. For the Δ_i operator we have the following.

$$\Delta_i\, x_k\, x_\ell = \frac{D\, x_k\, x_\ell}{D\, x_i} - \sum_j x_j\, \frac{D\, x_k\, x_\ell}{D\, x_j}$$

$$\frac{D\, x_k\, x_\ell}{D\, x_i} = \begin{cases} x_\ell & k = i,\ \ell \neq i \\ x_k & \ell = i,\ k \neq i \\ 2x_i & \ell = k = i \\ 0 & \ell \neq i,\ k \neq i \end{cases}$$

It follows that

$$\sum_k \sum_\ell h_{k\ell}\, \Delta_i\, x_k\, x_\ell = 2 \sum_k x_k\, h_{ik} - \sum_j x_j \;\; 2 \sum_k x_k\, h_{jk}$$

or

$$\sum_k \sum_\ell h_{k\ell}\, \Delta_i\, x_k\, x_\ell = 2(h_i - h_x) \qquad \text{(B.17)}$$

$$(h_i \equiv \sum_k x_k\, h_{ik})$$

and similarly

$$\sum_k \sum_\ell f_{k\ell}\, h_{k\ell}\, \Delta_i\, x_k\, x_\ell = 2((fh)_i - f_x\, h_x) \qquad \text{(B.18)}$$

$$((fh)_i \equiv \sum_k x_k\, f_{ki}\, h_{ki})$$

Derivatives of h_x and f_x with respect to mole fractions

From (B.11) and (B.17)

$$\Delta_i\, h_x = 2(h_i - h_x) + \sum_k \sum_\ell x_k\, x_\ell \frac{\eta_{k\ell}}{4} (h_{kk}^{1/3} + h_{\ell\ell}^{1/3})^2\, h_{kk}^{1/3} \frac{\Delta_i\, h_{kk}}{h_{kk}} \qquad \text{(B.19)}$$

Substituting (B.18) and (B.19) into (B.16) gives

$$\Delta_i\, f_x = 2\left(\frac{(fh)_i - f_x\, h_i}{h_x}\right) +$$

$$\sum_k \sum_\ell \frac{(f_{k\ell} - f_x)}{h_x} \frac{\eta_{k\ell}}{4} (h_{kk}^{1/3} + h_{\ell\ell}^{1/3})^2\, h_{kk}^{1/3} \frac{\Delta_i\, h_{kk}}{h_{kk}} +$$

$$\sum_k \sum_\ell x_k\, x_\ell \frac{h_{k\ell}\, f_{k\ell}}{h_x} \frac{\Delta_i\, f_{kk}}{f_{kk}} \qquad \text{(B.20)}$$

Derivatives of h_x and f_x with respect to temperature

Since $(\partial x_k \; x_\ell / \partial T)_V = 0$, there are no terms corresponding to (B.17) and (B.18).

$$\left(\frac{\partial h_x}{\partial T}\right)_V = \sum_k \sum_\ell x_k \; x_\ell \; \frac{\eta_{k\ell}}{4} \; (h_{kk}^{1/3} + h_{\ell\ell}^{1/3})^2 \; h_{kk}^{1/3} \; \frac{(\partial h_{kk}/\partial T)_V}{h_{kk}} \tag{B.21}$$

and

$$\left(\frac{\partial f_x}{\partial T}\right)_V = \sum_k \sum_\ell \frac{(f_{k\ell} - f_x)}{h_x} \; \frac{\eta_{k\ell}}{4} \; (h_{kk}^{1/3} + h_{\ell\ell}^{1/3})^2 \; h_{kk}^{1/3} \; \frac{(\partial h_{kk}/\partial T)}{h_{kk}}$$

$$+ \sum_k \sum_\ell x_k \; x_\ell \; \frac{h_{k\ell} \; f_{k\ell}}{h_x} \; \frac{(\partial f_{kk}/\partial T)_V}{f_{kk}} \tag{B.22}$$

$\underset{\sim}{D} \; h_{kk}$ and $\underset{\sim}{D} \; f_{kk}$ in terms of shape factors

Differentiation of equations (B.5) and (B.6) gives

$$\frac{\underset{\sim}{D} \; h_{kk}}{h_{kk}} = \frac{\underset{\sim}{D} \; \phi_k}{\phi_k} \tag{B.23}$$

and

$$\frac{\underset{\sim}{D} \; f_{kk}}{f_{kk}} = \frac{\underset{\sim}{D} \; \theta_k}{\theta_k} \tag{B.24}$$

The shape factors, θ_k and ϕ_k are functions of V_k^R and T_k^R

$$\underset{\sim}{D} \; \phi_k = \left(\frac{\partial \phi_k}{\partial T_k^R}\right) \; \underset{\sim}{D} \; T_k^R + \left(\frac{\partial \phi_k}{\partial V_k^R}\right) \; \underset{\sim}{D} \; V_k^R \tag{B.25}$$

and

$$\underset{\sim}{D}\ \theta_k = \left(\frac{\partial \theta_k}{\partial T_k^R}\right) \underset{\sim}{D}\ T_k^R + \left(\frac{\partial \theta_k}{\partial V_k^R}\right) \underset{\sim}{D}\ V_k^R \qquad \text{(B.26)}$$

Applying $\underset{\sim}{D}$ to equations (B.7) and (B.8) gives

$$\frac{\underset{\sim}{D}\ T_k^R}{T_k^R} = \frac{\underset{\sim}{D}\ \theta_k}{\theta_k} + \frac{\underset{\sim}{D}\ T}{T} - \frac{\underset{\sim}{D}\ f_x}{f_x} \qquad \text{(B.27)}$$

and

$$\frac{\underset{\sim}{D}\ V_k^R}{V_k^R} = \frac{\underset{\sim}{D}\ \phi_k}{\phi_k} - \frac{\underset{\sim}{D}\ h_x}{h_x} \qquad \text{(B.28)}$$

(Note, $\underset{\sim}{D}\ V = 0$)

Substituting (B.27) and (B.28) into (B.25) and (B.26) and simplifying the notation

$$D\ \theta_k = \theta_{T,k}(D\ \theta_k + D\ T - D\ f) + \theta_{V,k}\ (D\ \phi_k - D\ h) \qquad \text{(B.29)}$$

$$D\ \phi_k = \phi_{T,k}\ (D\theta_k + D\ T - D\ f) + \phi_{V,k}\ (D\ \phi_k - D\ h) \qquad \text{(B.30)}$$

where $D\ \theta_k = \frac{\underset{\sim}{D}\ \theta_k}{\theta_k}$, $D\ \phi_k = \frac{\underset{\sim}{D}\ \phi_k}{\phi_k}$

$$D\ f = \frac{\underset{\sim}{D}\ f_x}{f_x}\ , \quad D\ h = \frac{\underset{\sim}{D}\ h_x}{h_x}\ , \quad D\ T = \frac{\underset{\sim}{D}\ T}{T}\ ,$$

$$\theta_{T,k} = \left(\frac{\partial \theta_k}{\partial T_k^R}\right)\ \frac{T_k^R}{\theta_k}\ , \quad \phi_{V,k} = \left(\frac{\partial \phi_k}{V_k^R}\right)\ \frac{V_k^R}{\phi_k} \qquad \text{etc.}$$

Solving the two simultaneous equations, (B.29) and (B.30), for $D\ \theta_k$ and $D\ \phi_k$ gives

$$D\ \theta_k = \frac{(D\ T - D\ f)(\theta_{T,k} - \theta_{T,k}\ \phi_{V,k} + \theta_{V,k}\ \phi_{T,k}) - \theta_{V,k}\ D\ h}{1 - \phi_{V,k} - \theta_{T,k} + \theta_{T,k}\ \phi_{V,k} - \theta_{V,k}\ \phi_{T,k}} \qquad (B.31)$$

and

$$D\ \phi_k = \frac{\phi_{T,k}\ (D\ T - D\ f) + D\ h(\phi_{V,k}\ \theta_{T,k} - \theta_{V,k}\ \phi_{T,k} - \phi_{V,k})}{1 - \phi_{V,k} - \theta_{T,k} + \theta_{T,k}\ \phi_{V,k} - \theta_{V,k}\ \phi_{T,k}} \qquad (B.32)$$

Composition Derivatives

$\underset{\sim}{D} \equiv \Delta_i$ and $D\ T = 0$

$$\frac{\Delta_i\ \theta_k}{\theta_k} = \frac{-(\Delta_i\ f_x/f_x)(\theta_{T,k} - \theta_{T,k}\ \phi_{V,k} + \theta_{V,k}\ \phi_{T,k}) - \theta_{V,k}(\Delta_i h_x/h_x)}{1 - \phi_{V,k} - \theta_{T,k} + \theta_{T,k}\ \phi_{V,k} - \theta_{V,k}\ \phi_{T,k}} \qquad (B.33)$$

$$\frac{\Delta_i\ \phi_k}{\phi_k} = \frac{(\Delta_i\ h_x/h_x)(\phi_{V,k}\ \theta_{T,k} - \theta_{V,k}\ \phi_{T,k} - \phi_{V,k}) - \phi_{T,k}(\Delta_i f_x/f_x)}{1 - \phi_{V,k} - \theta_{T,k} + \theta_{T,k}\ \phi_{V,k} - \theta_{V,k}\ \phi_{T,k}} \qquad (B.34)$$

Temperature Derivatives

$\underset{\sim}{D} \equiv (\partial/\partial T)_V$ and $DT = 1/T$

$$\frac{(\partial \theta_k / \partial T)_V}{\theta_k} = \frac{\left[\frac{1}{T} - \frac{(\partial f_x / \partial T)_V}{f_x}\right] (\theta_{T,k} - \theta_{T,k}\, \phi_{V,k} + \theta_{V,k}\, \phi_{T,k}) - \theta_{V,k} \frac{(\partial h_x / \partial T)_V}{h_x}}{1 - \phi_{V,k} - \theta_{T,k} + \theta_{T,k}\, \phi_{V,k} - \theta_{V,k}\, \phi_{T,k}} \tag{B.35}$$

$$\frac{(\partial \phi_k / \partial T)_V}{\phi} = \frac{\frac{(\partial h_x / \partial T)_V}{h_x} (\phi_{V,k}\, \theta_{T,k} - \theta_{V,k}\, \phi_{T,k} - \phi_{V,k}) + \phi_{T,k} \left[\frac{1}{T} - \frac{(\partial f_x / \partial T)_V}{f_x}\right]}{1 - \phi_{V,k} - \theta_{T,k} + \theta_{T,k}\, \phi_{V,k} - \theta_{V,k}\, \phi_{T,k}} \tag{B.36}$$

Analytic solution for composition derivatives

Equation (B.19) and (B.20) may be written in the form

$$\Delta_i\, h_x = \sum_k \sum_\ell a_{k\ell} \frac{\Delta_i\, h_{kk}}{h_{kk}} - E_i \tag{B.37}$$

and

$$\Delta_i\, f_x = \sum_k \sum_\ell b_{k\ell} \frac{\Delta_i\, h_{kk}}{h_{kk}} + \sum_k \sum_\ell \frac{\Delta_i\, f_{kk}}{f_{kk}} - F_i \tag{B.38}$$

From (B.23), (B.24), (B.33), and (B.34) we can write

$$\frac{\Delta_i\, h_{kk}}{h_{kk}} = d_k\, \Delta_i\, h_x + e_k\, \Delta_i\, f_x \tag{B.39}$$

and

$$\frac{\Delta_i\, f_{kk}}{f_{kk}} = g_k\, \Delta_i\, h_x + m_k\, \Delta_i\, f_x \tag{B.40}$$

Substituting (B.39) and (B.40) into (B.37) and (B.38) - noting that $\Delta_i h_x$ and $\Delta_i f_x$ are independent of the summations over k and ℓ, we have

$$\Delta_i h_x = \Delta_i h_x \sum_k \sum_\ell a_{k\ell} d_k + \Delta_i f_x \sum_k \sum_\ell a_{k\ell} e_k - E_i$$

$$\Delta_i f_x = \Delta_i f_x \sum_k \sum_\ell (c_{k\ell} m_k + b_{k\ell} e_k)$$

$$+ \Delta_i h_x \sum_k \sum_\ell (c_{k\ell} g_k + b_{k\ell} d_k) - F_i$$

or

$$\Delta_i h_x = A_1 \Delta_i h_x + A_2 \Delta_i f_x - E_i \qquad \text{(B.41)}$$

$$\Delta_i f_x = B_1 \Delta_i f_x + B_2 \Delta_i h_x - F_i \qquad \text{(B.42)}$$

A_1, A_2, B_1, and B_2 are constants for the mixture and only E_i and F_i depend on the component i. The simultaneous equations (B.41) and (B.42) may easily be solved for the derivatives $\Delta_i f_x$ and $\Delta_i h_x$.

Analytic solution for temperature derivatives

Equations analogous to those for the composition derivatives may be derived in exactly the same way from equations (B.21) - (B.24), (B.35) and (B.36)

$$\left(\frac{\partial h_x}{\partial T}\right)_V = A_1 \left(\frac{\partial h_x}{\partial T}\right)_V + A_2 \left(\frac{\partial f_x}{\partial T}\right)_V - C_1 \qquad \text{(B.43)}$$

$$\left(\frac{\partial f_x}{\partial T}\right)_V = B_1 \left(\frac{\partial f_x}{\partial T}\right)_V + B_2 \left(\frac{\partial h_x}{\partial T}\right)_V - C_2 \qquad \text{(B.44)}$$

As before, these two simultaneous equations may be solved for the derivatives.

Appendix C Coefficients in Equations of State

The coefficients listed here are for the equations of state for methane developed in Chapter 3. Equations B, C, and D are of the same form as equation (3.1), equation E has the form of (3.20). In all cases numerical values of the coefficients give pressure in Pa for temperature in K and density in mol m^{-3}.

	EQUATION			
Coefficient	B	C	D	E
1	$.226039636517 \times 10^{-4}$	$.132448083038 \times 10^{-3}$	$.898183102418 \times 10^{-4}$	$.939889064830 \times 10^{-4}$
2	$.221476378730 \times 10^{-1}$	$.164377523021 \times 10^{-1}$	$.188570883291 \times 10^{-1}$	$.193627468613 \times 10^{-1}$
3	$-.553328789694$	$-.468759147842$	$-.507334853102$	$-.518953058182$
4	$.281858916729 \times 10^{2}$	$.216027995298 \times 10^{2}$	$.242440372451 \times 10^{2}$	$.228570280863 \times 10^{2}$
5	$-.295163245426 \times 10^{4}$	$-.265660017475 \times 10^{4}$	$-.275937243281 \times 10^{4}$	$-.252015241370 \times 10^{4}$
6	$.814088378598 \times 10^{-8}$	$.539736457336 \times 10^{-8}$	$.667706377937 \times 10^{-8}$	$.782777652516 \times 10^{-8}$
7	$.631986661316 \times 10^{-5}$	$.904035457663 \times 10^{-5}$	$.659554690590 \times 10^{-5}$	$-.185845317257 \times 10^{2}$
8	$-.542501277980 \times 10^{-2}$	$-.618667537915 \times 10^{-2}$	$-.475099859428 \times 10^{-2}$	$.636519495543 \times 10^{-9}$
9	$.474277618274 \times 10^{1}$	$.473048585074 \times 10^{1}$	$.941749168525$	$-.164834515660 \times 10^{-6}$
10	$.100268531959 \times 10^{-13}$	$.262533257810 \times 10^{-12}$	$.203123055432 \times 10^{-12}$	$.717057018772 \times 10^{-3}$
11	$-.409812261619 \times 10^{-10}$	$-.282057835912 \times 10^{-9}$	$-.882991375776 \times 10^{-10}$	$.498525092074 \times 10^{-20}$
12	$.331763473851 \times 10^{-6}$	$.385414795226 \times 10^{-6}$	$.269841136359 \times 10^{-6}$	$.136616192556 \times 10^{-8}$
13	$.178700501527 \times 10^{-13}$	$.196312923839 \times 10^{-13}$	$.163105161849 \times 10^{-13}$	$-.440199072120 \times 10^{-13}$

Coefficient	B	C	D	E
14	$-.114033814686 \times 10^{-14}$	$-.109992004660 \times 10^{-14}$	$-.965840913441 \times 10^{-15}$	$.300575118477 \times 10^{-24}$
15	$-.507875688482 \times 10^{-12}$	$-.509697089907 \times 10^{-12}$	$-.497527927565 \times 10^{-13}$	$-.567982014989 \times 10^{-29}$
16	$.416358397742 \times 10^{-19}$	$.386644229069 \times 10^{-19}$	$.388068765783 \times 10^{-19}$	$.562400436641 \times 10^{-37}$
17	$-.41698870897 \times 10^{-24}$	$-.375297743367 \times 10^{-24}$	$-.447156684621 \times 10^{-24}$	.469943326898
18	$.764256477191 \times 10^{-21}$	$.765121539971 \times 10^{-21}$	$.280554989023 \times 10^{-22}$	$-.615031567674 \times 10^{4}$
19	$-.124984074103 \times 10^{-25}$	$-.124844277709 \times 10^{-25}$	$-.496671746902 \times 10^{-28}$	$.895357307957 \times 10^{-4}$
20	$-.325367527345 \times 10^{1}$	$-.318318076937 \times 10^{1}$	.427414662506	$.125906059264 \times 10^{-16}$
21	$-.134372278007 \times 10^{3}$	$-.134820589100 \times 10^{3}$	$-.125241753250 \times 10^{3}$	$-.243775657125 \times 10^{-25}$
22	$-.460147430894 \times 10^{-7}$	$-.457050478675 \times 10^{-7}$	$-.102133310576 \times 10^{-7}$	$.125167059533 \times 10^{-33}$
23	$.799724700154 \times 10^{-4}$	$.751653775986 \times 10^{-4}$	$.788608202448 \times 10^{-4}$	$-.882320526724 \times 10^{-30}$
24	$-.123543435353 \times 10^{-15}$	$-.122534074823 \times 10^{-15}$	$-.374931459167 \times 10^{-17}$	
25	$.159537073866 \times 10^{-14}$	$.172230374498 \times 10^{-14}$	$.127111849576 \times 10^{-14}$	
26	$-.644137352786 \times 10^{-24}$	$-.650082069571 \times 10^{-24}$	$-.236364400069 \times 10^{-24}$	
27	$-.114224784265 \times 10^{-20}$	$-.116019192450 \times 10^{-20}$	$-.123455321379 \times 10^{-20}$	
28	$.217468601404 \times 10^{-34}$	$.339742415501 \times 10^{-34}$	$.204715659218 \times 10^{-33}$	
29	$.379692716559 \times 10^{-31}$	$.390850655316 \times 10^{-31}$	$.406242840085 \times 10^{-31}$	
30	$-.213397071743 \times 10^{-41}$	$-.216187310073 \times 10^{-41}$	$-.873417429883 \times 10^{-42}$	
31	$-.426924709358 \times 10^{-40}$	$-.469812724464 \times 10^{-40}$	$-.381661132665 \times 10^{-40}$	
32	$.255315476298 \times 10^{-39}$	$.755260720560 \times 10^{-39}$	$.532641296927 \times 10^{-39}$	
γ	$.97 \times 10^{-8}$	$.97 \times 10^{-8}$	$.97 \times 10^{-8}$	$.978454526721 \times 10^{-8}$